Presented To:

RCREEE
Regional Center for Renewable Energy and Energy Efficiency
المركز الإقليمي للطاقة المتجددة وكفاءة الطاقة

Scatec 200MW Wind Farm in Egypt

Detailed Flood Risk Assessment

24th March 2025

Presented By:

EcoConServ Environmental Solutions
12 El-Saleh Ayoub St., Zamalek, Cairo11211, Egypt
Tel: +20227359078 /27364818
Fax: + 20227365397
E-mail: *genena@ecoconserv.com*
URL: *www.ecoconserv.com*

Document History

Date	Version	Issued by	Revision Description	Reviewed by	Approved by
19/12/2024	1.0	EcoConServ	Issue for Client Review		
28/02/2025	2.0	EcoConServ	Issue for Client Review		
24/03/2025	3.0	EcoConServ	Issue for Client Review		

Table of content

List of Figures

List of Tables

1. Introduction

The project is in Wadi Dara area between Ras Shukeir – and Gebel El Zeit on the Gulf of Suez. This area is a part of the coastal strip that separates a high mountain range to the west (Red Sea Mountains) and the watercourse of the Red Sea and the Gulf of Suez (Figure 1). The site area is about 37 km2 covered by layers of clastic sediments resulting from the weathering and erosion of exposed rocks in the mountain range and mainly transported by rainwater. Due to the clastic nature of the sediments that cover this region, the high elevation difference between it and the mountainous regions to the west, and the impermeable nature of the rocks that form the mountain ranges, rainwater has been collected in many drainage basins causing surface runoff and forming many Wadies flow towards the Gulf of Suez. The intensity of surface runoff depends on many factors, the most important of which are the area of the drainage basin, the length of the wadi, the intensity of slope, the nature of the bed rocks and sediments, in addition to the intensity of the rainfall. This flow develops in certain basins and Wadies, forming a severe flood (Flash flood) that may cause great harm to the lives and facilities located on the mainstreams of these wadies or at the last on their outlets.

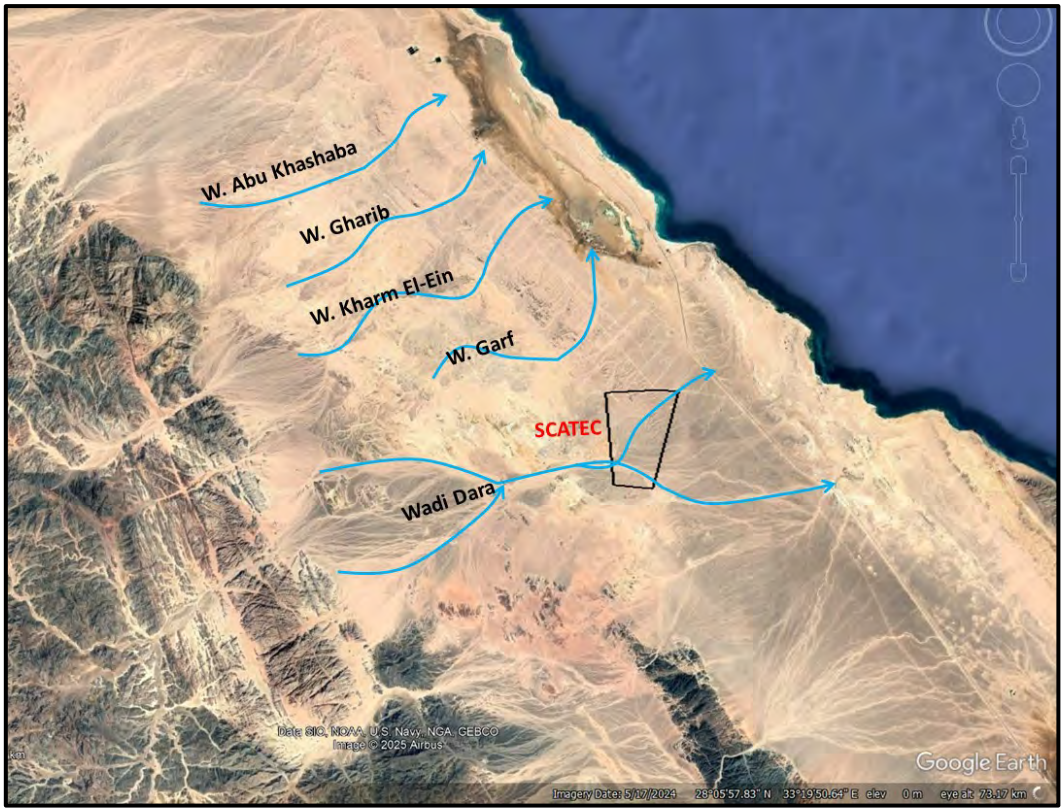

Figure 1: Location of the project site in the coastal area between the Red Sea Mountains and the Gulf of Suez. Note the numerous drainage lines running to the Gulf water crossing the whole area and the most obvious drainage are (Wadi Dara which crosses the site through two outlets at the north and south).

In the area surrounding the project site, there are many dry wadies that represent different drainage basins in natural and morphometric characteristics, which led to a variation in the intensity of floods that occur during rainstorm (Figure 1). Wadi Garf, Wadi Kharm El Ein, Wadi Gharib and

wadi Abu Khashaba are very close drainage basins to the north of the suite. Due to the small watershed areas of these basins no dangerous flood events have been recorded in all of them before unlike wadi Al Darb, Wadi Abu Had and Wadi Hawashyia at the far north which prompting the government to establish many applications and measures to mitigate the flood hazards which often occurred in them. Due to the presence of these wadies and the dangerous floods that have been recorded in some areas, a detailed study must be conducted to assess the risks of the expected floods in the project site, considering the consequences of global climatic changes.

In fact, the integrated record of the rainfall history represents the area of the project site is collected from El Gouna which is the closest station to the site (Figure 2). The collected rainfall data represent the last 10 years (2015 – May 2024) with the following parameters:

- The number of rainy days
- Rainfall intensity
- The largest amount of rain that fell in a day with date
- 6 Months records during the last 10 years from 2015 to 2024

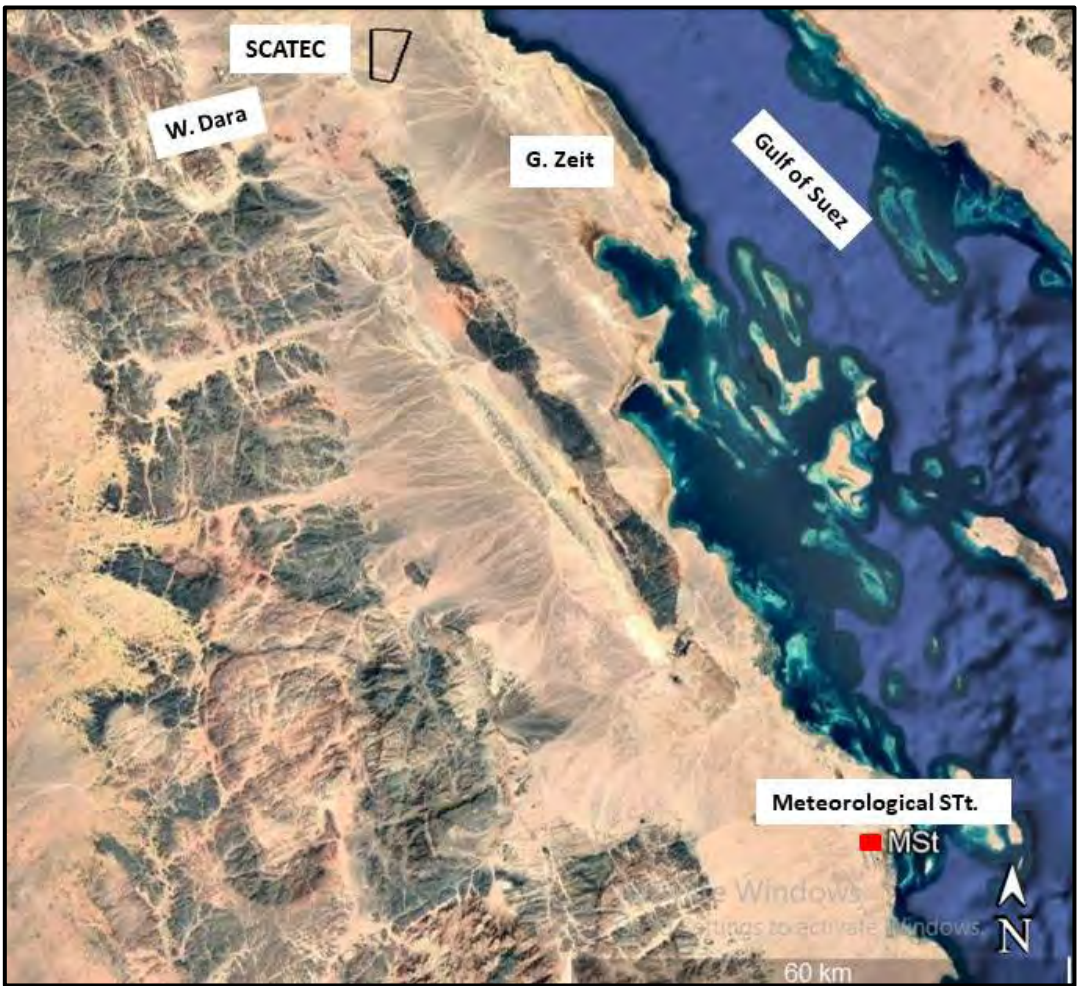

Figure 2: The weather stations close to project site

2. Scope of Work

The main objective of this report is to study in detail the floods expected to occur in the project area during rainstorms. Determine the extent of the danger of the surface runoff that passes directly in the project site through the drainage lines that cross it, in addition to locate the highly dangerous places within the site. Develop all suggestions that would overcome and mitigate the negative effects of floods and how to protect facilities and people live in the event of the occurrence of them. Develop a model to assess the risk of floods based on the natural characteristics of the region, the prevailing climatic conditions in the current climatic cycle, considering the active climatic changes and the resulting effects, especially the unexpected increase in rainfall intensity.

3. Methodology

a. **Previous work and literature review:** Collection of all available published articles, internal reports ... etc on the area concerned with the climate, rain, etc., and the flash flooding records.
b. **Installed level gauges data**: rainfall date during the period (2015 – 2024) of El Gouna weather station was collected from the General Authority of Meteorology.
c. **Flood risk assessment model:** morphometric analysis of the drainage basins in the area was carried out based on the SRTM satellite images of Egypt, using ARC-GIS software, and maximum rain fall intensity data recorded in the area. Then the severity and likelihood of the expected floods could be determined.
d. **Satellite Visual Analysis:** Satellite visualizations provide a suitable means for estimating the amounts of rain that fell anywhere on the surface of the Earth by tracking satellite images, **especially climatic satellites**. This helps in monitoring various climatic phenomena, including the phenomenon of rain. So, in addition to the 10-year records that will be collected from the active weather station in the area (El Gouna Station), the rainfall data will be extracted from climate satellite images by Neural Network Models.
The analysis of climate satellite images allows obtaining data of various elements such as rain, as the sources provide data and measurements of the amount of rain on a daily, weekly, monthly, and yearly basis. This data can be used after extracting it to track the movement of rainstorms and draw a hydrograph of rain, as well as the possibility of determining both the volume of rain and the intensity of rain according to mathematical equations. This model is based on calculating rainfall using GridSat-B1 infrared data and adjusting it using the monthly global climate data product. The extraction process will be done through the following steps:

- Download climate satellite data for the previous ten years
- Through CPC (Cartesian Perceptual Compression) and NOAA (National Oceanic and Atmospheric Administration) satellite images, rain can be monitored and tracked in the area as follows:
    - Obtaining the monthly averages amount of rain falling on the area during the study period, with the design of maps for each month in terms of the amount of rain falling.

- Tracking the strong rainstorms that the region has been exposed to, according to the depth of rain in each storm, and according to the amount of rain and the intensity of rain in each storm.
- From the previous data, it is possible to obtain the probability of the return of strong rainstorms and the time of their return.
- Estimation of the design depth of future rainstorms.
- Plotting hydrographs for the hydraulic drain values for the basin.
- It is also possible to calculate the hydrological factors of the basins, as well as calculate the water budget of the drainage basin and determine the degree of its danger.

e. Conducting a field visit to encounter any natural phenomena in the area that indicate the intensity of rain, the places where floods occur, the extent of the capacity of these floods and their impact on the surrounding environment. Also, to validate all the processed models and proposed mitigation measures on ground.

4. Project Location

The project site is located on the western bank of the Gulf of Suez, about 115 km north of Hurghada. The nearest settlements to the site are Ras Shukeir city to the north by about 10 km, where Ras Gharib and Zafarana cities are located at about 40 and 120 km north of the site respectively (Figure 3). The width of the project area (from west to east) is about 5 km while the length is about 6 km. The northern end of the Red Sea elevated mountains run in NW-SE at distance of about 20 km to the western boundary of the project site.

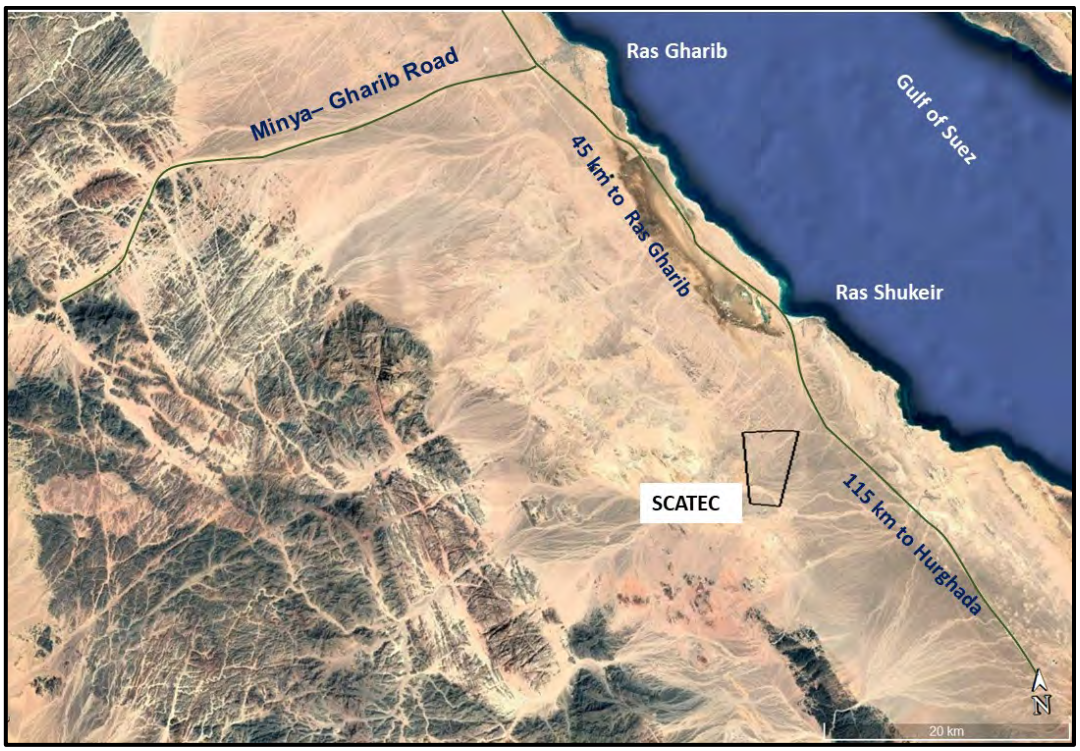

Figure 3: Location of the project site

5. Climate

Generally, the climate of the project area (Wadi Dara) is semi-arid, characterized by hot dry summers, moderate winters and very little rainfall. The climatic data in this study was collected from the world meteorological weather organization and from Hurghada Weather Airport Station (the nearest weather station to the site).

5.1 Temperature

The average maximum temperature in 30 years (1971-2000) is 46°C, while the average maximum temperature is 27.0°C. The mean minimum temperature is 18.74°C (Table 1).

Table 1: The meteorological parameters during the period 1971-2000 at Hurghada, the nearest weather station to Ras Gharib

Month	Jan	Feb	Mar	Apr	May	June	July	Aug	Sep	Oct	Nov	Dec	Av. annual
Av. Highest temp. °C	30	32	35	40	43	46	44	42	43	43	35	32	46
Av. lowest temp. °C	11	11.4	14	17.8	21.9	24.8	26.4	26.2	24.2	20.9	16.6	12.5	18.74
Av rainfall mm.	0.4	0.02	0.3	1	0.04	0	0	0	0	0.6	2	0.9	5.26
Av RH%	48	46	46	43	42	41	45	46	48	53	51	51	46.67
Sun rise Hs	279	290	310	300	341	360	403	372	330	310	270	279	3844

The range of temperature was 7°C during January and 46°C in May 2016 and the mean monthly temperature was 26°C (Table 2). The mean high temperatures reached 26 °C, while the average minimum temperatures were 21°C in 2016.

Table 2: The values of temperature, humidity, wind speed, rate of precipitation, visibility and pressure at sea level during the months of 2016 as recorded in the weather station in Hurghada International Airport (3).

Parameter	Max	Avg	Min	Sum
Max temperature	46. °C	32 °C	17 °C	
Mean temperature	32 °C	21 °C	7 °C	
Min temperature	32 °C	21 °C	7 °C	
Heating degree days (base 65)	10	1	0	199
Cooling degree days (base 65)	60	15	0	5561
Growing degree days (Base 50)	75	30	5	10859
Dew point	29 °C	11. °C	-22 °C	
Precipitation	40.9 mm	0.1 mm	0.0 mm	40.89 mm
Wind speed	74 km/h	19 km/l	-	-

5.2 Wind

The highest wind speed recorded in 2016 at Hurghada weather station was 74 km/hr, with an average of 19 km/hr (Table 2). From the study of the wind directions of Hurghada International Airport meteorological station, the prevailing winds blowing on area are the N or NE winds summer and autumn or S in winter.

5.3 Relative Humidity

The mean annual Relative Humidity in percentage ranged from 41% to 51% with a total annual average equal 46.67% during the period 1971-2000 as shown in Table (1). The air humidity decreases sharply when the country is exposed to the Khamaseen winds during the period March and June which is hot, dry and dusty that leads to stirring fine sand with a degree that may obscure the vision, in addition to low humidity, and it is associated with depressions from the Mediterranean and North Africa, or associated with the occurrence of weather conditions that are accompanied by instability situations in spring.

5.4 Solar Radiation

Hegazy and Effat (2010) reported that the average percentage of sunshine hours ranged from 65% to 70% during the winter months and 80% to 85% in the summer months, based on data from the period 1987-1996 at the Suez Marine Meteorological Station. They also noted that the investigated area, including Dara, experiences high solar radiation intensity, ranging from 1,900 to 2,600 Wh/m²/year. Additionally, the mean sunshine duration at Hurghada during the period 1971-2000 was 320.33 hours per month (Table 1).

5.5 Rainfall (Precipitation) and Evaporation

Data taken from the meteorological station at Hurghada International Airport indicated that the highest monthly total annual rain reached 40.89 mm during October 2016 and the mean lowest one was 0.1 mm in most months of the year (Table 2), while the total mean annual rainfall during the period 1971-2000 reached about 2 mm/year (Table 1). Meanwhile, the annual evaporation reaches 300 mm, and the maximum evaporation rate occurs in June and July, reported during the period 1987-1996 at Suez Marine Meteorological Station.

The monthly readings of the largest amount of rainfall that fell in one day at Hurghada station during the period 2015-2024 (Table 3). The maximum recorded rainstorm was 51.3mm on Oct. 27, 2016, followed by 16mm in 1st Jan 2022 (Table 3). The rainstorm recorded in 2016 resulted in a strong flash flood at Ras Gharib city.

Table 3: The monthly maximum rainfall in one day during the period 2015 -2024

Parameter	Jan	Feb.	Mar.	Abr.	May	Oct.	Nov.	Dec.	year
Max. in day mm	0	0.4	0	0	0	5.2	0	0	2015
Day						25			
Max. in day mm	0	0	0	0	0	51.3	0	0	2016
Day						27			
Max. in day mm	0	0	0	1.6	0	0	0	0	2017
Day				12					
Max. in day mm	0	2	0	0	2	0	0	0	2018
Day		23			6				
Max. in day mm	0.1	0.1	0	0	0	0	0	0	2019
Day	27	5							
Max. in day mm	0	0	3	0	0	0	0	0	2020

Day			12						
Max. in day mm	0	0.1	0	0	0	0	0	1.8	2021
Day		3						27	
Max. in day mm	16	2.1	0	0	0	0	0	0	2022
Day	1	15							
Max. in day mm	0.3	2	0.1	0	0	0	0	0	2023
Day	3		14						
Max. in day mm	0	0	0	0	1	0	0	0	2024
Day					30				

5.6 Topography

The project is in an area with drainage basins and dry wadis flows to the Gulf of Suez south of Ras Shukeir city. The project area belongs to two drainage basins, namely the Wadi Dara basin, Wadi North Dara (W. Mallaha). Astronomically, the project site extends between latitudes 27 ° 47' 47.5 ° - 28 ° 7' 45.9 ° North and longitudes 23 ° 44' 19.5 ° – 33 ° 24' 29.2 °East, (Figure 4). Topographic contour map of the area included the project site (Figure 5) shows no drastic change in topography along the project site. The ground elevation along the project site varies from 150 m amsl at the west to about 100 m amsl at the east.

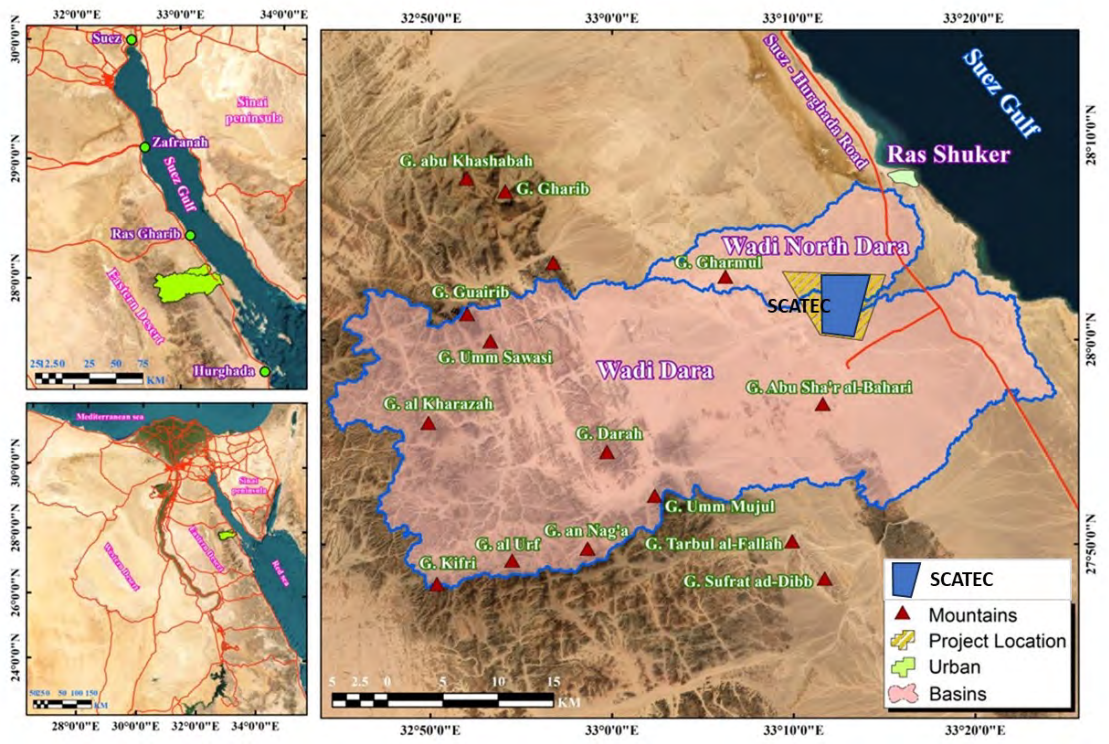

Figure 4: Map indicating the location and morphology of the two basins (Wadi Dara and W. Mallaha N. Dara) where the site is located at their downstream parts to the east.

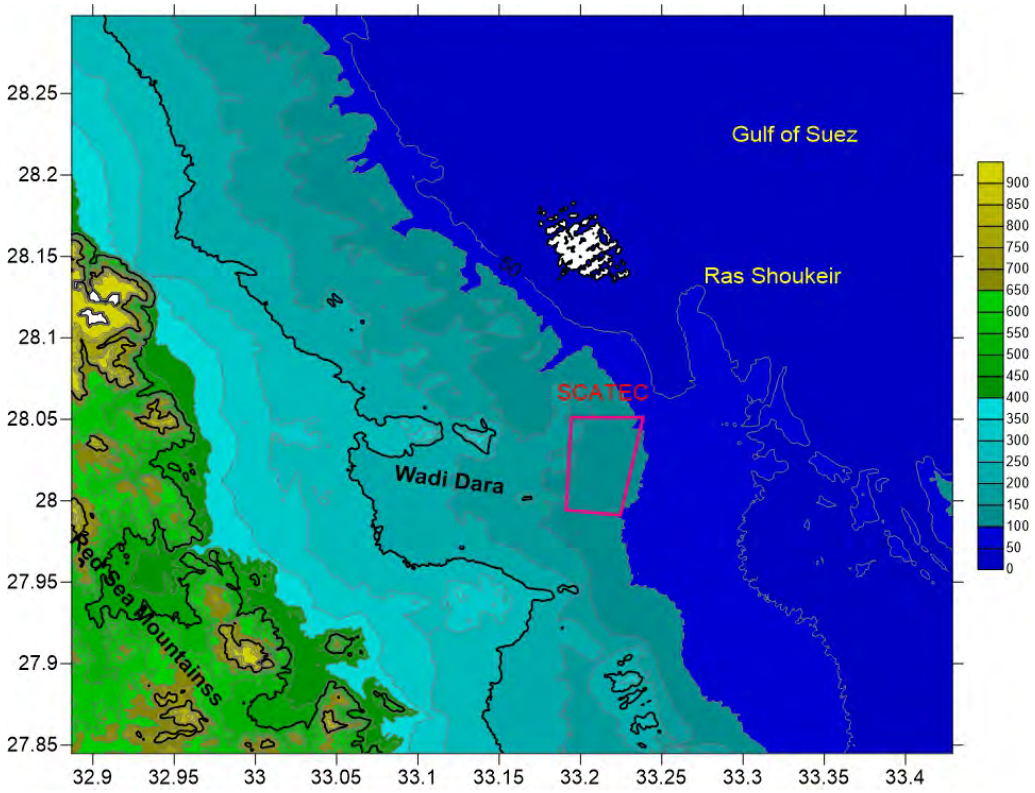

Figure 5: The topographic contour map of the area surrounding the project site.

6. Surface Geology

The Quaternary deposits (Post – Miocene) cover all the area of the project site (Figure 6). These deposits are composed of gravel, sand, clay, aeolian sand sheets and sand accumulations. They are mainly clastic sediments of different textures ranging from silt to gravel size. The composition of the Quaternary deposits is mainly the weathering products of the surrounding exposed rocks. In the area around the project with the occurrence of the igneous rocks of the Red Sea Mountain range in the far west and southwest, which consists mainly of granitic rocks rich in feldspars reddish in color, the soil cover in the area predominantly dark as it consists of fragments of younger granite and feldspars, the weathered products of granites (Figures 7, 8, 9).

The Quaternary sediments are the main cover of the eastern and southeastern parts of the project area on which major parts of construction works will be built, while at the west and southwest the construction foundations will be completely in Miocene evaporites (Figure 10). During the field survey, with the help of geological maps and aerial photographs, the different types of soil, characteristics and their location in the project area were investigated.

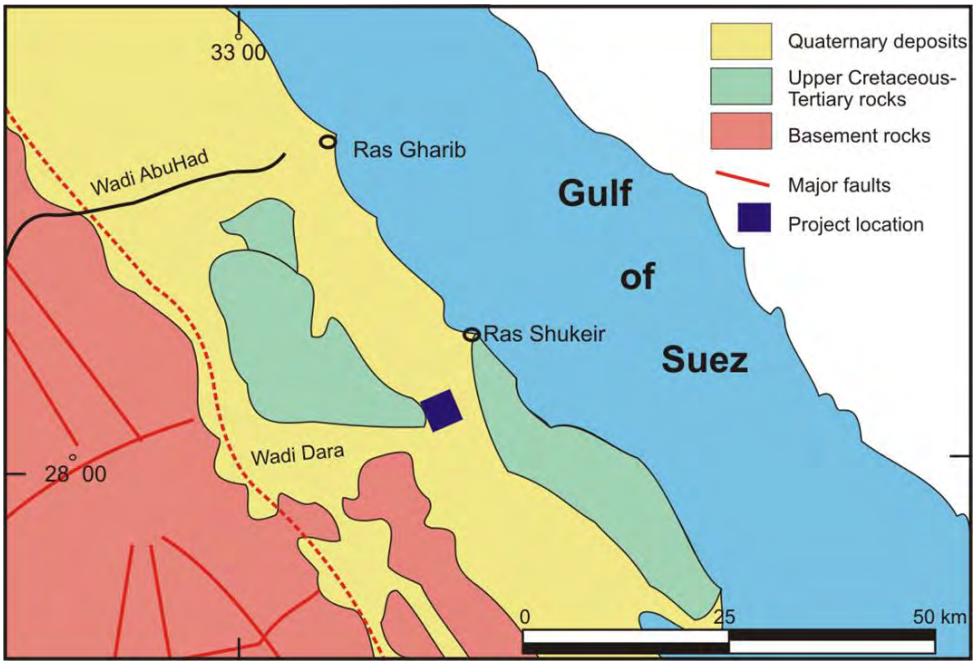

Figure 6: Regional geologic map of the area. Modified from the geologic map of Egypt

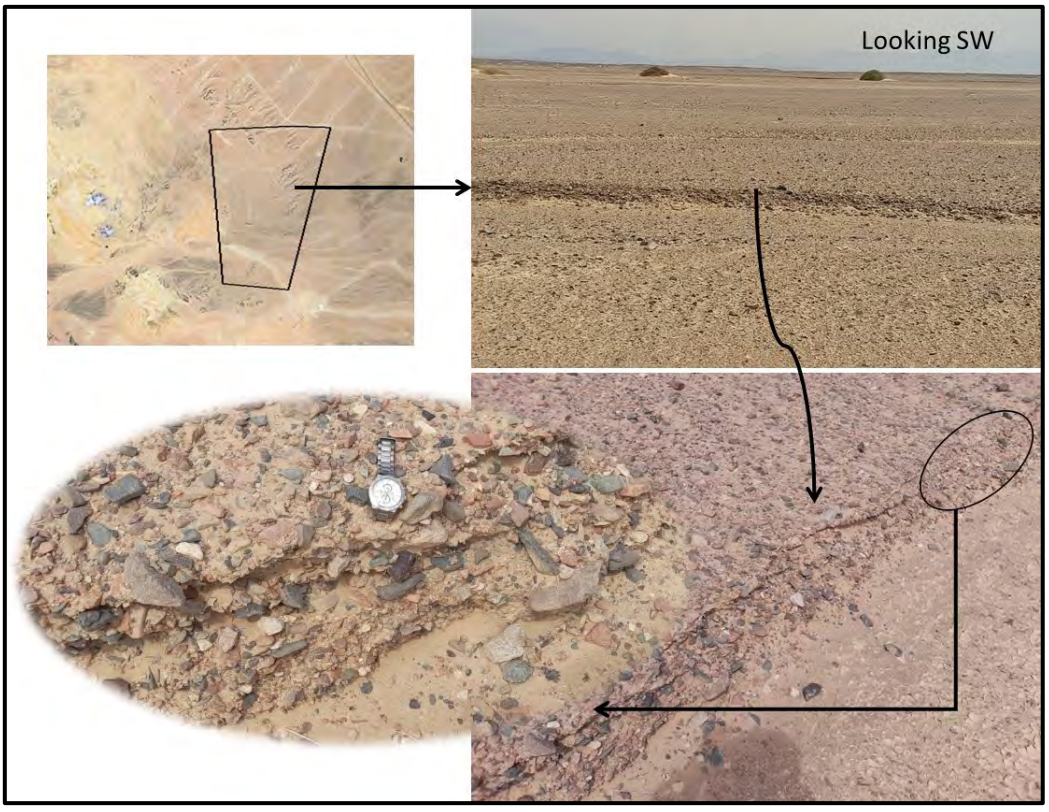

Figure 7: Field photograph of the Quaternary deposits at the mid-eastern part of the site.

**Note, the layer is composed of rock fragments of basement impeded in sand and silt.*

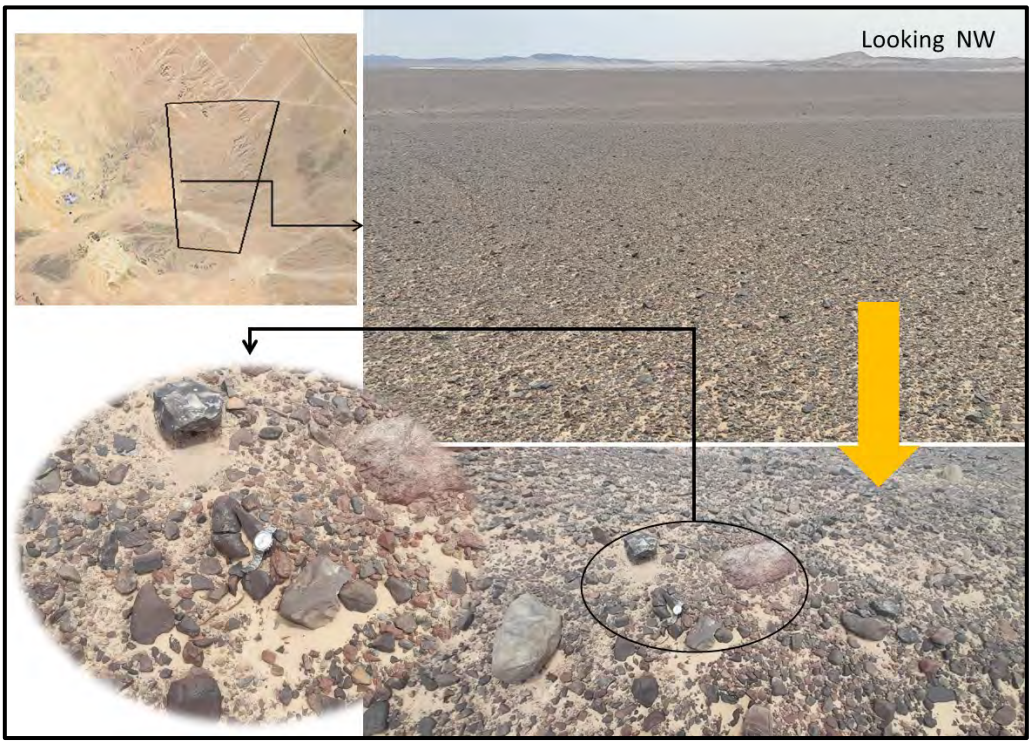

Figure 8: Field photograph of the Quaternary deposits at the mid-western part of the site.

**Note, the layer is composed of rock fragments of basement impeded in sand and silt, where the size of the fragment is slightly larger than the same deposits at the east.*

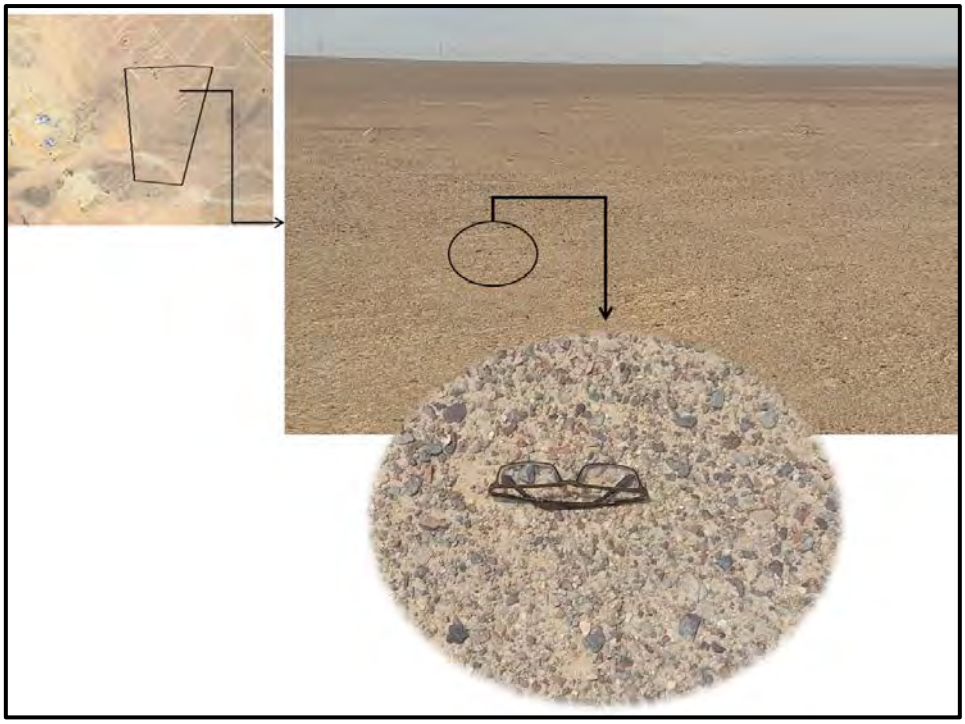

Figure 9: Field photograph of the Quaternary deposits at the NE part of the site. Note, the surface is covered by rock fragments of basement impeded in sand and silt, where the size of the fragment is much smaller than the same deposits at the west.

At the west and southwest, the Miocene evaporite is exposed on the surface of the site, sometimes covered by a very thin layer of Quaternary deposits (Figure 10).

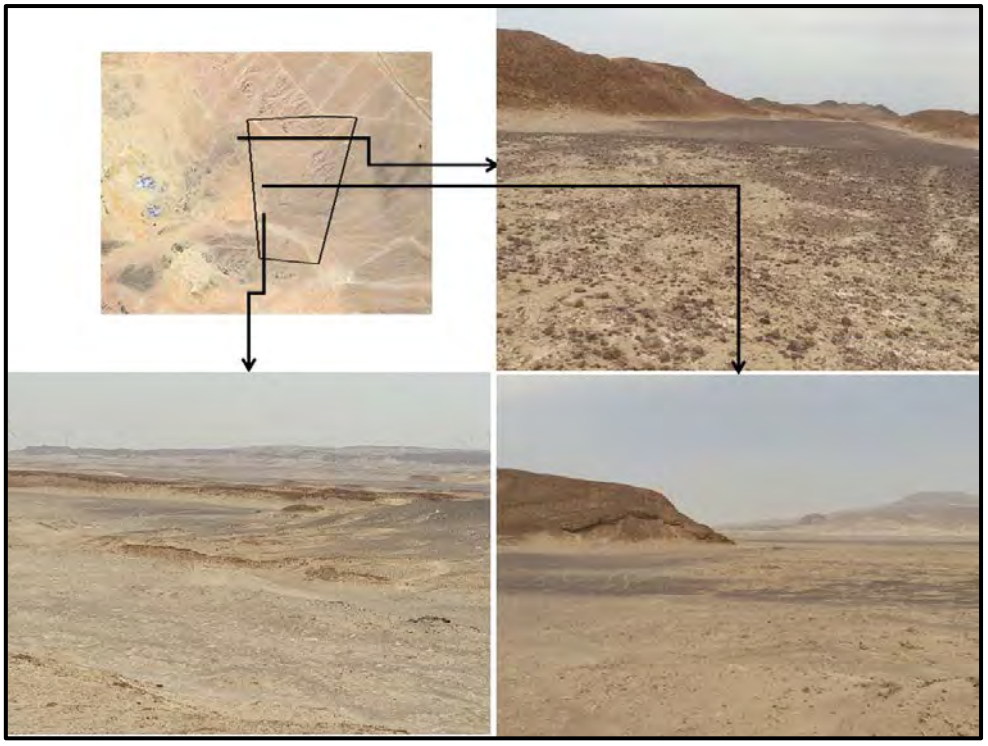

Figure 10 The evaporite exposed on the ground surface at the west and southwest

The soil covers almost all the projects (Figure 11) and is in the form of chains of alluvium terraces. Three alluvium terraces have been described in the project area and in the surrounding area during the site visit; T1, T2 and T3. The three terraces are deposited on the exposed main bed rocks which are mainly Basement rocks to the west outside the area of the project, Cretaceous sandstone at the southwest part of the site and Eocene limestone in the northwest part of the site. Their existence at different levels is mainly due to fluvial erosion in the direction of slope. They are of Quaternary age in periods of heavy rainfall. The grain size of the terraces decrease from the upstream to the downstream due to the decrease in the intensity of surface flow.

Terraces differ in their height from the floor of the wadi in addition to the type and size of their components. The terraces near the highlands in the west and southwest are located at higher altitudes, and the components are very close to those in the source and their size is large. T1 (the oldest terrace) is located close to the elevated exposures (Red Sea Mountains) either from the west or from the southwest. Going to east and northeast the fine the drainage lines getting very wide and almost disappeared except for the outlet of Wadi Dara at the south. The younger terraces formed on low lying successive levels, T2, T3. The youngest formed terraces (T3) are distributed along the floor of the shallow drainage that crosses the 2 and characterized by a successive layer of different deposits varies in grain size and thin layer of mud transported by sheet flow of rainwater. These terraces will be dealt with in some detail below.

T1: The older terrace

These terraces represent the top of the elevated land and the longitudinal shallow dissected hills at the west and northwest at the watershed area of Wadi Dara. This old terrace has been dissected by numerous shallow and wide tributaries drain eastward to the Gulf of Suez. The maximum elevation of the terraces at the west and southwest part is about 160 m (a.m.s.l) (Figures 11).

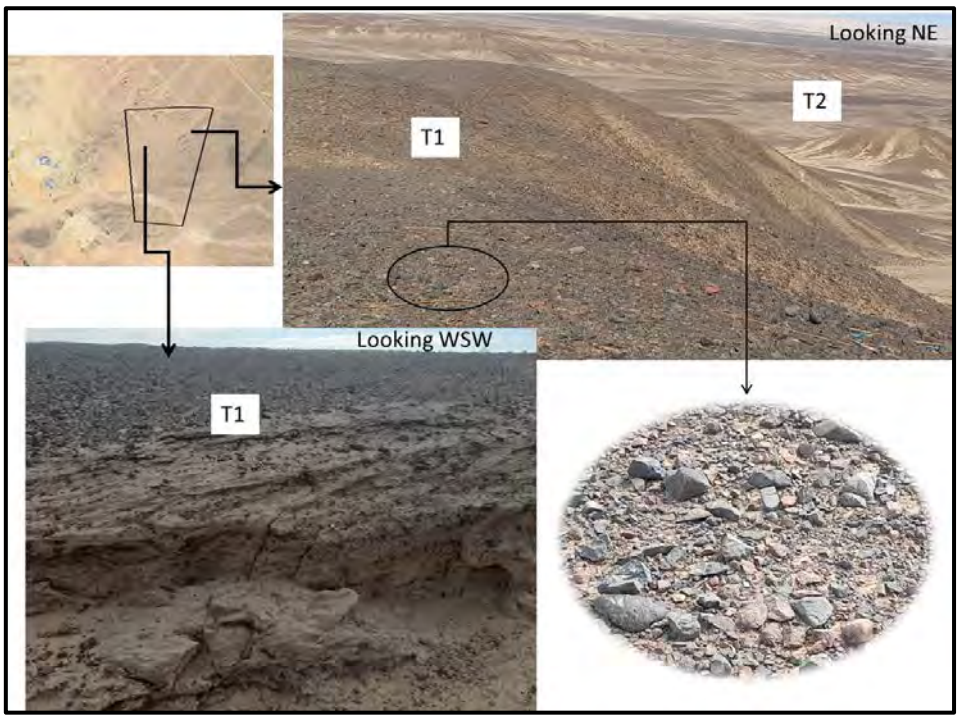

Figure 11: Field photographs of the terraces T1, T2

The thickness of the terrace or its height above the ground level (the level of the following terrace) varies from 1 m to about 2 m at the northwest while it varies from 1 m to about 3 m at the west and southwest. This terrace is composed of very coarse chert nodules, cobbles and boulders of granite, basalt, impeded in fine clay and sand (Figures 12, 13).

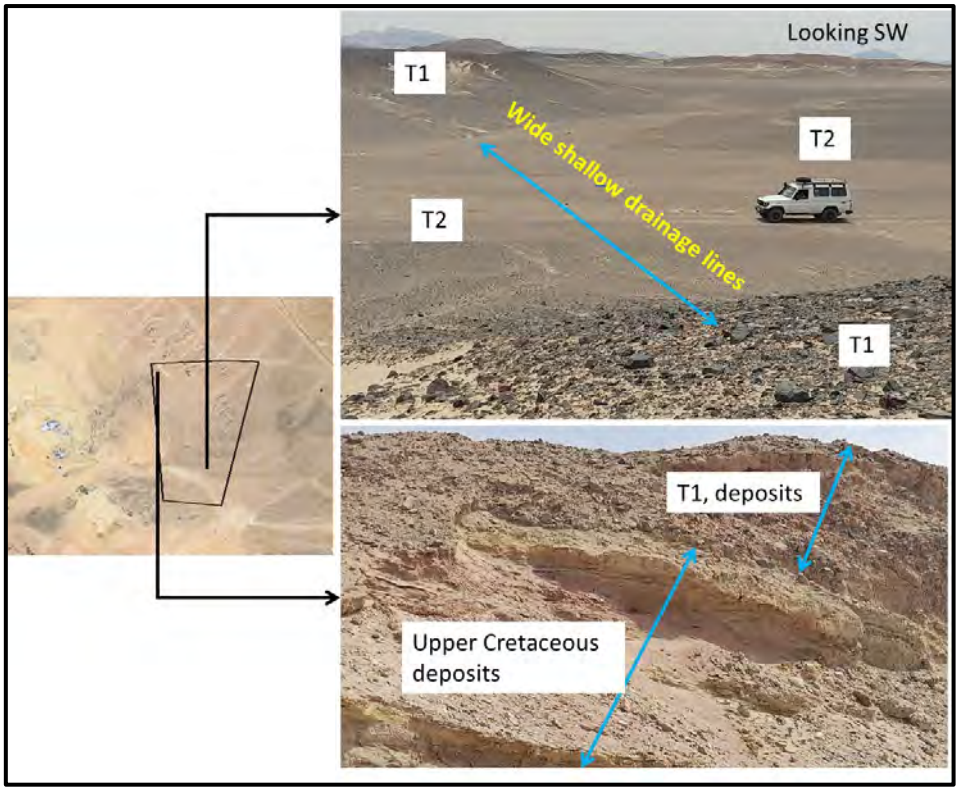

Figure 12: Field photographs of the terraces T1, T2

T2:

These terraces are exposed along the floor of the tributaries cutting through the terrace T1 (Figures 13, 14). The exposed thickness of the T2 (its elevation above the ground) varies from 0.5 m to about 1.5 m at the northwest while it varies from 0.5 m to about 2 at the southwest. This terrace is composed of medium sized chert nodules, fragments igneous rocks impeded in fine clay and sand. The fine clay and sand fraction is greater than that in the previous terrace (T1).

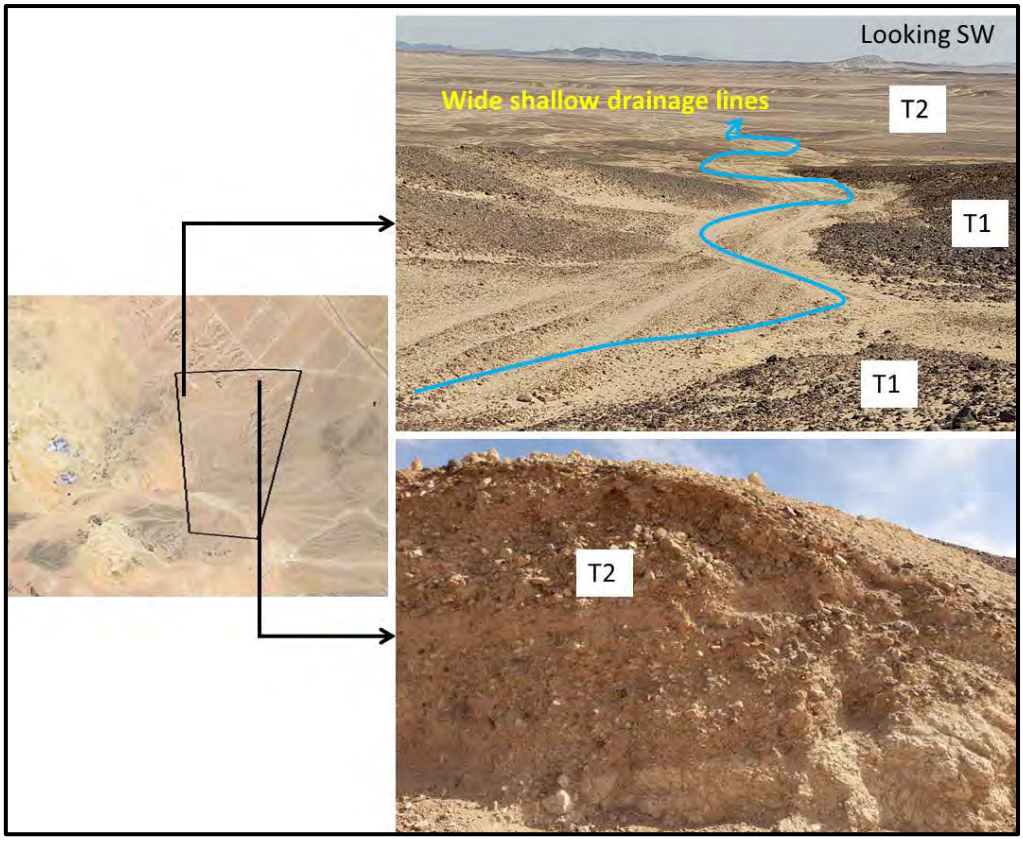

Figure 13: Filed photographs of the terraces T1, T2

T3:

These terraces are exposed along the floor of the tributaries cutting through the terrace T2 (Figures 14,15, 16). The exposed thickness of the terrace T3 varies from <0.5 m to about 1 m. at the northeast, while it varies from 0.5 m to about 1 at the middle and southeast. This terrace is composed of small nodules, fragments of igneous rocks impeded in fine clay and sand. The fine clay and sand fraction is greater than that in the previous terrace T2.

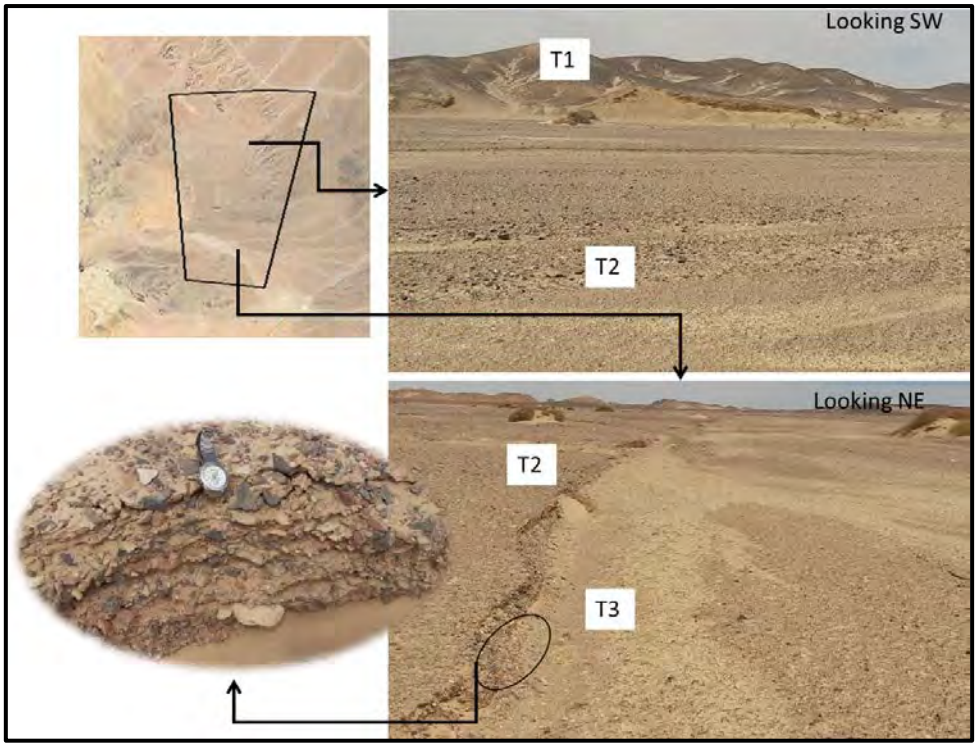

Figure 14: Field photograph of the T and T3 distribution in the project site

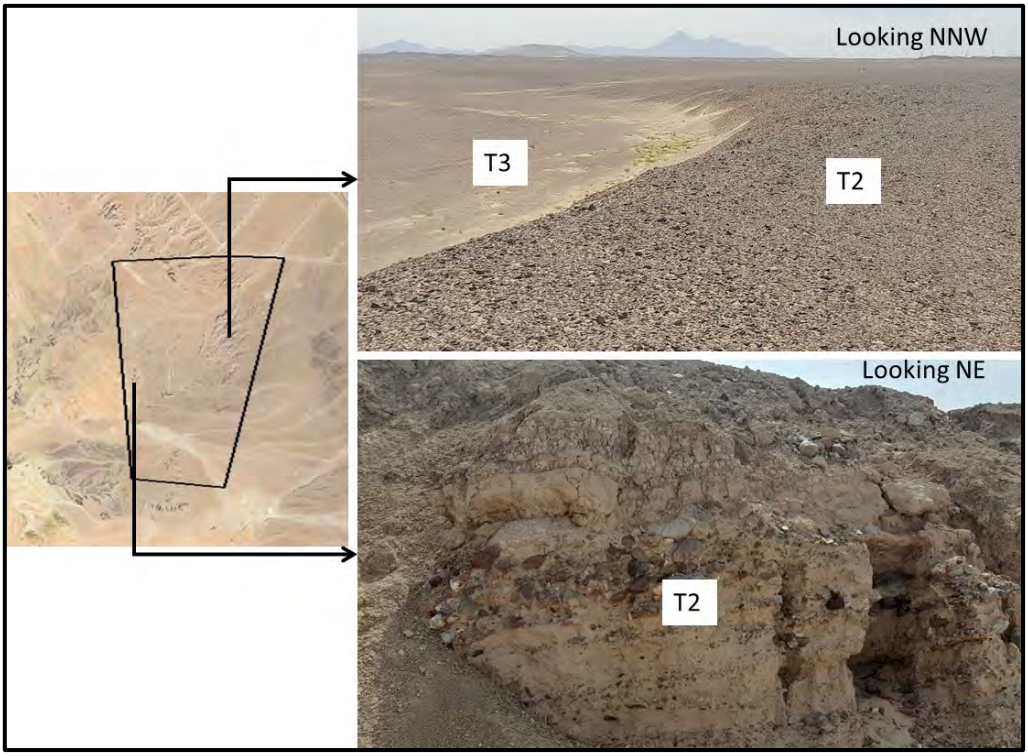

Figure 15: Field photograph of the T and T3 distribution in the project site

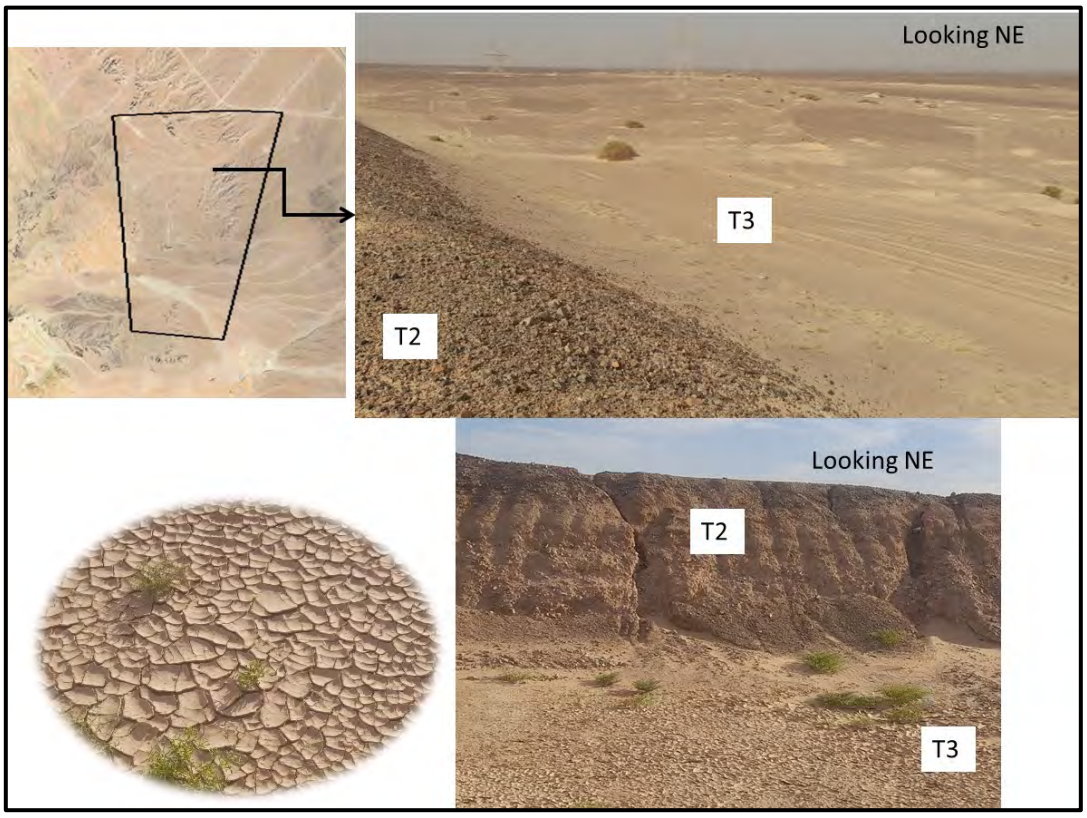

Figure 16: Field photograph of the T and T3 distribution in the project site. Note the mud cracks on the surface of the T3 terraces related to the last rainfall events. This means that the surface flow is very week.

7. Flood Risk Assessment

Flood risk can be analyzed through the lenses of the main terms of the risk equation: hazard, vulnerability, exposure, and capacity. In comparison to other types of risk, flood risk assessment suffers from a very strong imbalance in the level of maturity in assessing the different elements: whereas hazard modelling is well advanced, exposure characterization and vulnerability analysis are underdeveloped (UNISDR 2017).

The flood hazard assessment needs to physically and statistically model the initiation event (i.e. the trigger, which is usually rainfall) and after that to model the run-off/evolution of that event. In the case of flash flooding hazard, the run-off is modelled using a hydrological model to properly assess the routing of precipitation from rainfall to runoff and a hydraulic model to evaluate in detail the spatial extensions of floodable areas. In this context complete analyses of rainfall either from satellite climate data or actual records of rainfall, statistical analyses of the morphometric parameters of the drainage basins, and hydrologic and hydrogeologic analyses of the site will be conducted in the following sections. After the hazard assessment is completed, the flood risk is quantitatively assessed. The potential adverse consequences and impacts associated with the flash flood will be qualitatively and qualitatively considered.

The flood risk receptors are also considered based on the different land uses either in the project site or in the surrounding areas with relevant governmental bodies and stakeholders.

Vulnerability and exposure assessment will be conducted. Vulnerability represents an important step in properly evaluating flood impact and all quantitative indicators that are the final product of probabilistic risk assessment. So far, in flood risk assessment, this is probably the weakest link. Vulnerability is affected by factors such as settlements conditions, infrastructure, policy and capacities of the authorities, social inequities and economic patterns. This will be considered based on the different land uses and important flood receptors either in the site or in the surrounding areas. Vulnerability assessment is closely related to the ability to properly characterize the exposed elements to floods. The important flood exposures and flood receptors exist in the site will be considered and the level of their flood vulnerability will be evaluated through the site visits.

Based on the historical record of flash flooding in the area, the flood risk assessment models, the level of flood vulnerability of the site and important flood exposures and receptors, the areas with a significant flood potential and susceptibility within the site will be determined and mapped.

Then the appropriate mitigation measures will be suggested based on the nature of the facilities applied.

Combination of the following approaches will be used as possible:

* Historic flood risk assessment: information on flash floods that have occurred in the past,

* Predictive analysis assessing the areas that could be prone to flooding, and

* Flood mitigations measures based on the flood risk assessment models, potential of receptors, applied measures in the nearby facilities.

7.1 Literature review and Flood historical record

A flash flood is defined as a rapidly developed flood in just a few minutes or hours of excessive rainfall without visible signs of rain, or an accident like a dam or levee break. A flash flood can be generated during or shortly following a rainfall storm, especially when high-intensity rain falls on steep slopes with shallow, impermeable soil, exposed rocks and poor or sparse vegetation cover (Lin, 1999).

In recent years, flash floods became more frequent, causing life losses and significant damages in Egypt. Destructive flash flood frequently occurred in Egypt between 1972 and 2016 as shown in Table 4.

Table 4: Historical records of flash floods along the coastal areas of the Red Sea

Date	Area	Recorded damages & References
Oct. 2016	**Ras Ghareb**	**Local Authorities**

Feb. 2015	**Sinai, Red Sea region**	**Road Damages**
May. 2014	**Zafarana, G. Zeit, Taba, Sohag, Aswan, Kom Ombo Safaga**	**Dam Failure at Sohag, Road Damaged**
2013	**South Sinai**	**Two Deaths, Road Damaged**
2012	**W. Dahab , Catherine area**	**Dam Failure, Destroyed Houses**
17-18 Jan. 2010	**Along the Red Sea**	**Water Resources Research Institute (WRRI)**
Oct. 2004	**W. Watier**	**Road Damaged**
May 1997	**Safaga and El Qusier**	**- Information and Decision Support -- - Center in Red Sea Governorate, 2009. --The National Authority for Remote Sensing and Space Sciences (NARSS) – Red Sea Governorate, 1997**
Nov. 1996	**Hurghada and Marsa Alam**	
Nov. 1994	**Dhab, Sohag, Qena, Safaga, El-Qusier**	
Aug. 1991	**Marsa Alam**	**- Reports of Red Sea Governorate, 1994.** **- Red Sea Environmental Profile, 2008**
20 Oct. 1990	**Wadi El Gemal between Marsa Alam and Shalateen**	
23 Oct. 1979	**Marsa Alam and El Quseir**	
Jan. 1988	**W. Sudr**	**5 Deaths**
Oct. 1987	**South Sinai**	**1 Death, Roads Damaged**
May., Oct. 1979	**Aswan, Kom Ombo, Idfu, Assiut, Marsa Alam, El-Qusier**	**23 Deaths. Demolished Houses**
Feb. 1975	**W. El-Arish**	**20 Deaths, Road Problems**
1972	**Giza**	**Houses, Roads and Farms Damaged**

The area of Wadi Dara did not receive any heavy rainfall during October 26–27, 2016 while Ras Ghareb city which is at 45 km north of the sites was severely damaged due to flash flooding. (Figure 17).

Figure 17: Damaged caused by flooding in Ras Ghareb, October 2016

The intensity and distribution of damage caused by flooding in the study area were controlled by geologic, geomorphologic characteristics prevailed throughout the area. Also, huge amounts of precipitation in short time with uncontrolled and unplanned development increase the impact of the flood. The results indicate the presence of two drainage basins threatening Ghareb area with high possibility of flooding. Accordingly, establishing flood channel around the city, about 38 km long, is vital to protect the city from flood hazards in the future.

Youssef and Hegab (2005) utilized GIS and statistical analysis to develop a database management system for assessing flood hazards in the Ras Ghareb area. Their study identified nine drainage basins, two of which—Wadi Abu Had and Wadi El Darb—pose a threat to areas located north of the project site (Figure 18). Using the hazard degree approach proposed by El Shamy (1992b) and GIS modeling, they created a flood hazard and vulnerability map for the region (Figure 19).

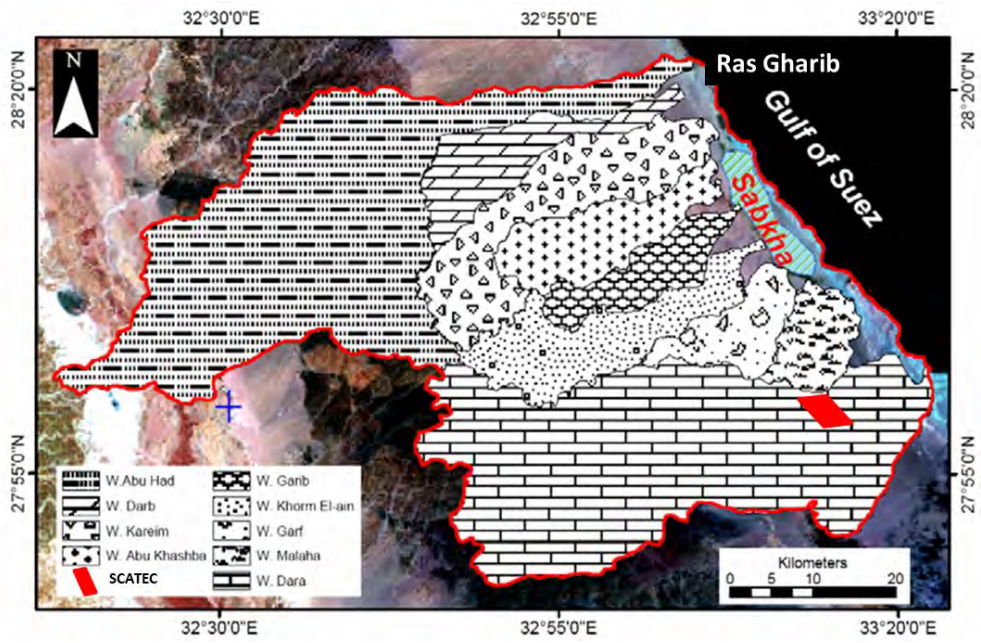

Figure 18: The drainage basins delineated in the area. Note that the project site lies within the basin of Wadi Dara. (Modified after Youssef and Hegab 2005).

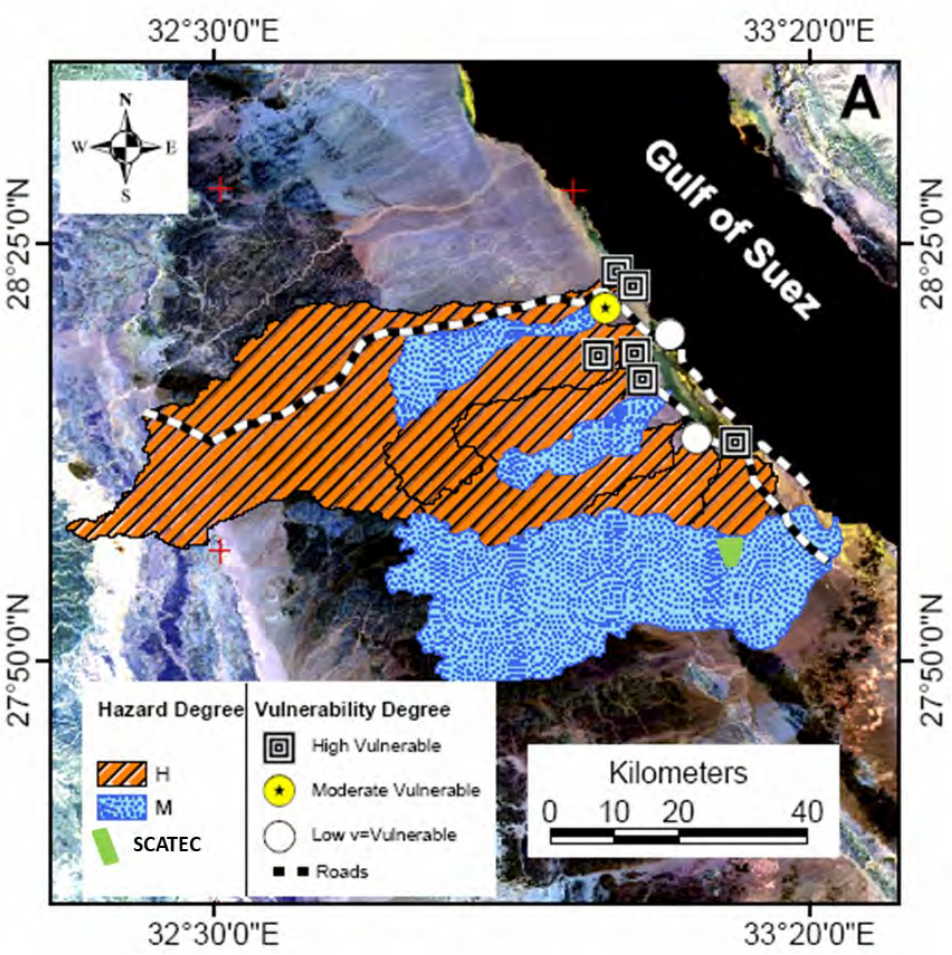

Figure 19: Drainage basins hazard and Vulnerability map of the area. The expected degree of flash flood hazard in the site is medium. After, (Youssef and Hegab 2005).

Elnazer et al. (2017) utilized GIS tools to study flash flood hazards impacting Ras Ghareb city. Their findings indicated that during periods of intense rainfall, Ras Ghareb faced significant flood risks from Wadi Abu Had and Wadi Al Darb, with the former affecting the city center and the latter impacting the southern part of the town (Figure 18). To mitigate flood impacts, they proposed constructing a 38 km-long channel directed north of the city (Figure 20). Additionally, Wadi Malaha and Wadi Garf were identified as having high flash flood hazards but low vulnerability, likely due to their small watersheds and drainage into a salt marsh (sabkha) with no residential activities. In contrast, Wadi Dara exhibited a medium flash flood hazard level but without associated vulnerability (Figure 20).

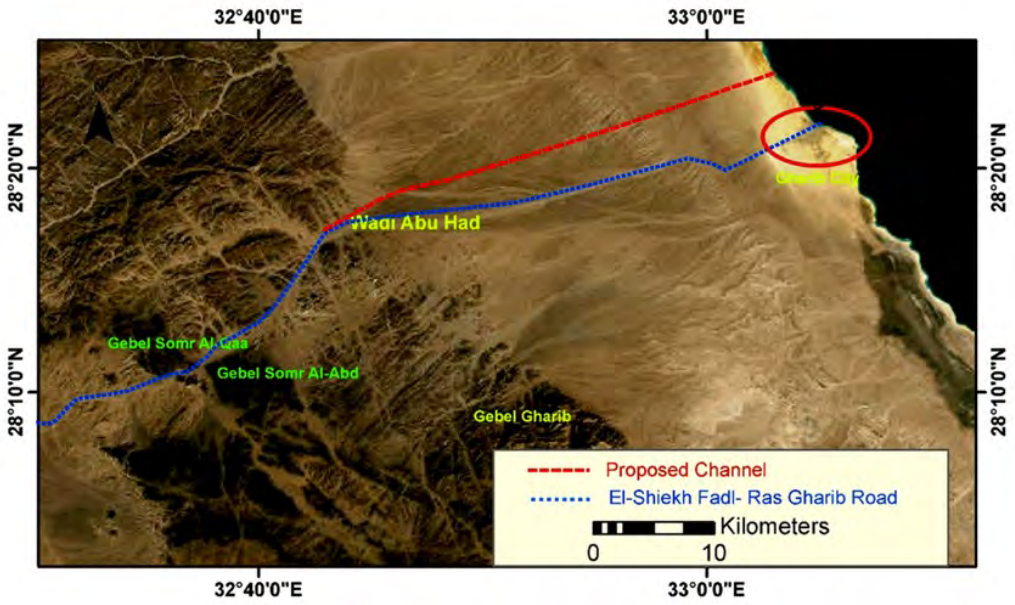

Figure 20: Proposed flash flood channel location in the study area. (After Alnazer et al., 2017)

7.2 Surface Water Conditions

The project site and its surroundings lack permanent fresh surface water bodies or streams. However, the area is traversed by shallow, dry drainage lines that channel occasional precipitation from the Red Sea Mountains toward the Gulf of Suez. These flash floods can be severe, potentially causing significant loss of life and property. The Red Sea region experiences seasonal flash floods characterized by high velocity, short duration, and sharp discharge peaks. Historical records highlight several significant flash flood events that have impacted the coastal areas along the Red Sea, as detailed in Table 7.

Yousif et al. (2024) analysed the soil characteristics and land use in the Wadi Dara area to estimate surface runoff volume within the basin. Their findings indicate that the average maximum annual precipitation of 73 mm/year over a total basin area of 1,175 km² (six basins) results in a total annual precipitation of 85 × 10^6 m³, of which 34 × 10^6 m³ contributes to surface runoff. Additionally, runoff estimation based on a single-day precipitation event proved significant. For instance, a storm delivering 27 mm/day (the maximum recorded daily rainfall) results in a total precipitation volume of 31 × 10^6 m³/day, generating 3.5 × 10^6 m³/day of surface runoff.

This indicates that approximately 40% of the annual precipitation contributes to surface runoff, while the remaining 60% is lost to infiltration and evaporation. Moreover, only about 11% of the total surface runoff is generated by a single storm event. These results highlight the high absorption capacity of soil in Wadi Dara, which effectively reduces the intensity of surface runoff.

7.3 Field Work

Prior to the site visit, an investigation was conducted using topographic maps, Landsat images, and digital elevation models (DEMs) generated from SRTM data. The topographic map of Egypt at a scale of 1:250,000 (sheets NH36-14 and NH36-15) reveals that the project site and its

surrounding areas are characterized by simple topography, with a gentle and consistent slope toward the Gulf of Suez (Figure 21). The site lies within a broad plain intersected by shallow, wide drainage lines (Figure 21).

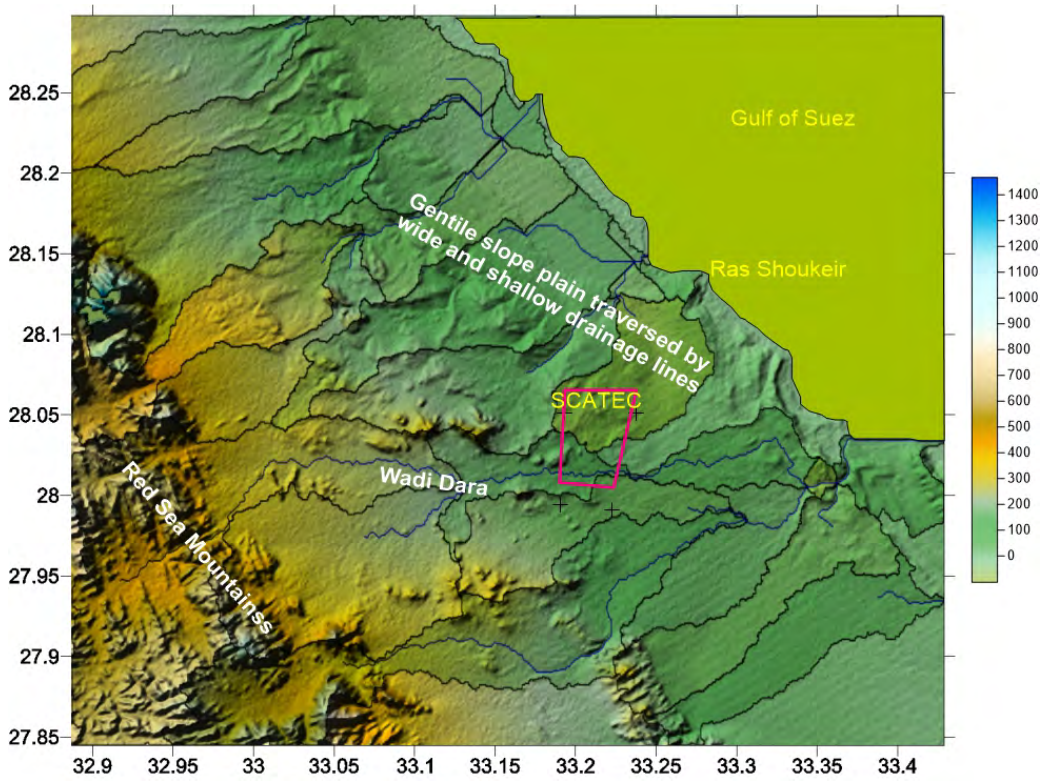

Figure 21: The drainage basins crossing the area around the project site. Note the project site lies at the downstream part of the watershed area of Wadi Dara. The constructed map is based on the DEM of the area using ARC-GIS software.

Wadi Dara is one of the dry wadis in the area, running east-west in the southern part of the project site (Figure 22), and is not prone to hazardous flash floods. To analyze the ground surface relief and slope of the project site, three topographic profiles were generated using the DEM model (Figure 23).

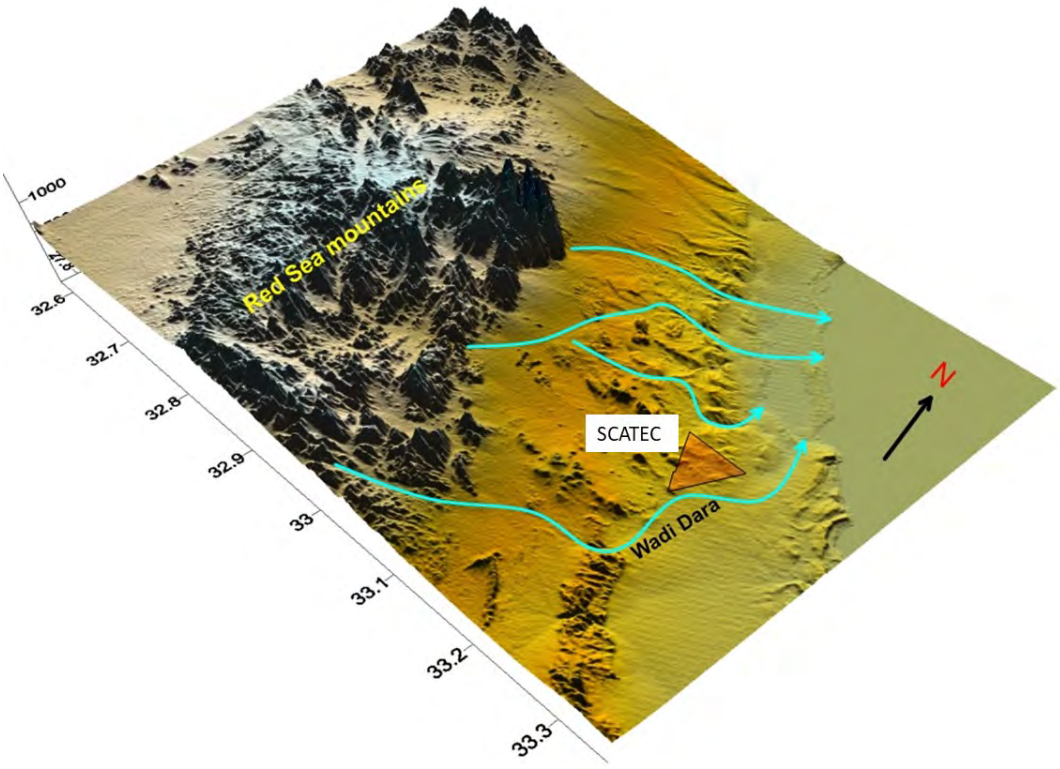

Figure 22: Figure 45: The 3D model of the area constructed from the SRTM maps using one of the professional GIS software showing course of W. Dara to the south of the site.

Two topographic profiles, P1 and P2, run east-west, aligning with the direction of the drainage lines across the site. Another profile, P3, intersects the drainage lines in a northwest-southeast direction through the central part of the site (Figure 23). The average ground surface elevation within the project site and its immediate surroundings ranges from 60 to 160 meters above mean sea level (amsl) (Figure 23).

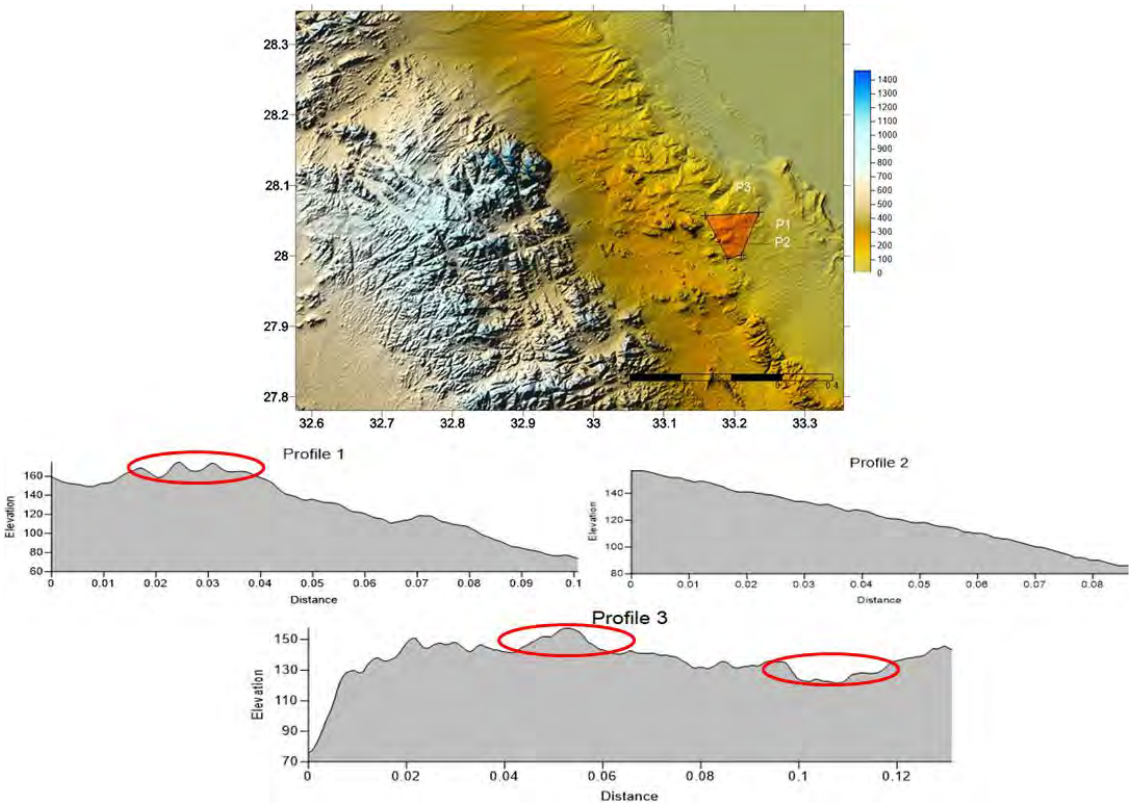

Figure 23: Three topographic profiles constructed along the project site.

The topographic profiles (P1 and P2) illustrate the low-relief ground surface of the project site, except for the western part, and show a gentle dip toward the east, parallel to the drainage lines, with a slope gradient of approximately 0.01. Perpendicular to the drainage lines, the ground surface exhibits a very gentle dip toward the south and southeast, with a slope gradient of about 0.002. Profile P3 highlights the shallow and wide configuration of the drainage lines, indicating the presence of shallow dissected hills traversing the project site, separated by broad, shallow drainage channels (Figure 24).

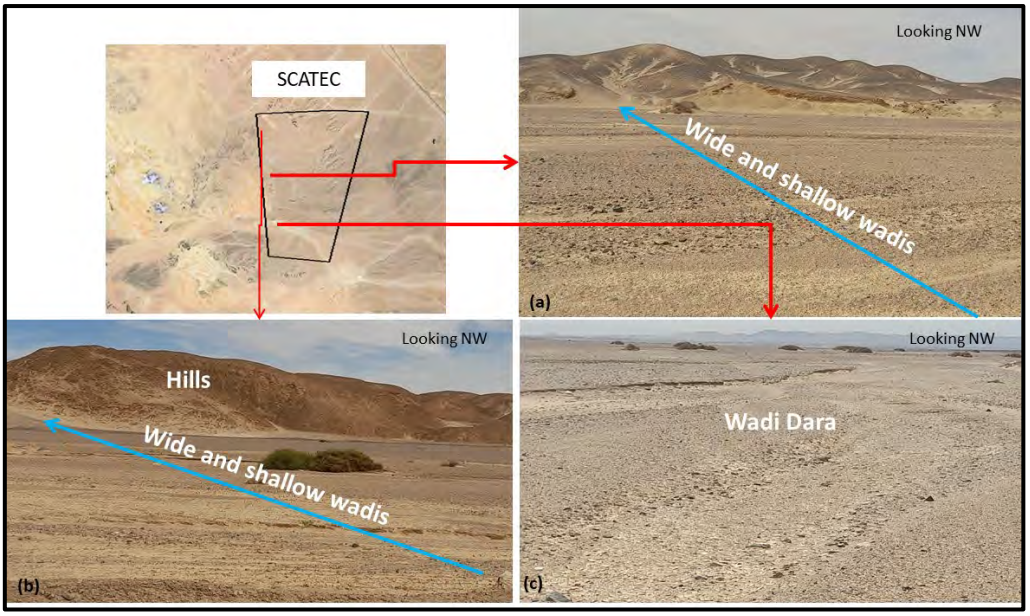

Figure 24: Shallow dissected hills separated by wide shallow drainage lines concentrated in the project site.

Regarding the potential for hazardous flash flooding in the project area, the site visit focused on identifying any actual evidence confirming the occurrence of flash floods specifically within the project area. The most common features observed on-site are summarized as follows:

1. The entire project area is wide and nearly flat, featuring numerous straight, shallow, and short tributaries. The simple relief and gently dipping ground surface indicate the weak intensity of runoff, which does not lead to the formation of deep channels.
2. The main trunk streams are shallow and wide, covered with fine sand and coarse-sized gravels, including chert and rock fragments. This reflects the weak flow intensity, insufficient to carry larger boulder-sized fragments.
3. Variable altitude hills, dissected by water tributaries, are exposed in the western and southwestern parts of the site.
4. Towards the eastern and southeastern parts of the site, shallow, very wide drainage lines have been exposed, with multi-sized grain deposits. The low sinuosity of these drainage lines further indicates the weakness of the surface flow.
5. The small tributaries are shallow, straight, and lack wide alluvial fans, reflecting the small volume of water carried and slow surface water flow.
6. A thick soil layer with high porosity and permeability, composed of multi-sized chert and rock fragments embedded in sand, covers the entire area. This results in a significant amount of rainfall infiltrating the surface, which reduces surface runoff.
7. The main course of Wadi Dara runs through the southern part of the site.

Based on the field study and the photographs presented above, it can be concluded that Wadi Dara basin is considered a medium-hazard basin in terms of flash flood events. Given the potential impacts of global warming and the anticipated changes in rainfall intensity over the area, it is recommended to develop flash flood models for the entire Dara basin. These models should incorporate various design densities and return periods to assess the severity of flash flood risks in the event of significantly heavier rainfall than currently experienced.

7.4 Source – Pathway – Receptors (SPR) of Flash Floods

The SPR provides a system model for the assessment of flash flood systems regarding individual components and their inter-relationships. It is used to describe the propagation of a flash flood from a source (Upstream) through pathways (drainage lines) to receptors in the drainage basin outlets (downstream).

The source of the flash flood along the whole Red Sea and Gulf of Suez coastal area is from the high elevated Red Sea Mountains at the west. In high intensity rainfall events, the surface flow following the regional topographic slope toward the east. At the upstream parts of the drainage basins, surface water is concentrated in many fine tributaries linked together forming larger drainage lines leading to a mainstream at the downstream parts. As a result, the source of flash flood is the elevated land, and the pathways are the mainstreams of the drainage basins. From the land uses either within the project site or in its close vicinity as indicated in the baseline part, flash flood receptors in the area are very limited and they are mainly engineering facilities (main roads with their services like check points, Ambulances and fuel stations, power lines, communication and weather towers, and substations. Households and farming activities in Wadi Dara, army units, crude oil and gas facilities. The only large, populated areas close to the site are Ras Gharib and Ras Shukeir cities. Many flood mitigation measures have been applied after the torrential storm that occurred in the area in 2016 such as culverts to protect the roads, surface flow storage and redirected dams, stone bricks and concrete fences around the base of the engineering structures. The mitigation measures applied in the areas very close to the site will be mentioned later in this report.

7.5Rain Fall in the Project Area

Rain is a key factor influencing runoff in the drainage basins along the Gulf of Suez coast. The speed and volume of runoff can determine the severity of flooding, which may impact both current and future development areas. Although the region has limited water resources, it is important to consider the potential benefits of flooding and reduce its negative impacts. For example, measures could be proposed to mitigate flood risks and capture rainwater in various areas for use in development projects.

Generally, rainfall in the study area is scarce, yet when it occurs, it can lead to flash floods in some basins. These flash floods vary in strength, volume, and speed depending on the amount of rain, which is often irregular and characterized by temporal and spatial variability. Annual rainfall amounts fluctuate significantly from year to year and across different locations within the study area. This variation in both quantity and timing are distinctive feature of desert rainfall, contributing to the occurrence of flooding.

7.4.1 Precipitation Measurements from Satellite Images

Satellite imagery is an important tool for studying weather and climate patterns, enabling continuous monitoring through remote sensing systems like NOAA satellites. These satellites images support mathematical models that analyze atmospheric pressure, temperature, and the thickness and density of atmospheric layers. By tracking cloud movement and using high-powered telescopes in visible and thermal ranges, satellites can calculate wind patterns and record

temperature gradients. Analyzing cloud layers provides comparative data, offering valuable insights into weather and climate conditions.

The study utilized data from the PERSIANN (Precipitation Estimation from Remotely Sensed Information using Artificial Neural Network) project, developed by the Center for Meteorology, Hydrology, and Remote Sensing at the University of California. This project extracts rainfall data from satellite images using Neural Network Models. The PERSIANN-CCS (Precipitation Estimation from Remotely Sensed Information using Artificial Neural Network – Cloud Classification System) data provides high-resolution spatial information with a cell size of 4 km x 4 km. The study covers the period from 2015 to 2024, during which the digital files were analyzed and modeled to assess the spatial and temporal changes in rainfall patterns over the study period. The following presents the results of the spatio-temporal analysis of these data sets:

7.4.1.1 Average Annual Precipitation in the Study Area

Table 5 presents the estimated annual averages of precipitation for the area, with the average annual precipitation calculated to be approximately 1.1 mm per year. Based on this, the drainage basin of Wadi Dara is expected to carry around 1.3 million m³ of rainwater annually at a minimum. This volume can vary over the years with higher precipitation rates, as well as during months with more intense rainstorms. Figures 25 and 26 illustrate the expected annual variation in potential precipitation across the study area, highlighting that 2018 recorded the highest amount of rainfall, with an average of approximately 1.6 mm.

Table 5: The annual change in rain expected to fall on the studied area basin during the period (2015-2021).

Year		2015	2016	2017	2018	2019	2020	2021	2022	2023	2024	AVE
Yearly	Year Avg.	1.3	1.3	1.5	1.6	1.4	0.5	0.7	0.8	0.9	0.5	1.1
	Total Rain	16	16.1	17.9	19.3	16.9	6.4	8.8	9.7	10.2	4.9	12.6
	Change (%)	-	0.00	15.38	6.67	-12.5	-64.3	40	14.3	12.5	-44.4	-6.15
Seasonally	Winter	1.53	1.07	1.27	3.9	3.73	0.5	1.13	1.5	0.37	1	1.6
	Spring	1.16	3.17	2.1	1.43	1.4	0.77	0.77	0.93	0.73	0.73	1.32
	Summer	0.27	0.07	0	0	0.4	0	0	0.17	1.37	0.27	0.26
	Autumn	2.47	1.37	0.47	2.9	0.3	0.6	0.73	1.03	0.87	0	1.07

Source: the analyses of the PERSIANN-CCS data during the period 2015-2024

Rainfall intensity leads to a total water volume of approximately 1.8 million m³ being received by Wadi Dara basin. The data from the attached table shows that the amounts of rainfall expected to fall on the basin vary throughout the study period (2015-2024).

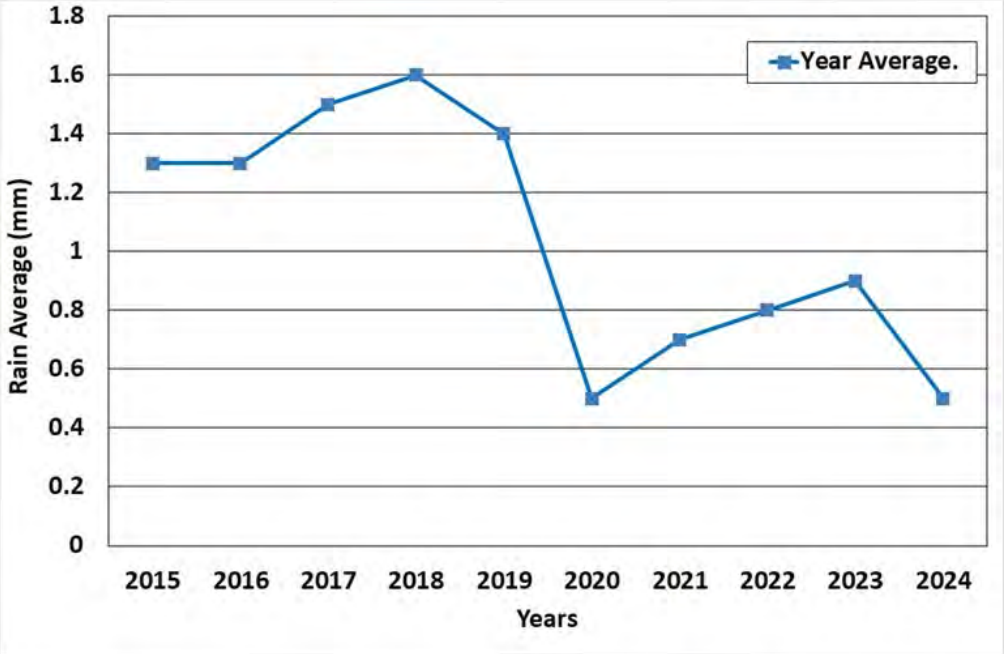

Figure 25:The annual averages rain expected to fall on the studied basin during the period (2015-2021)

The general trend for rainwater distribution increased from 2015 to 2018, due to the occurrence of several significant rainstorms. Notable flash floods during this period included the rainstorm on October 26-27, 2016, which triggered strong surface runoff across many regions of Egypt, causing widespread damage and resulting in 26 deaths and 72 injuries, primarily in the Red Sea, South Sinai, and Sohag governorates. Another major rainstorm occurred on April 25-26, 2018, which led to the closure of key roads, including the Katameya-Ain Sokhna, Ain Sokhna-Zaafarana, and Al-Karimat-Zaafarana routes, due to heavy flash flooding. Other significant rainstorms included those on January 25, 2016, which caused destructive flash floods, and December 24, 2016. The year 2018 was particularly impactful, with several intense rain events, such as the rainstorm on January 24, 2018, which resulted in road closures due to large torrents, and the December 26, 2018 rainstorm.

A decrease in rainfall from 2018 to 2020, despite several intense rainstorms, including the notable Dragon Storm (March 11-13, 2020), which caused severe flooding in northern Egypt can be observed. Additionally, rainstorms on November 7 and 20, 2020, contributed to this period of reduced precipitation. The average rainfall for 2020 was 0.5 mm. However, rainfall gradually increased in subsequent years, reaching 0.7 mm in 2021, 0.8 mm in 2022, and 0.9 mm in 2023. For 2024, the overall average potential precipitation is estimated to be around 0.5 mm for the first two-thirds of the year, with expectations of an increase, as the full data is not yet available. Significant rainstorms in 2024, including those on February 1 and March 8, are expected to further elevate the amount of rainfall for the year.

Overall, the percentage change in the average expected precipitation in the study area is -6.15%, reflecting a decrease in the frequency and intensity of strong rainstorms. This decline is attributed

to notable changes in the number and strength of rainstorms, which tend to increase significantly during the winter and spring seasons each year.

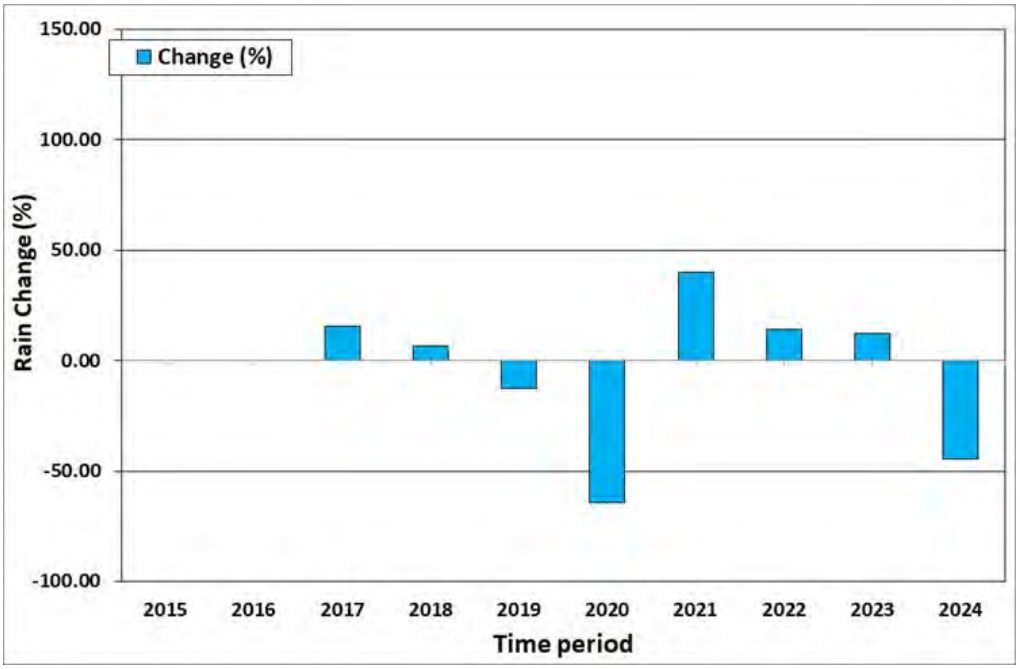

Figure 26: The annual change in the rainfall quantity expected to fall on the watersheds of the studied basin.

The figure below illustrates the spatial variations in rainfall across the Wadi Dara region, highlighting a concentration of significant rainfall in the northern and eastern parts of the study area. These regions represent the key catchments for the rainstorms that pass through the area.

From the study of the amounts of rain expected to fall in the region according to climate satellite data, the following can be concluded:

1. The expected change in the rate of rainfall over the region during the ten years (2015-2024) is -6.15.1%. This means that according to the prevailing climatic changes, the accumulation of clouds causes rain decrease over the study area (Table 5).
2. The heavy accumulations of clouds that cause rain are concentrated in the eastern parts of the study area. This may be because of winds on these dense clouds and moving them to the east.
3. The occurrence of torrential rains at the exits of the Wadies is largely related to the amounts of accumulated clouds and the rain that falls on the Eastern parts of the area.

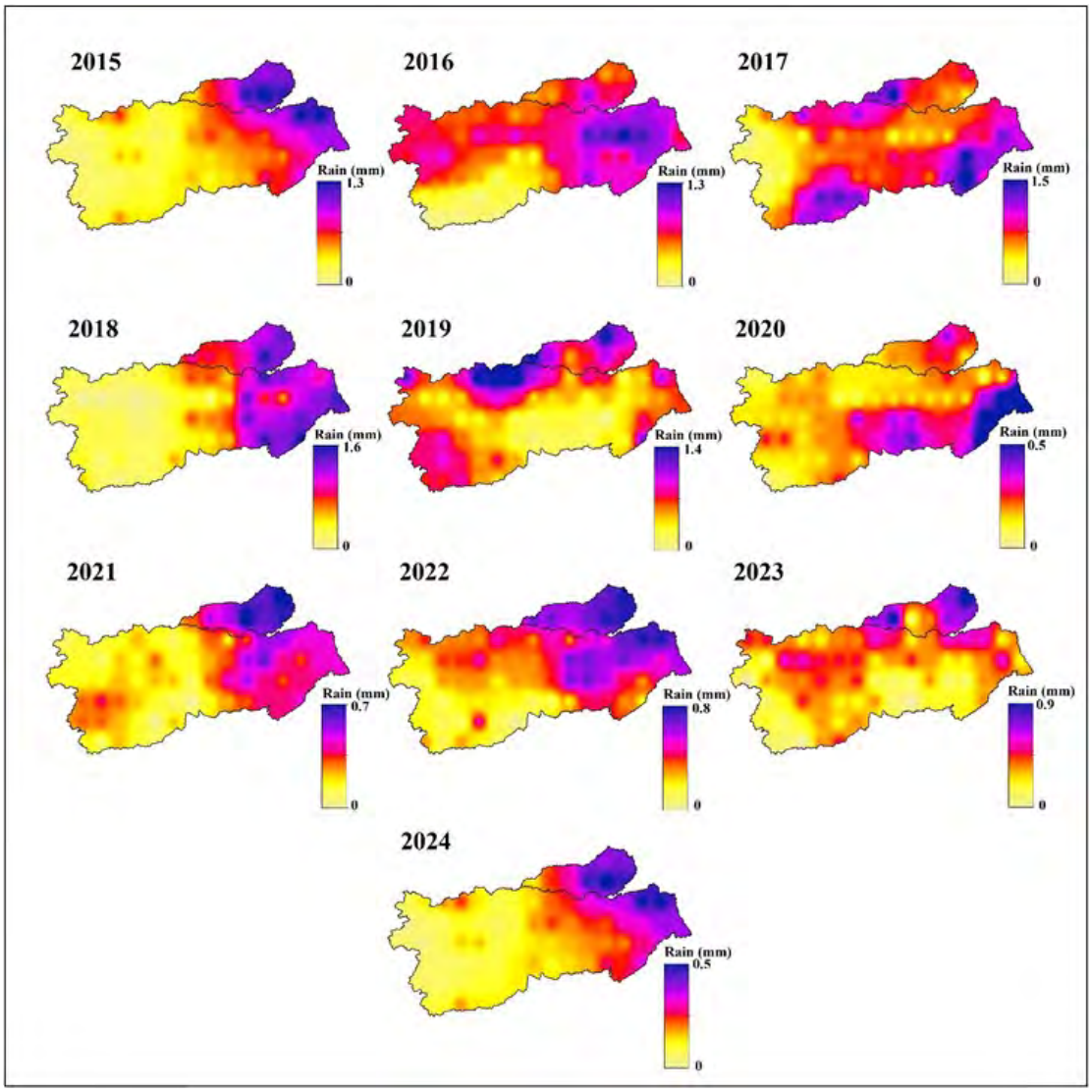

Figure 27: Spatial and temporal changes in the amount of rain expected to fall on Wadi Dara basin during the period (2015-2021)

4. Rainfall in the middle part of Wadi Dara, even if it is heavy, does not cause torrential flood, which may threaten the facilities on the site. This is because most of the surface runoff the tributaries that cross the site are mainly due to direct rainfall on the site
5. With this negative trend in decreasing the amounts of clouds accumulating in the middle and eastern parts of the region because of climate changes, the volume of surface runoff may decrease, which requires simple applications to protect any facility that may be in mainstreams of the drainage lines.

7.4.1.2 Average Expected Monthly Precipitation in the Study Area

Table 6 and Figure 28 present the probable monthly averages of rainfall in the study area for the period from 2015 to 2024. February and March stand out as the months with the highest expected rainfall, with an average of approximately 1.8 mm. These months mark the transition from winter to spring, coinciding with the peak occurrence of air depressions over the eastern region of Egypt. These atmospheric changes, including shifts in pressure and wind patterns, lead to instability in weather conditions, thereby contributing to the increased rainfall during this period.

In March, the highest average monthly rainfall was recorded in 2016, with an expected rainfall of 7.4 mm. Additionally, March recorded 1.9 mm of expected rainfall in 2018. As for February, it experienced the highest expected rainfall in 2018, at 5.3 mm, followed closely by 2019 with 5.2 mm, and then 2015, with 2.1 mm.

October and November are the second highest months for expected precipitation in the region, marking the beginning of Autumn, which is the primary rainfall season. During this period, temperatures start to drop, and the frequency of atmospheric depressions passing over the northern coasts increases, leading to higher chances of rainfall. In October, the highest recorded monthly average rainfall occurred in 2015, with 6.2 mm, while 2016 and 2018 saw 2.8 mm and 2.5 mm, respectively. Other years generally recorded lower rainfall values. November saw the highest expected rainfall in 2018, with 5.2 mm, and 2.2 mm in 2020.

Table 6: Probable monthly averages of rainfall in the area during the period (2015-2021).

Months	Jan.	Feb.	Mar	Apr	May	Jun	Jul	Aug	Sep	Oct	Nov	Dec	Ave	Total
Average	1.5	1.8	1.8	1.4	0.8	0.7	0.0	0.1	0.1	1.7	1.7	1.6	1.1	13.2

Source: the analysis of the PERSIANN-CCS data during the period 2015-20254

December ranks third in terms of expected average precipitation, with an average of about 1.6 mm, peaking at 6.4 mm in 2017 and 2.1 mm in 2021. January follows with an average precipitation of 1.5 mm, reaching 5.0 mm in 2019 and 2.9 mm in 2017. The summer months—July, August, and September—record the lowest precipitation rates. Figure (28) illustrates the variations in monthly precipitation amounts in the Wadi Dara region from 2015 to 2024, showing increased precipitation during the winter, spring, and autumn months, and a decrease during the summer months.

Figure 28: The monthly change in the amount of precipitation expected area during the period (2015-2021)

7.4.1.3 Average Seasonal Precipitation in the Study Area

Table 7 and Figure 29 exhibit the possible seasonal averages of rainfall in the studied basin during the period (2015-2024). Winter is the highest season of the year in terms of the amount of rain expected to fall with an average of about 1.6 mm during the study period. This quantity increased to reach 3.9 mm in the winter of 2018 and 3.73 mm in 2019 which is linked to the occurrence of several rainstorms and the prevalence of many weather fluctuations in these years. It reached 1.5 mm in the winter of 2015 and 2022.

Table 7: Expected seasonal averages of rainfall on area during the period (2015-2021)

Months	2015	2016	2017	2018	2019	2020	2021	2022	2023	2024	AVE
Winter	1.53	1.07	1.27	3.9	3.73	0.5	1.13	1.5	0.37	1	1.6
Spring	1.16	3.17	2.1	1.43	1.4	0.77	0.77	0.93	0.73	0.73	1.32
Summer	0.27	0.07	0	0	0.4	0	0	0.17	1.37	0.27	0.26
Autumn	2.47	1.37	0.47	2.9	0.3	0.6	0.73	1.03	0.87	0	1.07

Source: the analysis of the PERSIANN-CCS data during the period 2015-2021

The spring season ranks second in terms of rainfall, with an average of 1.32 mm during the study period. This can be attributed to weather disturbances, including the passage of depressions over northern Egypt, which triggered the Khamaseen monsoon and increased rainfall. Autumn recorded its highest rainfall in 2018, with 2.9 mm, followed by 2015 at 2.47 mm and 2016 at 1.37 mm. However, in 2019, the autumn rainfall dropped to its lowest value of about 0.3 mm.

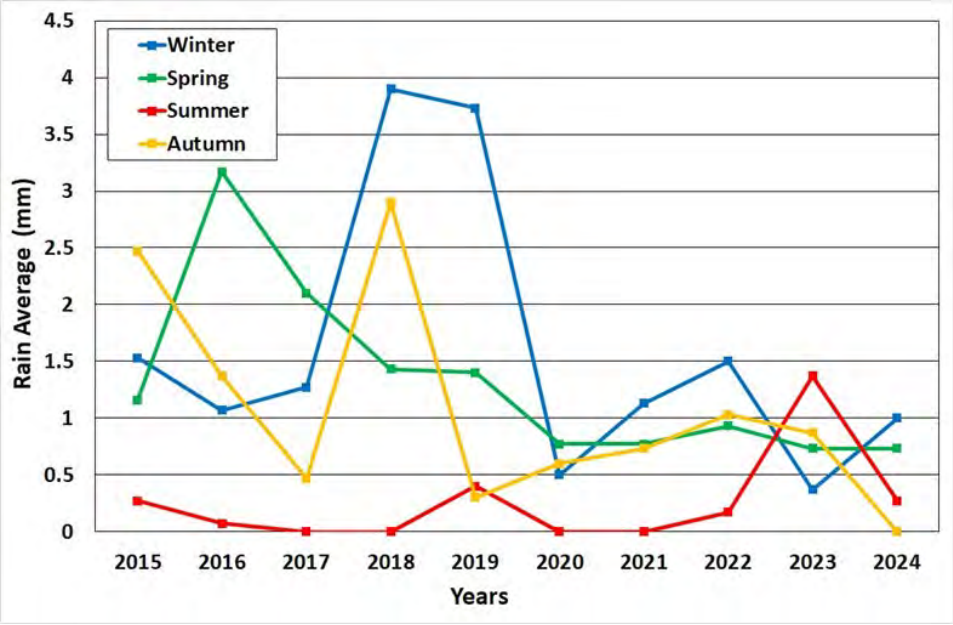

Figure 29: The expected seasonal average precipitation on study area during the period (2015-2021)

Summer is the driest season of the year, with an average rainfall of about 0.26 mm during the study period. This is due to the area's very hot, dry, and humid summer conditions, which limit the occurrence of rainfall.

7.4.1.4 Monthly Average of the Largest Amounts of Precipitation during the Study Period

Table 8 presents the expected monthly average precipitation with the highest quantities during the study period 2015-2024. November emerged as the month with the highest expected precipitation, with an average of 16 mm in 2018. The maximum recorded rainfall occurred in April 2019 with 98 mm, followed by May 2018 with 89 mm, and December 2021 with 83 mm.

The data indicates that the highest monthly averages of rainfall are observed during the winter months, gradually decreasing through autumn and spring, with minimal rainfall during the summer months. The average rainfall recorded in November, January, February, and March was approximately 5.2 mm, 4.7 mm, 4.1 mm, and 4.5 mm, respectively. Winter is the season with the highest expected rainfall, averaging about 4.17 mm across December, January, and February, compared to 3.03 mm in autumn, 2.97 mm in spring, and 0.53 mm in summer.

Table 8: Average precipitation of the largest amount of rain expected per month during the period (2015-2024)

Month	Jan	Feb	Mar	Apr	May	Jun	Jul	Aug	Sep	Oct	Nov	Dec	AVE
2015	4.0	5.0	9.0	1.0	2.0	1.0	0	0	0	13.0	4.0	1.0	3.3
2016	3	3	15	2	2	1	0	0	0	7	4	0	3.1
2017	10	1	2	8	4	0	0	0	0	0	4	14	3.6
2018	0	13	6	2	3	0	0	0	2	5	16	2	4.1
2019	18	13	3	5	1	2	0	0	0	0	1	1	3.7
2020	2	0	4	1	0	0	0	0	0	2	6	5	1.7
2021	3	1	1	1	3	0	0	0	0	2	3	7	1.8
2022	4	3	3	1	1	1	0	0	0	1	4	1	1.6
2023	1	0	0	2	2	6	3	0	1	2	5	2	2.0
2024	2	2	2	2	1	1	0	1	0	-	-	-	1.2
M AVE	4.7	4.1	4.5	2.5	1.9	1.2	0.3	0.1	0.3	3.6	5.2	3.7	2.7

Source: the analyses of the PERSIANN-CCS data during the period 2015-2021

7.4.1.5 Annual Analysis of the Calculated Average Amounts of Rain Expected to Fall during the Study Period

From the analysis of the PERSIANN-CCS satellite data during the period 2015-2024, the calculated annual average precipitation expected in the area (Table 9 and Figures 30-409) revealed the following:

2015: The expected annual average precipitation for 2015 was approximately 1.3 mm. This average increased to 6.2 mm in October, while it decreased to zero in July, August, and September. The

Autumn season recorded the highest expected precipitation for the year, with an average of about 2.47 mm, followed by the **Winter season** at 0.53 mm (Table 9 and Figure 30).

Table 9: The calculated annual and monthly average precipitation in the study area during the period (2015-2021)

Months	2015	2016	2017	2018	2019	2020	2021	2022	2023	2024	AVE
Jan.	1.3	1.1	2.9	0	5	1.1	1.3	1.2	0.2	0.9	1.5
Feb.	2.1	1.2	0.9	5.3	5.2	0	0.9	1.2	0	1	1.8
Mar.	1.7	7.4	1.1	1.9	1.4	1.4	0.5	1.2	0	1.1	1.8
Apr.	0.8	1	4.3	1.1	1.9	0.9	0.9	0.9	1.1	1	1.4
May	1	1.1	0.9	1.3	0.9	0	0.9	0.7	1.1	0.1	0.8
Jun	0.8	0.2	0	0	1.2	0	0	0.5	3.7	0	0.7
Jul.	0	0	0	0	0	0	0	0	0.4	0.7	0
Aug.	0	0	0	0	0	0	0	0	0	0	0.1
Sep.	0	0	0	1	0	0	0	0	0.2	-	0.1
Oct.	6.2	2.8	0	2.5	0	0.9	1.1	0.9	1.1	-	1.7
Nov.	1.2	1.3	1.4	5.2	0.9	0.9	1.1	2.2	1.3	-	1.7
Dec.	0.9	0	6.4	1	0.4	1.2	2.1	0.9	1.1	-	1.6
Ave.	1.3	1.3	1.5	1.6	1.4	0.5	0.7	0.8	0.9	0.5	1.1

Source: the analyses of the PERSIANN-CCS data during the period 2015-2021

2016: The expected annual average amount of precipitation in this year was about 1.3 mm, increased to reach 7.4 mm in March, 2.8 mm in October, and 1.3 in November. Spring is the highest season of the year in terms of the expected precipitation rate, which reached 3.17 mm, followed by autumn with about 1.37 mm, then winter with about 1.07 mm (Table 9 and Figure 31).

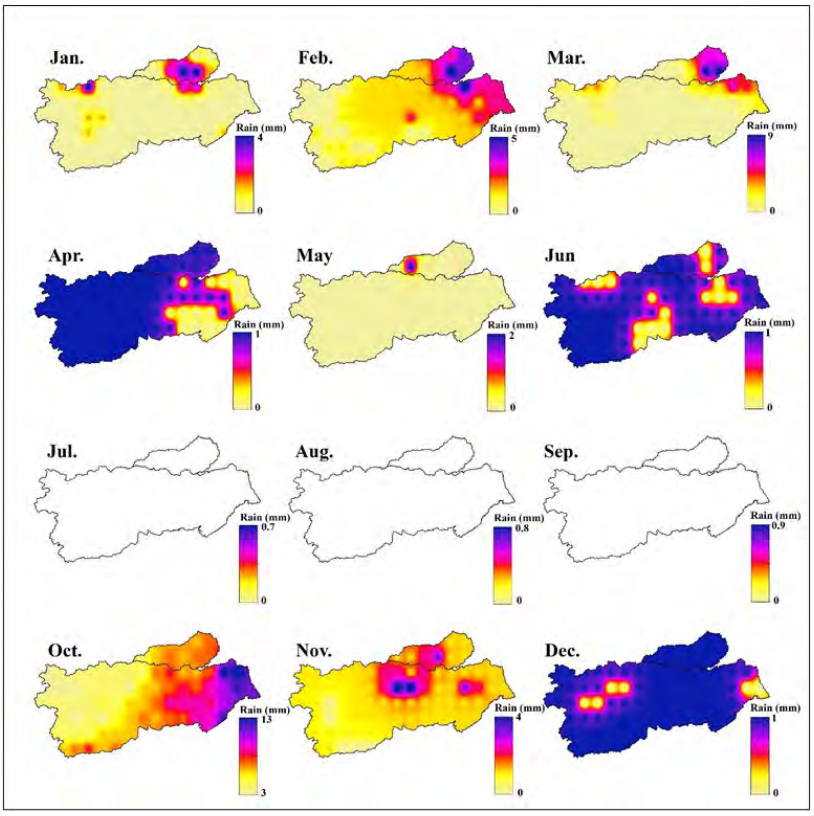

Figure 30: The expected monthly rainfall of the year 2015 on the area.

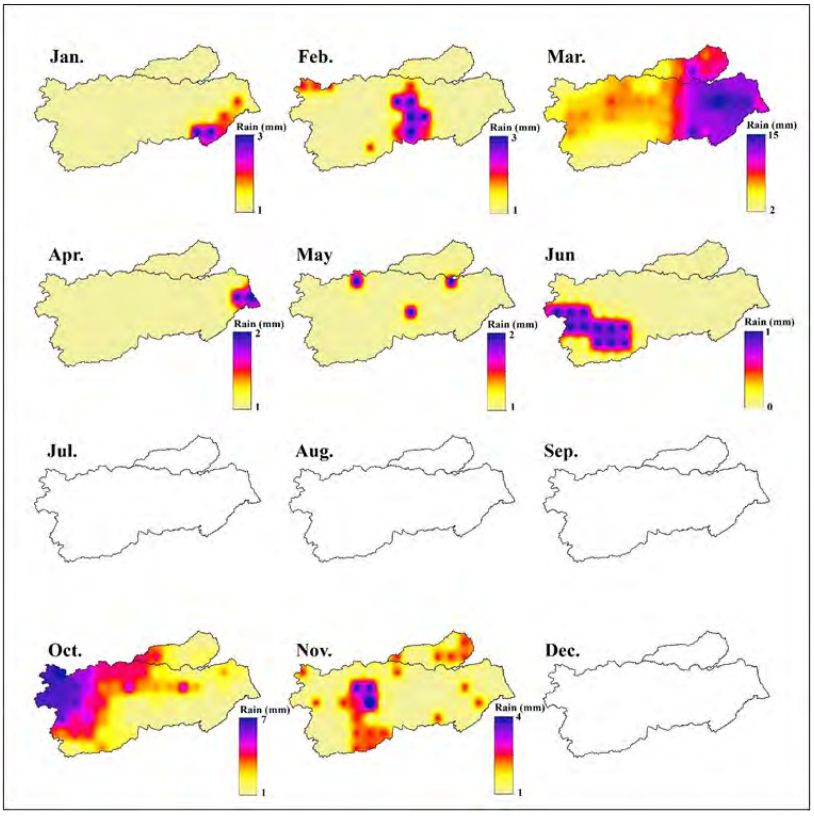

Figure 31: The expected monthly rainfall of the year 2016 on the area.

2017: The expected annual average amount of precipitation in this year increased to about 1.5 mm in a rate of about 15.38%. The highest value in December was about 6.4 mm, followed by January with about 2.9mm. The spring season came first in terms of the expected rainfall rate of about 2.1 mm, followed by the Winter season with about 1.27 mm, then the Autumn season with about 0.47 mm (Table 9 and Figure 32).

2018: This year is the highest year in terms of expected rainfall obtained from satellite images with an average of about 1.6 mm. The highest value was in February (5.3mm). In the 23rd., of February, a strong rainstorm passed, resulting in a large flow of water in the basins of the middle and south of the Gulf of Suez. November came in the second category this year, reaching about 5.2 mm followed by October with 2.5mm. Winter was the highest season this year with an average of about 3.9mm, followed by Autumn with about 2.9 mm, and then Spring with about 1.43 mm (Table 9 and Figure 33).

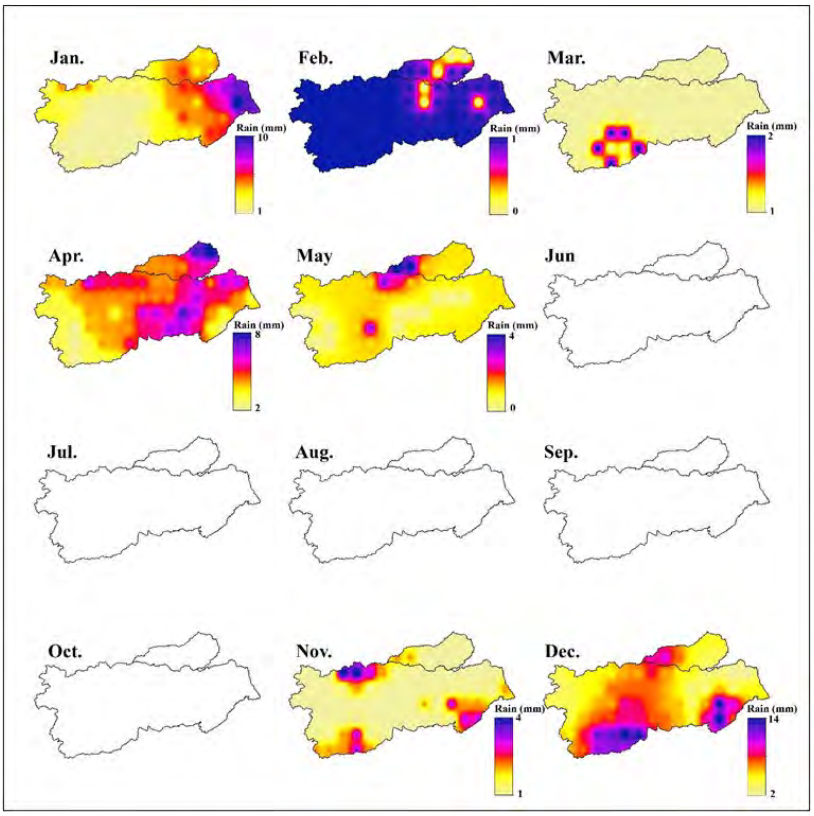

Figure 32: The expected monthly rainfall of the year 2017 on the area.

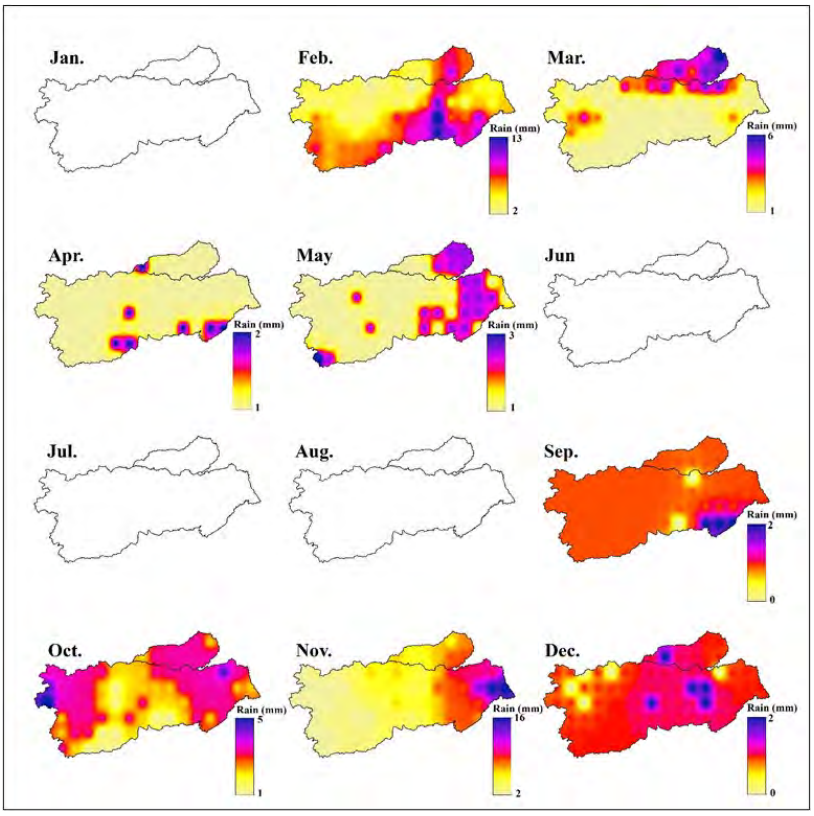

Figure 33: The expected monthly rainfall of the year 2018 on the area.

2019: The expected annual average precipitation decreased in this year compared to the previous year, as the annual average precipitation was about 1.4 mm, with a decrease rate of 12.5%. February is the highest month of the year with an average of about 5 mm, followed by Abryl with a precipitation of 1.9 mm. In terms of seasons, winter is the highest season of this year which amounted to about 3.73 mm, followed by spring with an average precipitation of 1.4 mm, and then Summer with 0.4 mm (Table 9 and Figure 34).

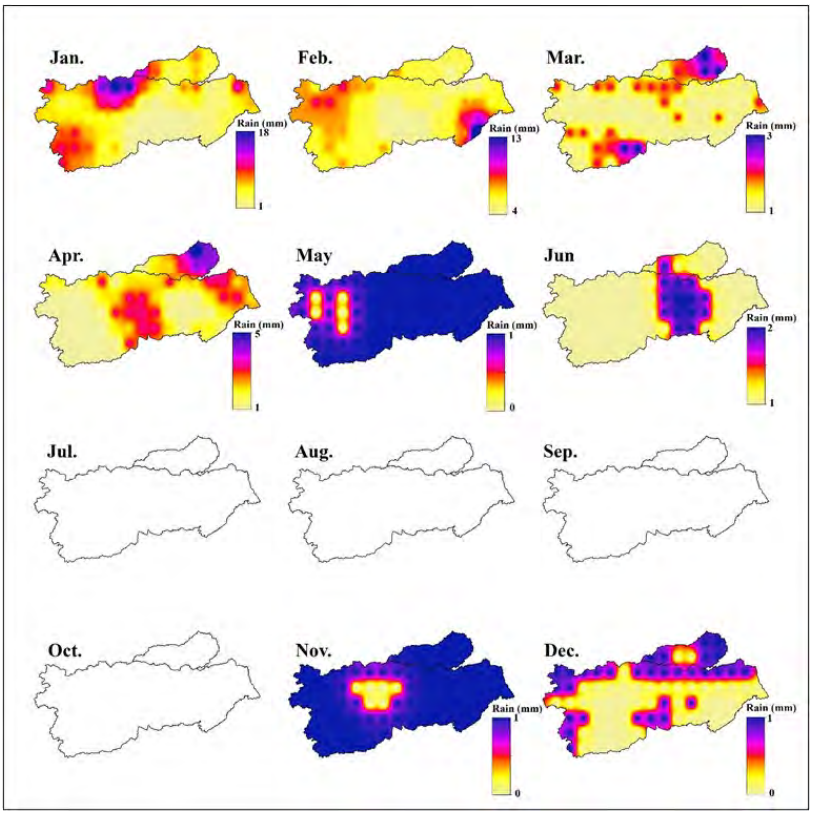

Figure 34: The expected monthly rainfall of the year 2019 on the area.

2020: The expected average of precipitation this year was about decreased to about 0.5 with a reduction rate of 64.29%. mm. March is the highest month of this year with an average of about 1.4 mm. In terms of seasons, Spring is the highest season of this year with an expected average precipitation reaching about 0.77 mm, followed by Autumn 0.6 mm then Winter 0.5 mm (Table 9 and Figure 35).

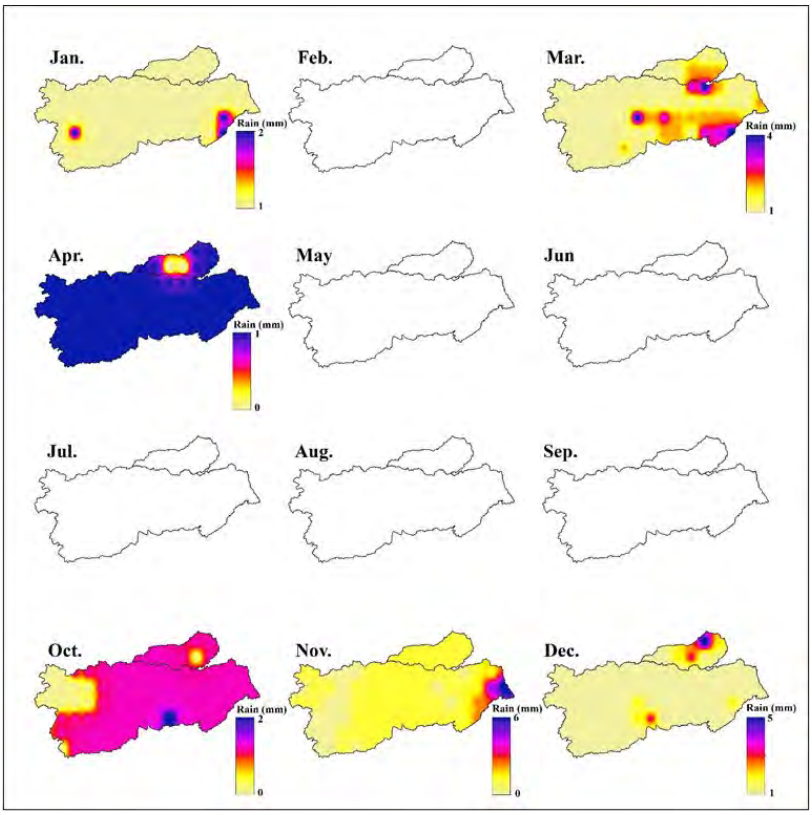

Figure 35: The expected monthly rainfall of the year 2020 on the area.

2021: The general average precipitation increased in this year, reaching 0.7 mm, with an increase rate of 40% over the previous year. December is the highest month of this year with a rate of about 2.1 mm, followed by January by about 1.3 mm then October and November with about 1.1 mm. Minter was the highest season of expected precipitation with about 1.13 mm, followed by the spring with 0.77 and Autumn 0.73 mm (Table 9 and Figure 36).

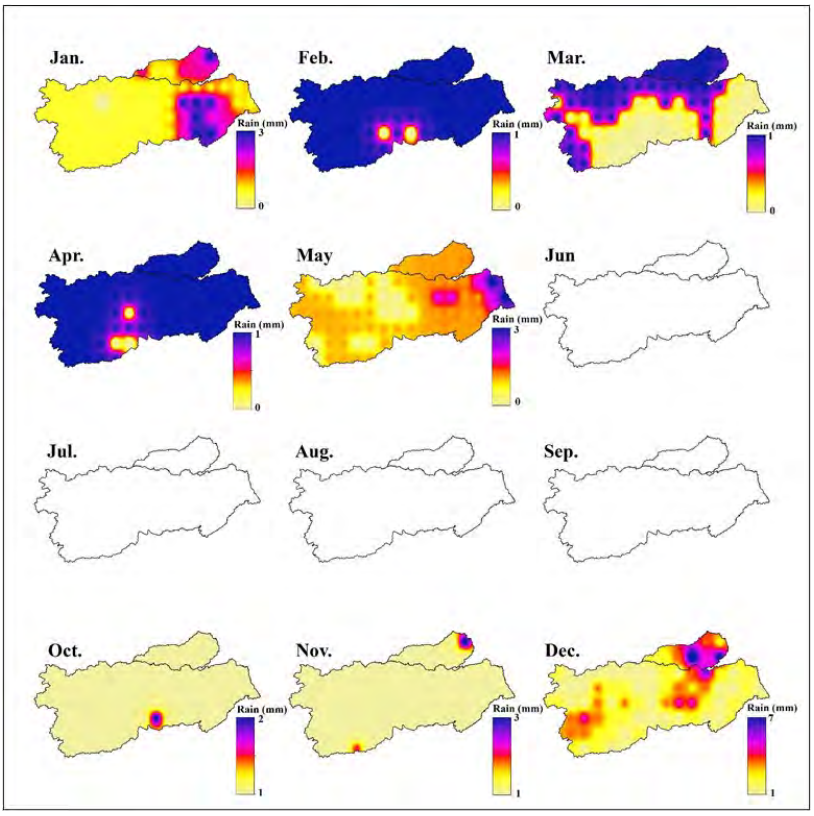

Figure 36: The expected monthly rainfall of the year 2021 on the area.

2022: The average precipitation this year was about 0.8 mm, which increased of about 14.29% over the previous year. November is the highest month this year in terms of precipitation at about 2.2 mm, followed by January, February and March with about 1.2 mm each. At the seasonal level, winter is the highest season this year in terms of average precipitation, which amounted to about 1.5 mm, followed by autumn with an average precipitation of 1.03 mm, and then spring with 0.93 mm (Table 9, Figure 37).

2023: The average precipitation increased to 0.9 mm, an increase of 12.5% over the previous year. June is the month with the highest precipitation rate at 3.7 mm, followed by November at 1.3 mm. Summer is the season with the highest precipitation rate at 1.37 mm, followed by autumn at 0.87 mm, spring at 0.73 mm, and finally winter at 0.37 mm (Table 9, Figure 38).

2024: The annual average precipitation decreased this year compared to the previous year, as the potential annual average of precipitation was about 0.5 mm. The reduction rate of -44.44%, due to the unavailability of satellite images for the last third of this year as the images are available only for the winter, spring and summer seasons. March is the month with the highest precipitation rates, with an average of about 1.1 mm, followed by February and April with a potential precipitation rate of 1.0 mm each. At the seasonal level, winter is the highest season this year in terms of average precipitation, which amounted to about 1.0 mm, followed by spring with an average precipitation of 0.73 mm, then summer with 0.27 mm, and no data is available for the Autumn season (Table 9, Figure 39).

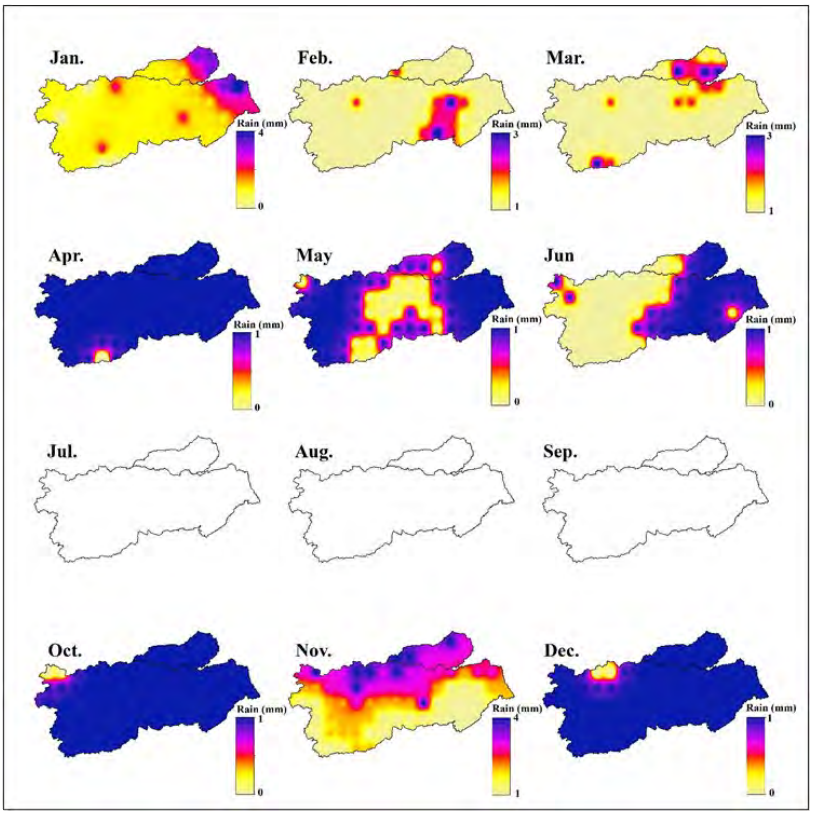

Figure 37: The expected monthly rainfall of the year 2022 on the area.

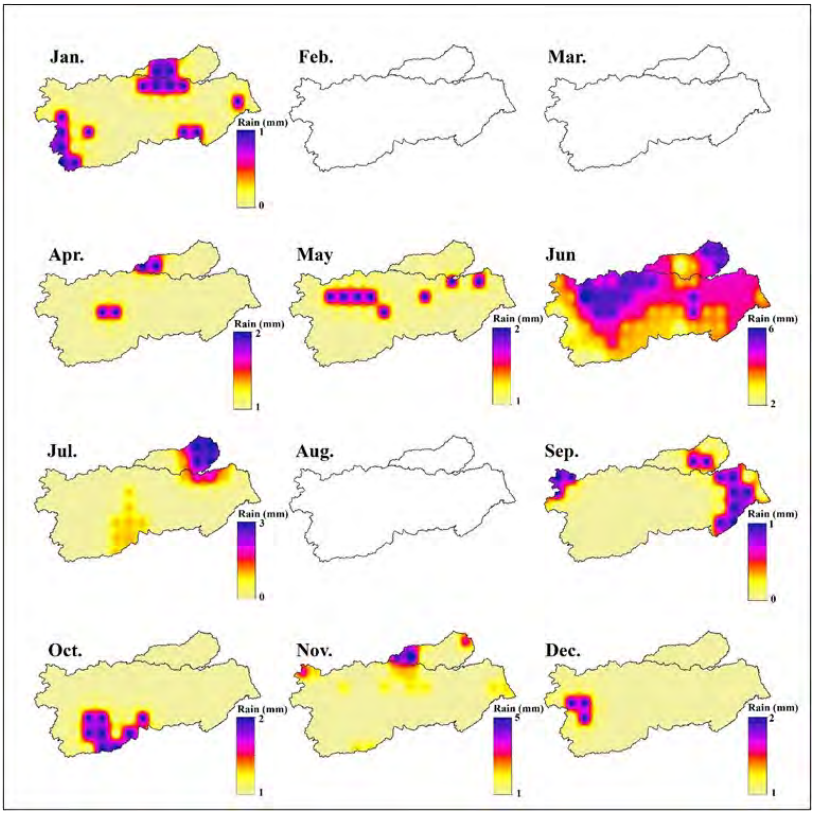

Figure 38: The expected monthly rainfall of the year 2023 on the area.

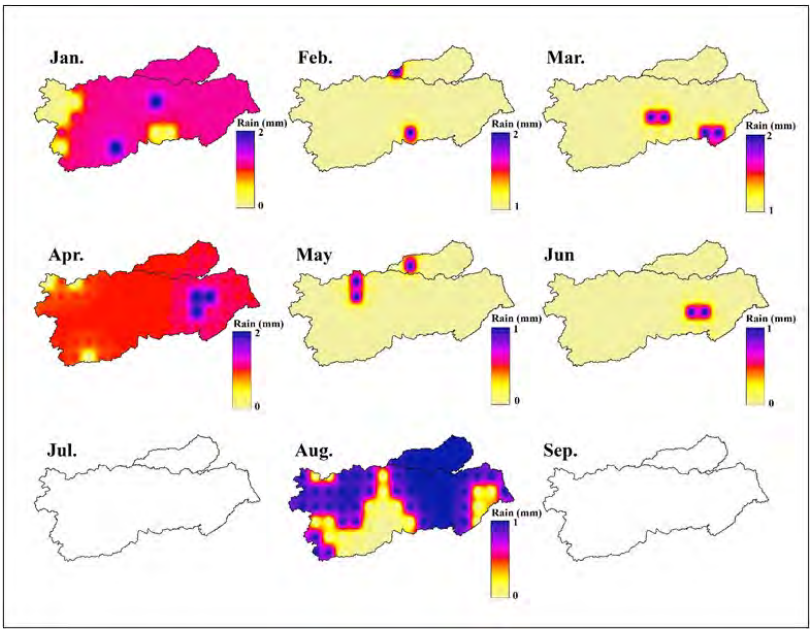

Figure 39: The expected monthly rainfall of the year 2024 on the area.

7.4.2 Measured Rainfall Data and Rainstorms Design

Actual rainfall data used in this part was collected from the Egyptian Meteorological Authority for the nearest meteorological station to the study area, which is the El Gouna station (Figure 40). The data covers a 10-year period from 2016 to 2024, aligning with the selected climate satellite images for consistency.

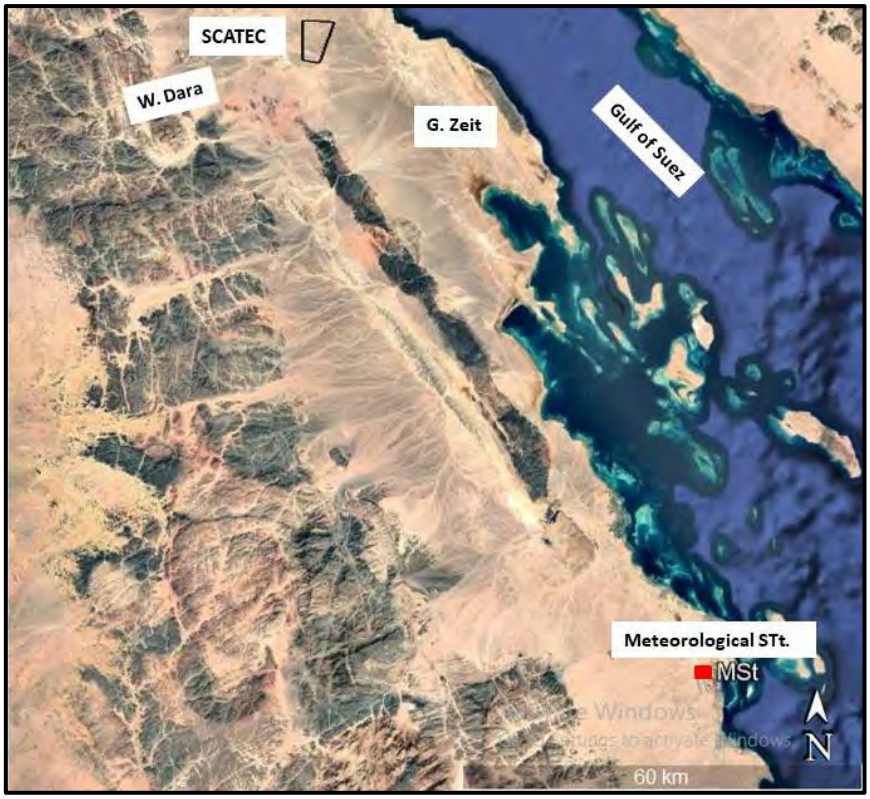

Figure 40: The weather stations close to the area basin

7.4.2.1 Recent rainfall data

Based on the comparison between the rainfall data expected from the satellite images and that measured (Tables 10 and 11), important notes can be revealed:

- In October 2016, the study area experienced heavy rainfall that led to a dangerous flood in the City of Ras Ghareb. The satellite data estimated the rainfall depth at 7 mm, while the actual measured rainfall from the closest meteorological station was 51.3 mm. In 2022, the expected rainfall was 4 mm, but the measured amount at El Gouna and Hurghada stations was 16 mm (Table 10). This discrepancy is unusual, as typically, actual rainfall is lower than the values estimated from satellite data. The difference may be due to the significant distance (more than 75 km) between the site and the weather station, coupled with the southeast wind direction, which likely reduced cloud density during the rainfall event at this distance.
- October 2016 and January 2022 are the only two months in the past decade where the actual rainfall exceeded the amounts calculated from satellite images. Notably, October 2016 witnessed severe flooding in the Ras Ghareb area, located about 40 km north of the study site, where the actual rainfall significantly surpassed the satellite estimates.

Table 10: Monthly maximum rainfall in one day during the period 2015 -2024. El Gouna weather station

parameter	Jan	Feb.	Mar.	Abr.	May	Oct.	Nov.	Dec.	year
Max. in day mm	0	0.4	0	0	0	5.2	0	0	2015
Date						25			
Max. in day mm	0	0	0	0	0	51.3	0	0	2016

Date						27			
Max. in day mm	0	0	0	1.6	0	0	0	0	2017
Date				12					
Max. in day mm	0	2	0	0	2	0	0	0	2018
Date		23			6				
Max. in day mm	0.1	0.1	0	0	0	0	0	0	2019
Date	27	5							
Max. in day mm	0	0	3	0	0	0	0	0	2020
Date			12						
Max. in day mm	0	0.1	0	0	0	0	0	1.8	2021
Date		3						27	
Max. in day mm	16	2.1	0	0	0	0	0	0	2022
Date	1	15							
Max. in day mm	0.3	2	0.1	0	0	0	0	0	2023
Date	3		14						
Max. in day mm	0	0	0	0	1				2024
Date					30				

Table 11: Expected rainfall compared with the actual rainfall depths during the period (2016 to 2021)

Month	2015		2016		2017		2018		2019		2020		2021		2022		2023		2024	
	E	M	E	M	E	M	E	M	E	M	E	M	E	M	E	M	E	M	E	M
Jan.	4	0	3	0	10	0	0	0	18	0.1	2	0	3	0	4	16	1	0.3	4.7	0
Feb.	5	0.4	3	0	1	0	13	2	13	0.1	0	03	1	0.1	3	2.1	0	0	4.1	0
Mar	9	0	15	0	2	0	6	0	3	0	4	0	1	0	3	0	0	0.1	4.5	0
Apr	1	0	2	0	8	1.6	2	0	5	0	1	0	1	0	1	0	2	0	2.5	0
May	**2**	**0**	**2**	0	4	0	3	2	1	0	0	0	3	0	1	0	2	0	1.9	1
Jun	1	0	1	0	0	0	0	0	2	0	0	0	0	0	1	0	6	0	1.2	
Jul	0	0	0	0	0	0	0	0	0	0	0	0	0	0	0	0	3	0	0.3	
Aug	0	0	0	0	0	0	0	0	0	0	0	0	0	0	0	0	0	0	0.1	
Sept	0	0	0	0	0	0	2	0	0	0	0	0	0	0	0	0	1	0	0.3	
Oct	13	5.2	7	51.3	0	0	5	0	0	0	2	0	2	0	1	0	2	0	3.6	
Nov	4	0	4		4	0	16	0	1	0	6	0	3	0	4	0	5	0	5.2	
Dec	1	0	0		14	0	2	0	1	0	5	0	7	1.8	1	0	6	0	3.7	

E.: Expected precipitation based on analyses of the satellite images
M. Measured precipitation data from the El Gouna meteorological station

7.4.2.2 Estimation of the rainstorms returns probability

To estimate the probability of flood occurrences and their return period in the study area, rainfall data from the El Gouna meteorological station (2015-2024) were analyzed. The highest recorded rainfall in one day during this period was 51.3 mm in 2016 and 16 mm in 2022, with a total of 16 readings (Table 11). These values were sorted in descending order, with the highest rainfall value ranked first, followed by the remaining values, as shown in Table (12). The probability of flash floods (P (%)) in the region was then calculated using the equation provided by Critchley & Siegert (1991), as follows:

$$P\ (\%) = \frac{m - 0.375}{N + 0.25}\ X\ 100$$

$$P(\%) = \frac{m - 0.375}{N} + 0.25)\ X\ 100$$

P = probability in % of the observation of the rank m

M = the rank of the observation

N = the total number of observations used

By applying the equation to the maximum rainfall data, it is evident that the probability of the October 27, 2016 floodthe strongest torrent to occur in the region during the study period—is 3.8%. Since the amount of rainstorm water is inversely correlated with the probability of flash flood occurrence, larger floods are less likely to happen compared to smaller-scale ones. Additionally, the return period (Tp) for floods was calculated using the following equation:

$$T = \frac{100}{P1}\ (years)$$ TP = 100/P

Using the previous equation, the return time for floods was calculated, which is inversely proportional to the probability of occurrence. A higher probability of a flood means a shorter return period, and conversely, a lower probability leads to a longer return period (Table 13 and Figure 41). Based on this, the return period for the flood of March 12, 2020, is approximately 26 years. Consequently, it is anticipated that a flood of similar magnitude to the 2016 event could recur by the year 2042.

Table 12: The calculated data of rainstorm returned probability

Date	year	Rain $_{max}$ **(mm)**	Rank	P (%)	T_p **(yr)**
17/2	2015	0.4	11	65.4	1.5
25/10	2015	5.2	3	16.2	6.2
27/10	2016	51.3	1	3.8	26.0
12/4	2017	1.6	9	53.1	1.9
23/2	2018	2.0	6	34.6	2.9
6/5	2018	2.0	7	40.8	2.5

27/1	2019	0.1	13	77.7	1.3
5/2	2019	0.1	14	83.8	1.2
12/3	2020	3.0	4	22.3	4.5
3/2	2021	0.1	15	90.0	1.1
27/12	2021	1.8	8	46.9	2.1
1/1	2022	16.0	2	10.0	10.0
15/2	2022	2.1	5	28.5	3.5
3/1	2023	0.3	12	71.5	1.4
14/3	2023	0.1	16	96.2	1.0
30/5	2024	1.0	10	59.2	1.7

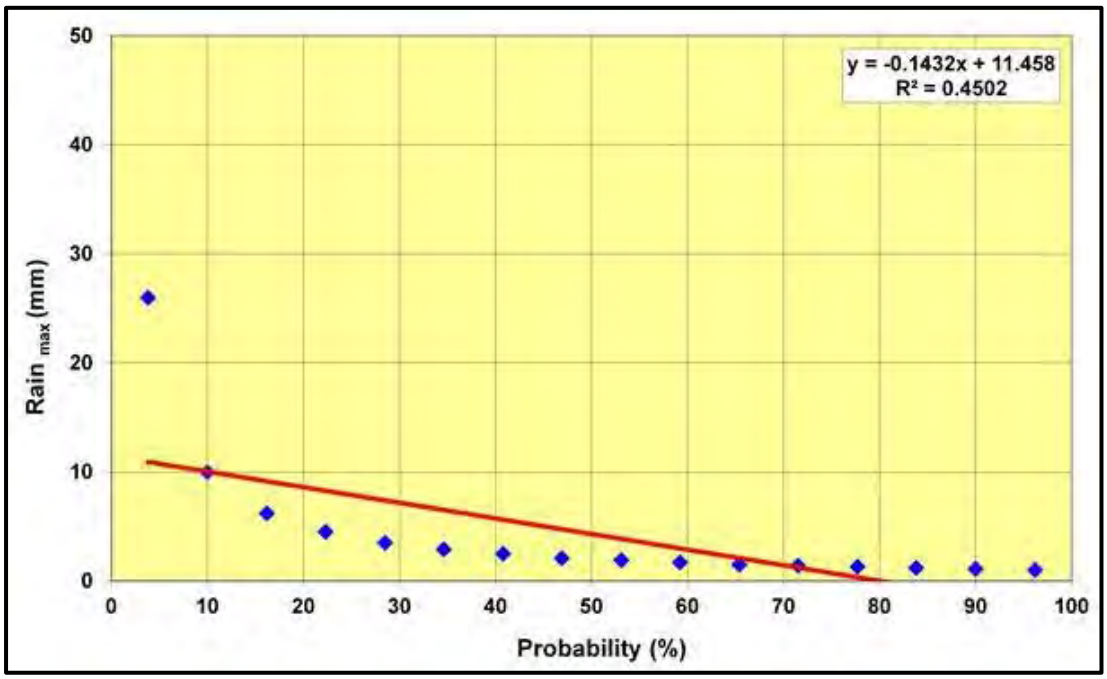

Figure 41: The rainstorm returned probability

7.4.2.3 The intensity of rainfall and designed flood

The rainfall depth for certain return periods (2, 5, 10, 25, 50, and 100 years) was calculated using the Log-normal statistical distribution (Maximum Likelihood). This method enabled the prediction of the maximum rainfall amounts that could occur in a single day, as shown in Table 13 and Figures 41 and 42. The predicted maximum rainfall amounts for each of these return periods are as follows:

Table 13: Maximum rainwater could be received in one day

Return Period (year)	Rain Depth (mm)
2	3.31
5	8.52
10	12
25	16
50	19.6
100	22.8

It is observed from the data in the previous table that the maximum amount of rain expected to fall in one day increases as the return period increases. Specifically, the predicted rainfall depth is approximately 3.31 mm for a 2-year return period, while it is expected to reach about 22.4 mm for a 100-year return period. This trend indicates that with longer return periods, the intensity and volume of rainfall expected to occur in a single day increases, reflecting the rarity and severity of such events.

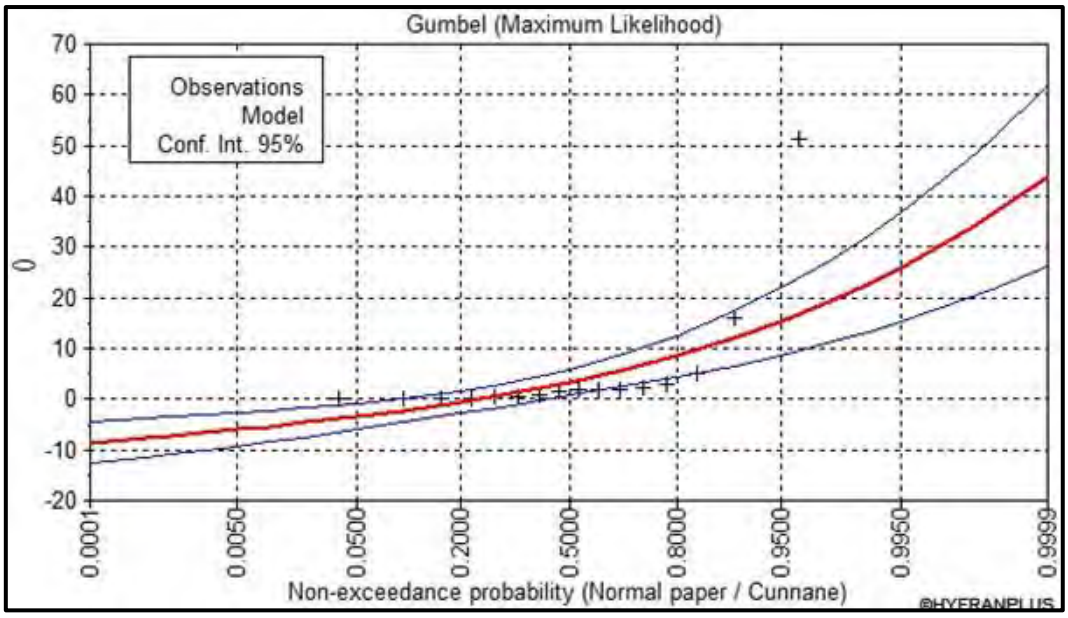

Figure 42: The probability of rain falling intensity

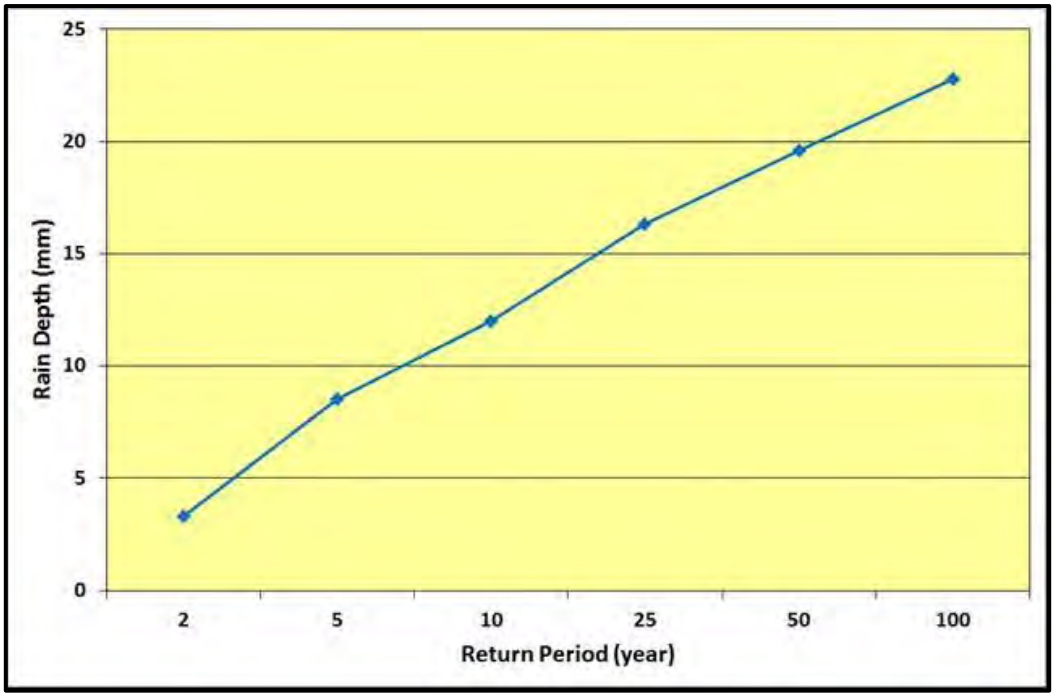

Figure 43: The returned periods of the maximum rainfall intensity.

Based on the above detailed study of the actual rainfall data collected from the closest meteorological stations to the project site (El Gouna), the following points could be concluded:

- In October 2016 when the study area received heavy rainfall, no strong flash flood was recorded in Wadi Dara like the one recorded in Ras Ghareb area north of the site by about 40km.
- In the years 2016 and 2022 when the above station recorded 7-mm and 4-mm rainfall depth respectively, the area of study received rainfall with about 51.3 and 16 mm for the two years respectively.
- Global warming phenomena were taken into consideration when designing the rainstorms and their return periods through; 1) increase the amount of recorded precipitation by about 25%, and 2) calculation based on the maximum rainfall depths recorded in one day in the station (October 2016).
- Rainstorms that recorded 51.3 mm at El Gouna station could be returned in a period of about 26 years.
- Rainstorm depth recorded at El Gouna Station in one day during the occurrence of flooding in Ras Gharib area (53.1 mm) could be returned in the study area in a period of more than 100 years.
- After the catastrophic flood event of 2016, mitigation measures were applied along the dangerous drainage basins in the area, such as three successive dams with artificial lakes along the main stream of Wadi Hawashyia, 60 km to the north of the site, a group of successive dams with road lining and culverts underneath to prevent the flow of water above the road along Wadi Abu Had, about 40 km to the north, and a dam with an artificial lake at the mouth of Wadi Al Darb, 35 km to the north of the site. However, no flood mitigation measures were constructed in Wadi Dara.

7.5 Flood Risk Assessment in the Studied Basins in the General Framework of the Gulf of Suez Basins

7.5.1 Morphometric Characteristics of Drainage Basins

Morphometric refers to the process of numerical analysis of earth surface features from topographic maps, Land Sat images and DEM that are supplemented by aerial, space and field measurements. Morphometric analyses of the studied basins (Wadi Dara and Wadi N Dara) were done using ARC-GIS software and the values were compared to the limits of the basins along the Red Sea. The morphometric studies of the drainage basins are important to determine the hydrological characteristics of them so that it is easy to predict the severity of the floods.

The morphometric parameters of the basin include the:

- Basin dimension
- Basin shape
- Topographic features of the basin.

a) Basin Dimensions

They are represented by the area, length, width and perimeter.

Basin Area (A) km^2

The area of the drainage basin measures the region that includes all the tributaries located within the basin territory and which is surrounded by the water-dividing line. The area of the basin is affected by the growth of the watercourse network and its distribution pattern.

There is an inverse relationship between the area of the drainage basin and the volume of sediments that the wadi transports to the downstream part, the greater the area, the less the volume of sediments the wadi carries to the downstream part. The potential power of the drainage basin to retain sediments increases with the increase in its area. The larger the drainage basin area, is the greater the capacity of the basin to retain and store sediments temporarily or permanently within the drainage basin itself (Muhammad Abd al-Latif, 2008, p. 57).

The area of the basin has an influential role in the possibility of floods, as there is a direct relationship between the areas of the basins and the discharge volume. The larger the area of the basin, the greater the volume of rain it receives and the higher the possibility of flooding (Jouda etal, 1991). Therefore, there is a greater probability of flooding in large-sized basins than small ones (Cooke et al., 1985).

The area of the Red Sea basins ranges from 1796.5 km^2 (high flood risk) to 2.8 km^2 (low flood risk). Based on the software, the areas of the studied two basins are indicated in Table 14. The total area of the studied basins is about 1323.1 km2 with an average of 661.55 km2. The area of the basins ranges from 152.2 km2 (Wadi N. Dara), to 1170.9 km2 (Wadi Dara). Based on the role of basin area in expecting floods, Wadi Dara has the highest possibility of expecting floods rather than the other one.

Table 14: The morphometric parameters of the studied two basins crossing the project site.

	W. Dara	W. N Dara	Average
A (km2)	1170.9	152.2	661.55
LB (Km)	65.2	25.3	45.25
W (Km)	18.5	5.9	12.20
Pr (Km)	243.4	75.8	159.60
Rc	0.25	0.33	0.29
Re	0.59	0.55	0.57
Ish	0.28	0.24	0.26
SH	2.01	1.73	1.87
K	0.91	1.05	0.98
R/w	3.52	4.29	3.91
Rf	1308	407	857.50
Rh	20.06	16.09	18.08
Rr	0.54	0.54	0.54
Rn	4.82	1.61	3.22
Gn	4.19	1.75	2.97
Hi	0.9	0.37	0.64
Sl	1.15	0.92	1.04
Kc	7	6	-
Snu	8879	1197	5038.00
Slu (Km)	4314.7	601.4	2458.05
Rb	4.4	3.96	4.18

A; area of the basin (km^2), BL basin length (km), W basin width (km), Pr perimeter of the basin (km), Re elongation ratio, Rc circularity ratio, Ish shape index, SH compactness ratio, K Lemniscates ratio, Rlw Length / Width Ratio, Rf relief (m), Rh relief ratio, Rr Relative relief, Rn ruggedness number, Gn Geometric Number, Hi Hypsometric Integral, Sg slope index, kc order of trunk channel, Snu sum of stream numbers, Slu sum of stream lengths (km), Rb bifurcation ratio, D drainage density by Horton method (km^{-1}), F stream frequency (km^{-2}), Rm Stream Maintenance Ratio, Lo length of overland flow (km), Rt texture ratio (Km^{-1}).

Basin Length (LB) km

The length of the basin is one of the basic dimensions on which to calculate certain morphometric parameters that depend on the length of the basin, especially the shape coefficients, and to determine some of the shape and topographic characteristics of the drainage basins (Gregory & Walling, 1973).

The length of the basin is influenced by several factors and processes which are as follows the growth direction and development of watercourses, which in turn are subject to the direction of the faults and fractures, the head ward erosion towards the water divide line or downstream with the growth of flood alluvial fans.

The length of the basin was measured using the ARC GIS software based on the method adopted from Schumm, 1956. The length of the basin is the distance from the mouth of the mainstream to the furthest point on the perimeter parallel to the mainstream.

The total length of the studied drainage basins is about 90.5 km, with an average of 45.25 km, where Wadi N. Dara the less length among them of about 25.3 km followed by W. Dara (65.2 km) (Table 14).

The shorter the length of the basin is, the stronger the water flow through it. Accordingly, Wadi Dara basin could have strong surface water flow during the rainfall storms higher than the N. Dara basin.

Basin Width (W) km

The width of the basin contributes to the identification of its shape.

In general, it is possible to say that the basins of small length and width are the most dangerous ones. This is because their basins areas are small, short in length and width. Therefore, they can be totally covered by rainstorms in a short period with limited water loss by leakage and evaporation. Thus, the surface runoff takes a short time to reach the outlet of the Wadi.

The total width of the basins studied is about 24.4 km. Like the basin length, the shorter the width, the higher the water flow, so W.N Dara basin is expected to have lower water flow than W Dara.

Perimeter of the Basin (Pr) km

The perimeter is the water divide line which separates one basin from the adjacent basins.

The importance of measuring the perimeter of the basin is that it is used to calculate other morphometric parameters such as shape coefficients, basin elongation and basin circularity (Khader, 1997 and Mahsoub, 2002).

The basin Perimeter is affected by several factors, such as the development of first order tributaries, the emergence of seasonal small tributaries which arise after the rainstorms, and by the decline of slopes that their peaks represent water dividing lines of basins. Based on the software, the total perimeters of the basins reached 319.2 km. Wadi N Dara has the shortest perimeter of about 75.8 km followed by Wadi Dara 243.4 km (Table 14).

Based on the foregoing, the shorter the basin perimeter, the less its area and the rest of its dimensions and the greater its risk levels concerning flood possibility and vice versa. Therefore, Wadi N. Dara basin is considered to have a lower flood risk compared to Wadi Dara.

b) Basin Shape

The shape of a basin and its resemblance to a circular or rectangular form influence the time it takes for floodwaters to reach the outlet of the basin, which in turn affects the extent of its impact

on surrounding areas. Additionally, the shape of the basin influences its aquifer recharge potential (Rashidi, 1994).

The shape of the discharge basin significantly influences water flow; elongated basins tend to have a more uniform time distribution of water discharge and lower quantities compared to circular basins. Conversely, circular basins are characterized by a higher volume of water, as they accumulate from most tributaries into a central area within a short period, quickly reaching the basin's outlet and increasing the risk of flooding.

Some morphometric parameters have been developed using the Arc GIS software that determines the degree of affinity of the drainage basin shape as follows:

Elongation Ratio (Re)

Elongation is one of the most accurate morphometric factors in measuring the forms of drainage basins, as it compares the shape of the drainage basin and the shape of the rectangle. The values of this ratio range between (0: 1). A higher value, closer to 1, indicates that the shape of the basin more closely resembles a rectangle, and vice versa (Gardiner, 1975).

The elongation ratio reflects the flow characteristics within a basin. A greater basin length, indicated by a higher elongation ratio and increased irregularity, corresponds to reduced water flow and a lower likelihood of flooding. The average elongation ratio for the studied basins is approximately 0.57, suggesting a general tendency toward elongation. The elongation ratio of the Red Sea basins ranges from 0.32 (high risk) to 0.83 (low risk). The Elongation ratios in the two studied basins are listed in table 14. This ratio indicates that the studied drainage basins exhibit a low to medium potential for flooding.

Circulatory Ratio (Rc)

The circulatory ratio indicates the degree of similarity of the basin boundary to a circular shape. It examines the relationship between the area of the basin and the area of a circle with a perimeter equal to the basin's perimeter. The small value of this ratio, close to zero, reflects the following:

- The irregular shape of the basin (closer to elongation).
- Increased meandering of the water divides lines.
- Reduced flood risk within the basin.
- A high value of this ratio, close to unity, indicates that the basin shape approaches a circular form (Al-Wedani, 2007).

Basins with small areas are often more circular as they have not yet reached the advanced geomorphological stage compared to larger basins which are often inclined to elongation. Circular shapes lead to the accumulation of the water from most tributaries in the main course at the same time resulting in a sudden high discharge leading to devastating floods (Morisawa, 1958). The circularity ratio can be calculated according to the following equation (Gregory & Wallind, 1979):

$$Rc = \frac{4\pi A}{P2}$$

Where Rc = Circularity Ratio, π = 3.14, A = Area (km2), and P = Basin Perimeter

The circularity of the Red Sea basins ranges from 0.13 (low risk) to 0.52 (high risk). The average circulatory ratio of the studied basins is 0.29. The basins studied are characterized by low flood possibilities as their circularity values are close to zero (Table 14).

Shape Index (Ish):

The shape index (Ish) expresses the degree of consistency between the dimensions of the basin where the shape of the basin is compared to triangle or square shape. The sha was calculated by the following equation (Horton, 1932), using the ARC – GIS software.

$$\mathbf{Ish = A/L^2}$$

Where; Ish = shape index, A = basin area (km2), and L = basin length (km)

A low value of the shape index indicates that the basin resembles a triangular shape, which is associated with a lower flood risk. Conversely, a high value of this factor suggests that the basin approaches a square shape, which is associated with a higher flood risk. The shape index is a numerical metric (Horton, 1932) commonly used to quantify basin shapes. The international range for this factor typically falls between 0.1 and 0.8. The shape indices of the studied basins are presented in Table 14, with an average shape index of 0.09 for the three basins.

The shape index of the Red Sea basins ranges from 0.08 (low risk) to 0.54 (high risk). A smaller value of this factor indicates a more elongated basin, while a higher shape index (above 0.8) suggests a basin with higher peak flood flows occurring in a short period. On the other hand, an elongated drainage basin with a low shape index is characterized by a lower peak flow of floodwater spread over a longer period. Based on the calculated shape index factor of the studied basins (Table 14) and its comparison with the shape index values of the entire Red Sea basins, it can be concluded that the studied basins exhibit an elongated, triangular shape, and thus, they are associated with a low flood risk possibility.

Length / Width Ratio (R/W)

The length over width ratio is a simple morphometric factor used to assess the orientation of the basin's shape, whether closer to circular or rectangular. A higher value of this ratio indicates that the basin's shape is more rectangular. The ratio is calculated as follows:

$$\mathbf{R/W = L/W}$$

Where; R/W = length/width ratio, L = basin length, and W, basin width.

The average length/width ratio for the studied drainage basins is 3.91. A high value of this ratio indicates that the basins are more elongated, with the length being significantly greater than the width. The ratio values for the studied basins range from 4.29 for Wadi N Dara to 3.52 for Wadi Dara, suggesting that both basins are more rectangular in shape, which correlates with a lower risk of flooding.

c) Morphological Features of Drainage Basins

The surface characteristics of a basin significantly influence its hydrology, particularly regarding surface runoff. Gentle slopes tend to promote greater evaporation and infiltration, as rainwater takes more time to flow off the surface. In contrast, steep slopes reduce these losses, allowing

water to flow more rapidly (Khedr, 1997). The surface characteristics of the drainage basins are assessed based on several morphometric parameters, including:

1) Maximum Relief, 2) Relief ratio, 3) Relative Relief, 4) Ruggedness Value, 5) Geometric Number, 6) Hypsometric Integral, and 7) Slope Gradient.

Maximum Relief (Rf)

Maximum relief refers to the difference between the lowest point at the outlet of the basin and the highest point at the water divide.

There is a direct relationship between the maximum relief and the slope gradient, on one hand, and the intensity of surface flow and the number of transported materials, on the other. As the maximum relief increases, the slope becomes steeper, leading to a higher flow of water. The maximum relief of the Red Sea basins ranges from 30 meters (indicating low flood risk) to 2088 meters (indicating high flood risk). The maximum relief values of the studied basins, as shown in Table 14, have an average value of 857.5 meters. Compared to the average values of the Red Sea drainage basins, the studied basins are categorized as having a low to medium flood risk potential.

Relief Ratio (Rh)

The Relief Ratio measures the relationship between the maximum relief and the length of the basin, providing an indicator of the basin's slope. Unlike the maximum relief, which does not account for the horizontal distance between the highest and lowest points, the Relief Ratio takes both vertical and horizontal dimensions into consideration. This ratio, which reflects the steepness of the basin's surface, was calculated using the equation proposed by Strahler (1957).

Relief Ratio (Rh) = Maximum Relief (m) / Basin Length (km)

The type of rock, rainfall volume, and the morphological stage of the basin are key factors contributing to a low Relief Ratio (Moussa, 2000). A higher Relief Ratio indicates a steeper slope, which correlates with an increased risk of flooding. The Relief Ratio for Red Sea basins range from 7.4 (low flood risk) to 109.5 m/km (high flood risk). The average Relief Ratio for the studied basins is 18.08, with Wadi N Dara exhibiting the lowest value at approximately 16.09, while Wadi Dara has a value of 20.06 (Table 14). When compared with the Red Sea basins, the studied basins fall into the low flood risk category in the event of heavy rainfall.

Relative Relief (Rr)

Relative Relief measures the relationship between the maximum relief (the difference between the highest and lowest levels in the basin) and the basin perimeter. It can be calculated using the following equation (Gregory & Walling, 1979):

Relative Relief = [Maximum Relief (m)/ Basin perimeter (km)]*100

The Relative Relief coefficient is inversely related to the area of the basin and the degree of rock resistance to erosion under constant climatic conditions (Jode et al., 199). The relative relief of the Red Sea basins ranges from 0.2 (low risk) to 3.4 (high risk). Based on the software, the average relative relief of the studied basins is 0.54. This value may indicate the low resistance of rocks to erosion in both Wadis. The Relative Relief values of the studied basins suggest a low flood risk in their outlet areas.

Ruggedness Number (Rn)

This coefficient examines the relationship between the topography of the basin and the length of its drainage network, addressing the mutual relationship between multiple variables. It measures how the basin's relief relates to the length of its streams and the basin area. Ruggedness expresses the relationship between the basin's relief and the drainage density and is therefore highly dependent on factors such as the type of rock and the amount of rainfall (Awadallah, 2005). The ruggedness value was calculated using ARC-GIS based on Strahler's (1964) formula.

Ruggedness = Basin topography (m) × Drainage density (km/km^2) / 1000

The ruggedness value of the Red Sea basins ranges from 1.3 (low risk) to 30.9 (high risk). Based on the software, the average ruggedness ratio for the studied basins is 3.22. The value for W. N Dara is 1.61, while W. Dara has a value of 4.82. These values indicate that the studied basins have low flood risk potential.

Hypsometric Integral (Hi)

The hypsometric integral represents the developmental stage of a basin based on the relationship between its area and topography (Khader, 1997). The hypsometric integration of basins was calculated using the following equation (Mustafa, 1982) with ARC-GIS software:

Hypsometric Integral = Basin area (km^2) / Maximum basin topography (m)

The values of the hypsometric integral for the Red Sea basins range from 0.02 (low risk) to 1.6 (high risk). According to the software analysis, the hypsometric integral values for the studied basins are 0.37 for W. N Dara and 0.9 for W. Dara. This suggests that W. N Dara has a low flood risk, while W. Dara has a medium flood potential.

Slope Index (SI)

The slope index measures the relationship between the horizontal distance (basin length) and the vertical distance (the difference between the lowest and highest elevations expected in the basin). This index provides an indication of the extent of basin erosion (Khader, 1997). The relationship is expressed by the following equation:

Slope Index = [(Maximum basin topography/Maximum basin length) *1000] *57.3

Basins with a low slope index are characterized by a gentle gradient, slow surface water flow, and lower flood risk, whereas basins with a high slope index have a steeper gradient, faster flow, and higher flood risk. The slope gradient values of the Red Sea basins range from 0.9 (low risk) to 13.4 (high risk). For the studied basins, the hypsometric integrals are 0.92 for Wadi N Dara and 1.15 for Wadi Dara. These values suggest that the studied basins have a low slope gradient, which results in slower surface water flow and indicates low flood risk at their outlet areas.

7.5.2 Morphometric Analyses of Drainage Networks

The term "drainage network" refers to the overall layout of a collection of drainage channels in a region (Figure 44). This network includes a main channel that is fed by several tributaries, each corresponding to a wadi proportional to its size. All these tributaries converge, forming a network that descends toward the main channel.

The drainage network results from a complex interplay of surface characteristics, such as rock type, hardness, sensitivity, permeability, and structural properties, including cracks, joints, faults, and folds, as well as climatic conditions. The morphometric parameters of the drainage network for the studied basins are provided in Table 15.

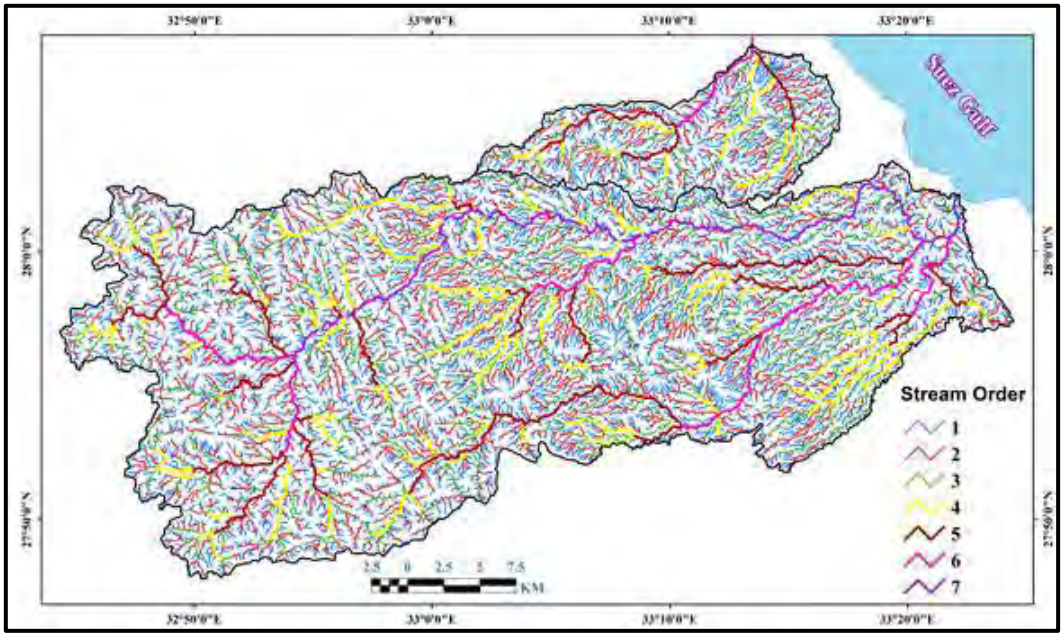

Figure 44: The drainage network in the area

Table 15: The drainage network parameters

	Wadi	Dara	N.Dara	Total		Wadi	Dara	N.Dara	Total
Order 1	Num	6979	924	7903	Order 5	Num	23	3	26
	(Km)	2132.9	309.3	2442.2		(Km)	159.2	26.4	185.6
Order 2	Num	1441	208	1649	Order 6	Num	5	1	6
	(Km)	1054	151.8	1205.8		(Km)	68.9	9.6	78.5
Order 3	Num	345	48	393	Order 7	Num	1	-	1
	(Km)	573.5	71.5	645		(Km)	71.4	-	71.4
Order 4	Num	85	13	98	Total	Num	8879	1197	10076
	(Km)	254.8	32.8	287.6		(Km)	4314.7	601.4	4916.1

Stream Order (Kc)

The Stream Order is the first step in the morphometric study of drainage networks, allowing for the identification of the network's size and density. The stream order is defined by the arrangement of streams, with each stream being classified into a specific order based on its position within the network. This classification is done by dividing the drainage network into distinct channels, each consisting of one or more links according to its order.

Using the internationally recognized method (Strahler, 1958), which is incorporated in the software, the stream order for the two basins ranges from 6 in W. N Dara to 7 in W. Dara.

Stream Number (Snu)

The number of streams is one of the important indicators of the size of the drainage network, and clearly shows the developmental stage reached by the basin. The greater the number of streams is, the higher the maturity of the basin. There is also a direct relationship between the area of the basin and the number of streams. The larger the area, the greater is the number of streams and vice versa.

The number of streams must be taken into consideration in estimating the risk of the floods. The increase in the number of streams increases the efficiency of the drainage network to transfer the surface water and accordingly, the flood probability increases.

The stream number of the Red Sea basins ranges from 183 (low risk) to 6630 (high risk). The stream numbers of the studied basins are 1197 in W. N Dara basin and 8879 in W. Dara basin. (Table 14). The stream numbers of the basins studied compared with the stream numbers of the Red Sea basins indicated that W. N Dara has medium risk while W. Dara has high flood risk possibilities.

Stream Lengths (SLu) Km

The length of the stream constitutes the distance travelled by the flow in its tributaries until it reaches the main valley and then to the outlet of the basin. The length of the stream reflects the erosion process of water movement, the surface characteristics of the slope and the kind of rocks and structural elements prevailed in the area. The lower the gradient, the longer the water course is and the more the lateral sculpting is, thus leading to the formation of the shallow, meanders and wider drainage lines. In the case of a steep slope, the vertical sculpting processes predominate, making the drainage lines shorter, deeper and straighter.

The length of the stream plays a significant role in determining flood hazards. In longer streams, the water takes more time to reach the outlet, with additional losses occurring due to evaporation and leakage during the extended journey. In contrast, shorter streams experience reduced losses, allowing the water to reach the basin outlet more quickly, potentially increasing the risk of flooding in a shorter time frame.

The length of stream of the Red Sea basins ranges from 108.2 km (high risk) to 9813.7 km (low risk). Based on the ARC GIS software, the length of streams of the studied basins in km are 601.4 of W. N. Dara and 4314.7 of W. Dara. (Table 14). The length of the streams in the studied basins, when compared to the streams in the Red Sea basins, indicates that Wadi N. Dara has a high flood risk, while Wadi Dara has a medium flood risk potential.

Bifurcation Ratio (Rb)

The bifurcation ratio refers to the ratio between the number of streams of an order and the number of streams to the following order. The bifurcation ratio was calculated by entering the following equation:

Bifurcation Ratio = No. streams at a given order/ No. of the next order

The bifurcation ratio is associated with the shape of the basin; rectangular basins tend to have a higher bifurcation ratio, meaning that water takes longer to reach the main valley compared to circular basins. In circular basins, the flow is more intense due to the shorter length of the discharge period.

Based on the above, the bifurcation ratio is inversely proportional to the risk of floods. The lower the bifurcation ratio, the higher is the risk of floods, and vice versa. The value of the bifurcation ratio of the Red Sea basins ranges from 1.6 (high risk) to 10.9 (low risk). Based on the ARC GIS software, the bifurcation ratios of the studied basins are 3.996 for W. N. Dara and 4.4 for W. Dara (Table 14). The bifurcation ratios, when compared with those of the Red Sea basins, indicate that the two basins crossing the site are associated with medium flood risk possibilities.

Drainage Density (D) Km^{-1}

Drainage density is a key indicator of how extensively a basin is divided by drainage lines. It reflects the influence of factors such as rock type, soil, and topography (Rashidi, 1994). A high drainage density suggests that the bedrocks are weak and respond rapidly to erosion, with low permeability, which increases flood risk. Conversely, a low drainage density indicates hard, permeable rocks and, therefore, a lower flood risk.

The drainage density was calculated by using the following equation (Horton, 1945):

Drainage Density = Total lengths of streams (km) / Basin area (Km^2).

Strahler, Morisawa has rated the discharge density in several categories as shown in the following table:

Table 16: The ranks of the drainage density (Strahler, 1957 & Morisawa, 1985)

Rank	Morisawa, 1985	Strahler, 1957
Low	< 8 (permeable rocks, wet, dense vegetation	< 5 km/km^2
Medium	8-20 permeable rocks, high rain, dense vegetation	5-13.7 km/km^2
High	20-200 impermeable rocks, low rain and vegetation	13.7: 155 km/km^2
V. High	> 200 (200 impermeable rocks, no rain and vegetation, weak rocks)	> 155.3 km/km^2

The drainage density of the Red Sea basins ranges from 5.4 (low risk) to 77 (high risk). The drainage density of the studied basins is 3.95 for W. N. Dara and 3.68 for W. Dara. All the basins studied are of low flood risk possibility, concerning the values of drainage density.

Stream Frequency (F) Km^{-2}

The frequency of streams is a measure that reflects the relationship between the total number of streams in a basin and its area. It provides valuable insight into the extent of surface incision within the drainage basin and the efficiency of the drainage network in facilitating water flow. A higher stream frequency indicates a more fragmented basin with a dense network of tributaries, which can contribute to faster runoff and increased flood risk. This measure can be calculated using the following equation (Horton, 1945, p.285):

Stream Frequency = No. of Streams / Basin Area (km2)

The stream frequency is influenced by various surface characteristics, including the permeability of the soil and the presence of impervious surfaces. For example, clogged clay surfaces tend to increase stream frequency due to their reduced permeability, which leads to faster surface runoff and higher flood risks. In contrast, highly permeable sandy and gravel surfaces tend to reduce stream frequency by allowing more water to infiltrate the ground, decreasing runoff and flood risk (Salloum, 2004).

The stream frequency of the Red Sea basins ranges from 9.5 (low risk) to 123 (high risk). For the studied basins, the stream frequency values are 7.86 for Wadi N. Dara and 7.58 for Wadi Dara. These values indicate that both basins exhibit low flood risk possibilities, as their stream frequencies fall within the lower range observed for the Red Sea basins.

Stream Maintenance Ratio (Rm)

The stream maintenance ratio is a key factor in understanding the hydrological characteristics of a basin. It represents the average unit area required for feeding the longitudinal unit of the drainage network. A higher stream maintenance ratio indicates a larger basin area relative to the drainage network, which typically results in lower drainage density and, consequently, a lower flood risk. This ratio is influenced by several factors, including climatic conditions, rock types, porosity, permeability, and vegetation cover (Jode et al., 1991).

In the studied basins, the stream maintenance ratio was calculated using the equation developed by Schumm (1956):

Stream Maintenance Ratio = Basin Area km2 / Total Stream Length

The stream maintenance ratio for the Red Sea basins ranges from 0.01 (high risk) to 0.18 (low risk). For the studied basins, the stream maintenance ratio is 0.25 for the drainage basin of W. N Dara and 0.27 for the drainage basin of W. Dara. These values suggest that both basins exhibit a high flood risk possibility.

Surface Flow (Lo) Km

Surface flow refers to the excess water that begins to move on the slopes after evaporation and leakage to feed the groundwater reservoir. This movement is unfocused in different directions, covering a large part of the surface (Saleh, 1999).

Surface flow covers the area between the water divide line and the beginning of the stream where the surface water accumulates and move in a concentrated flow. The water depth, velocity, and length of movement up to the first streams vary according to the geomorphological and hydrological characteristics of each basin (Saleh, 1999).

The average length of surface flow was calculated using the following equation (Horton, 1945):

Mean Surface Flow = 1/2 Drainage Density km/km2

The surface flow of the Red Sea basins ranges from 2.7 (low flood risk) to 38.5 (high flood risk). The surface flow is 1.98 for W. N Dara and 1.84 for W. Dara. These values indicate that all the studied basins are characterized by low flood risk possibility.

Texture Ratio (Rt) Km^{-1}

The texture ratio of the topography reflects the degree of proximity of the drainage lines in the basin, irrespective of their lengths. The importance of this factor lies in the fact that it is used to determine the extent to which the basin is being dissected by drainage lines (Gouda et al., 1991, p. 330).

The texture ratio is influenced by both climate and rock type. In wetter regions, basins are often characterized by a higher number of streams, indicating a more dissected and finer texture. In contrast, arid and semi-arid areas typically have fewer streams, leading to a coarser texture. The type of rock also plays a significant role in determining the texture of the basin. Weak, easily eroded rocks contribute to a finer texture, while harder, more resistant rocks result in a rougher texture. Additionally, the lack of vegetation in certain areas can further contribute to the formation of a rough texture. The texture ratio is calculated using the equation proposed by Horton (1945, p.288).

Texture Ratio = No. Streams / Basin Perimeter

The classification of the basins studied according to the Smith classification is as follows:

Table 17: Texture Ratio classification (Smith, 1950)

Texture ration classification, Smith, 1950	
Rough Texture	<4 stream/km
Medium Texture	4 - 10 stream/km
Soft texture	> 10 stream/km

The texture ratio of the Red Sea basins ranges from 6.7 (high risk) to 100.6 (low risk). The texture ratio of the basins that were studied is 15.79 for W. N Dara and 36.48 for W. Dara. Compared with the Red Sea basin's texture ratio values, W. N Dara has low flood risk while W. Dara has medium flood risk possibilities.

7.5.3 Factors Affecting the Occurrence of Flooding

The flood flow is controlled by several factors, the most important of which are (Table 18):

- Hydrological factors of drainage basins.
- Hydrological budget of drainage basins.

Table 18: The hydrologic parameters of the studied basins. (The parameters automatically calculated by the ARC-GIS software)

Wadi	Dara	N Dara	Average
TL	645.9	101.2	373.6
TC	1076.5	168.6	622.6
Dr	866.5	138.1	502.3
Dv	1844.2	345.4	1094.8
Td	1.84	0.70	1.27
Lt	3.6	9	105.3
Pre	60067170.0	7807860.0	33937515.0
EL	1250803.9	61845.6	656324.7
Lti	1008371.9	20531.0	514451.5
Se	341226.5	16871.8	179049.2
L	2600413.1	99250.1	1349831.6
Ru	57466756.9	7708609.9	32587683.4

LT Lag – Time (min), CT concentration Time (min), DR Drainage rate, DV Drainage Volume (m³), DT Discharger Time (h), FV Flow velocity (m/sec), Pre precipitation (mm), EL Evaporation Losses (m³), LTI Lag time infiltration (min), Se Seepage (m³), TL total losses (m³), Ru Run off

a) Hydrological Factors of Drainage Basins

Hydrological factors are influenced by a combination of morphometric properties and climatic conditions within a given basin. Utilizing LandSat images, Digital Elevation Models (DEM), and average climatic data, key hydrological factors for the studied basins were calculated using Arc-GIS. The impact of these hydrological factors on the three basins will be analyzed through several hydrological parameters, which include Lag-Time, Concentration Time, Discharge Volume, Flow Volume, Discharge Time, and Velocity of Water.

Lag-Time (TL) Min

Lag time refers to the interval between the onset of rainfall and the initiation of surface runoff. It is characterized by high rates of subsurface leakage and evaporation. A longer lag time indicates higher evaporation and leakage rates, which consequently reduces the likelihood of flooding. Studying lag time is important to determine the period required for the flow to begin, as well as to estimate the net flow through the leakage during this time. Lag time is influenced by the basin's lithology; rocks that are highly permeable, porous, and have cracks and joints lead to increased lag times. Additionally, the surface slope plays a role: steeper slopes reduce lag time because the increased flow velocity reduces leakage and evaporation losses. Thus, a shorter lag time correlates with a higher flood risk. The lag time for the studied basins was calculated using the equation provided by the US Conservation Services (1972).

LT= KI CT

Where; TL =Lag-Time, KI= constant (0.6), CT (Concentration Time (min)

The lag time factor for the two basins is 101.2 minutes in W. N Dara and 625.9 minutes in W. Dara. Based on these values, both basins are less vulnerable to flooding at their downstream outlets, as the longer lag time suggests lower flood risk.

Basin Concentration Time (CT) Min

Concentration time refers to the period that the rainfall needs from the farthest point at the water divide to reach the outlet of the basin in the form of running water (Goroshkov, 1979). The time-concentration equation depends on the effect of basin length and the vertical difference on the surface water velocity. Calculation of the concentration time based on the following equation:

CT = 0.28 (L/V)

Where; CT = concentration time (min), L = the mainstream length (m), V= flow velocity (L m/T min)

The concentration time is useful in identifying the time required for the flow to reach the outlet of the Wadi and determining the Wadies that are suitable for setting up flood warning stations. Sometimes the concentration time may decrease in some Wadies to a degree that cannot be warned. The CT values of the two basins are 168.6 mins in W. N Dara and 1076.5 mins in W. Dara. (Table 18). The concentration time for W. N Dara is about 3 hours while in W. Dara is about 18 hours, therefore it is not necessary to set a flood warning stations in these basins.

Discharge Rate (DR) m^3/sec

The discharge rate is the volume of water that passes through an area of one square kilometer in cubic meters per second. This factor considers that all the parts (any drop of rain fall on any square centimeter has been taken into consideration) of the basin are added to the volume of discharge. The discharge rate can be calculated from the formula of the "Centre for Development and Technological Planning".

DR = 1.5*A^$^{0.9}$ "This equation calculates the discharge rate ignoring the leakage and evaporation percentages." Where; DR is the discharge rate, A is the area of the basin, 0.9 is a constant to refer to the basin characters.

The discharge rate of the Red Sea Basins ranges from 3.8 m^3/sec (low risk) to 1273.4 m^3/sec (high risk). The discharge rates of the studied basins are 138.1 for the drainage basin of W. N Dara and 866.5 for W Dara. Compared to the Red Sea basins discharge rates, W. N Dara has low flood risk while W. Dara has medium flood risk possibilities at their downstream outlets.

Discharge Volume (DV) m3

The volume of discharge is the total amount of water that can be discharged by the drainage network, measured in a thousand cubic meters. A greater flow indicates a higher flood risk for the basin. The discharge volume can be calculated using the equation provided by the Centre for Development and Technological Planning.

DV = 1.5 * (LT)^0.85

Where; DV is the discharge volume in m3, LT is the sum of all tributaries length, and 0.85 is a constant to refer to the basin characters.

The discharge volume of the drainage basins in the Red Sea varies from 80.4 thousand m3 (low risk) to 3708.1 thousand m3 (high risk). The discharge volumes of the two basins are 345.4 of W. N. Dara and 1844.2 of W. Dara. The calculated values of the discharge volume of the basins compared to the average values of the Red Sea basins indicated that W. N Dara is of low risk while W. Dara is of medium flood risk possibility.

Discharge Time (TD) h

The discharge time is the time required for a basin to drain all its water from the upstream to the outlet area. The discharge time of the basin was calculated by the following equation, (Salwa, 1989):

$$\mathbf{TD= (0.305\ L)^{1.15} / 7700\ (0.305\ H)^{0.38}}$$

Where; TD = discharge time, L = the main stream length, H = the elevation difference

The average discharge time of the Red Sea basins ranges from 0.05 h (high risk) to 4.9 h (high risk). The discharge times in the two basins are 0.7 h for the drainage basin W. N Dara and 1.84 h for W. Dara. As a result, W. N. Dara has low flood risk and W. Dara has medium-flood risk possibilities.

Flow Velocity (Lt) km/h

The velocity of any moving object can be calculated by the following mathematical equation:

Velocity = Distance / Time

This equation is based on the calculation of water flow velocity:

Flow Velocity (Lt) = Basin length (L) / Concentration Time (CT)

The flow velocity of surface water in the Red Sea basins ranges from 5.2 km/h (Low risk) to 39.9 km/h (high risk). The flow velocities in the two basins are 9 km/h in the drainage basin of W. N Dara and 3.6 Km/h in Wadi Dara. Based on the surface flow velocity, it can be stated that the drainage basin of W. N Dara has medium flood risk while the drainage basin of W. Dara has low flood risk possibilities.

b) Hydrologic Budget of the Basins

The hydrological budget is based on the calculation of the amount of water falling on the basin, the evaporation and the leakage losses to determine the net flow and thus to identify the possibility of runoff (Saber, 2007). The hydrologic budget was studied through the following elements:

- The volume of water falling on drainage basins.
- The volume of losses.
- The volumes of net flow.

Volume of Rain Falling on Drainage Basins (Pre) m^3

The volume of water falling on each basin depends on the area of the basin and the largest amount of rain falls in one day. The volume of water falling on the basin can be calculated. The largest

quantity of rain falls in one-day from the closest meteorological station was 53.1 mm in 27 October 2016 where the average evaporation in the same year was 13.9 mm. The water volumes were calculated by the following equation:

Amount of Water Falling (Pre) = Area of the Basin × Largest Amount of Rain Fall in One Day

The volumes of rainfall on the two basins that were studied in case of the highest precipitation value (53.1 mm) are 7,807,860.0 m3, in W. N Dara and 60,067,170.0 in W. Dara.

Loss Volume m^3

The water lost by evaporation and leakage affects the flow. The flow is the remaining rain after evaporation and leakage.

There are many types of water losses:

- Evaporation during runoff.
- Leakage during Lag-time.
- Fixed leakage during discharge time.

Evaporation Loss During Runoff (EL) m^3

Due to the arid climatic conditions prevailed in the area, the evaporation rates increase due to the high temperature, especially during the summer. In addition to the temperature, the period of precipitation also affects the evaporation; where the shorter the period of precipitation is, the less is the chance of evaporation. Also, the time of precipitation affects evaporation; the evaporation increases in daytime fall, while it decreases at night (Mustafa, 2004). In addition, the slope gradient affects evaporation; evaporation increases on gentle slope gradient surfaces, while it decreases on steep surfaces. The evaporation data from the closest meteorological station has been used to calculate the evaporation during runoff through the following set of equations

Total Daily Evaporation = Mean Evaporation x Basin Area

The total evaporation in an hour is then calculated by the following equation:

Total Hourly evaporation = Total Daily Evaporation / 24

The values resulting from the calculation of the discharge time of basins are then used to calculate evaporation during discharge time, as shown in the following equation:

Evaporation during Discharge Time (EL) = Total Evaporation/Hour × Basin Discharge Time

The evaporation losses of the two basins are 61,845.6 m3 in W. N Dara and 1,250,803.9 m3 in the drainage basin of W. Dara.

Leakage during Lag-Time: (LTI) m^3

Leakage is the infiltration of water through the soil surface. The soil has a higher infiltration limit (infiltration capacity) as it cannot pass more than this limit. When the amount of rain falling is much greater than the soil infiltration capacity, runoff begins to form by collecting the rainwater

above the soil surface. The degree of water leakage through the soil depends on the degree of porosity of the rock, its permeability and the degree of slope of the surface, as well as the depth and type of the surface layer. The following table (Table 19) shows the volume of leakage through the soil layers (Wilon & Lane, 1980).

Table 19: The volume of leakage in soil sediments

Type of sediments	Grain size	inch/h	Notes
Gravel, coarse sand	2 mm	5	
Clean sand, Gravel	2	2:5	Agricultural land
Sand, gravel, silt, clay	Varies	3:1	Few silt & Clay
Sand, gravel mixed with silt and clay	Varies	0.25	Much silt & clay
Consolidated materials, high % of silt and clay	varies	0.1-0.001	
Average		1.93	0.08mm/min

Leakage is calculated during lag-time using the following equation:

Leakage during Lag-Time = Basin Area × Lag Time × 0.08 mm/min

Where; 0.08 mm/min is the average amount of leakage for all types of surface sediments (Wilson & Lane, 1980).

Leakage during lag-time is known as the leakage that occurs at the onset of rainfall and continues until the water appears on the surface of the earth and begins to flow. The (LTi) for the two basins is 20,531.0 for the drainage basins of W. N Dara and 1,008,371.9 for the drainage basin of W. Dara. The drainage basins of Wadi Al Darb and Wadi Kharim loss volume of water through infiltration less than that in Wadi Abu Khashba.

Fixed leakage during Discharge Time (Se) m^3

Fixed leakage values reflect the amount of leakage within the bed rock that lies beneath the surface soil sediments that cover the sides and bottoms of the basin (Awadallah, 2005).

The constant leakage is calculated during the discharge time of the basin through the following equation:

Fixed leakage values (Se) = Basin Area × Discharge Time × w

Where (w) = Constant expressing the original rock type

The fixed leakage values of the two basins are 16,871.8 in the drainage basins of W. N Dara and 341,226.5 In W. Dara. The fixed leakage during the discharge time in W. Dara is significantly higher than in W. N Dara.

Total loss (L) m^3

The total loss is the amount of water lost, either by evaporation or by leakage, since the amount of net flow is determined. The loss is calculated by collecting evaporation and leakage values previously calculated as follows:

Total Loss = Evaporation during runoff + leakage during lag-time + Fixed leakage values

The total loss of Red Sea basins varies from $0.02*10^6$ m3 to $2.1*10^6$ m3. The total losses in the two basins are 99,250.1 m3 in W. N Dara and 2,600,413.1 in W. Dara**.** These values are high due to the climatic conditions, as well as the surface characteristics and geological composition of the area.

Net flow volumes in drainage basins (Ru) m^3

The net flow is the remaining water after subtracting evaporation and total leakage losses out of the total rainfall. The increase in net flow indicates a higher probability of running off (Saber, 2007). Thus, net flow is calculated by subtracting total losses from total precipitation.

Net flow (Ru)= total precipitation - total losses

The values of net flow in the two studied basins are 7,708,609.9 m^3 in the drainage basin of wadi N. Dara and 57,466,756.9 in the drainage basin of W. Dara. These net flow in the drainage basins could form flash flood at the outlet of them in case of rain falling up to 53.1 mm in 24 h duration time. This is a large amount of water compared to the large drainage basins on the coast of the Red Sea and the Gulf of Suez, and may pose a threat to the facilities that would be built in the main streams of the drainage lines especially in the middle and downstream parts of the area when the amount of rain falls similar to the largest amount that fell according to global warming. Therefore, the necessary measures must be taken to protect these facilities from the strong surface runoff.

7.5.4 Summary of the Studied Basins According to the Measured Parameters

To assess the risk and hazard rate of surface flow in the studied basins, three key morphological characteristics of the drainage basins were analyzed. The morphometric features of the drainage basins along the Red Sea were also referenced. The flood risk level for each drainage basin was determined based on a combination of these morphometric variables. The selected parameters were chosen for their significant role in characterizing the basin and their relevance to flood risks, as outlined below:

1. Shape Properties: The circulatory ratio was selected as an important indicator to measure the risk of runoff in the region.

2.Geomorphological Characteristics: The rates of relief ratio, ruggedness value, and hypsometric integral were selected as indicators to measure the risk of flow in the basins.

3. Morphometric Characteristics of the Drainage Network: The parameters of the (drainage density, stream frequency, texture ratio) have been selected to indicate the effect of bed rock characteristics on the surface flow.

4. Hydrological Factors: The coefficients of (lag-time - concentration time - water velocity) were selected as indicators to measure the risk of flow in the two basins.

The following conclusions can be drawn based on the limits of each parameter for the two basins, in comparison with their values across all basins along the Red Sea and Gulf of Suez:

- In terms of circulation, the two basins are characterized low flood risk.
- In terms of the relief factor, all basins fall within the low-risk category.
- Regarding ruggedness, the values of the ruggedness ratio reflect low flood risk risk in the studied basins**.**
- In terms of the hypsometrical integral, the drainage basin of W. N. Dara shows low flood risk while W. Dara exhibits medium flood risk.
- In terms of drainage density, both basins present low flood risk.
- In terms of stream frequency, both basins present low flood risk.
- Regarding topographic texture, W. N Dara presents low flood risk while W. Dara presents medium flood risk.
- In terms of the lag-time, both basins are of low flood risk.
- Regarding concentration time, it is not necessary to establish flood warning stations for either basin.
- In terms of water velocity coefficient, the drainage basin of W. N. Dara is of medium risk while W. Dara is of low flood risk.

7.5.5 Flash Flood Risk Assessment

The numerical data produced from the morphometric analysis of the two drainage basins that were studied has been processed statistically within the framework of the general data available to the Red Sea basins (Figure 45). The most important morphometric parameters were chosen to categorize the studied drainage basins according to the severity of flooding. 5 parameters out of the 23 parameters which have background limits in the Red Sea area were chosen for simple statistical processing to throw in-depth insight into the severity level of the two basins. The chosen five parameters are (area, circularity, slope index, drainage density, and net flow). These parameters are the most important factors in the morphometric analyses of the drainage basins. The actual reasons for choosing the previous five coefficients in the severity calculations are:

1) Basin dimension parameters collectively determine the basin area.
2) Circularity parameter reflects other basin shape characteristics.
3) Slope index is the final product of the interplay of topographic features.
4) Drainage density is considered one of the most important parameters among the morphometric parameters of the basin.
5) Factors controlling flood occurrence such as climatic conditions, hydrological factors, and hydrologic budget are directly linked to the net flow.

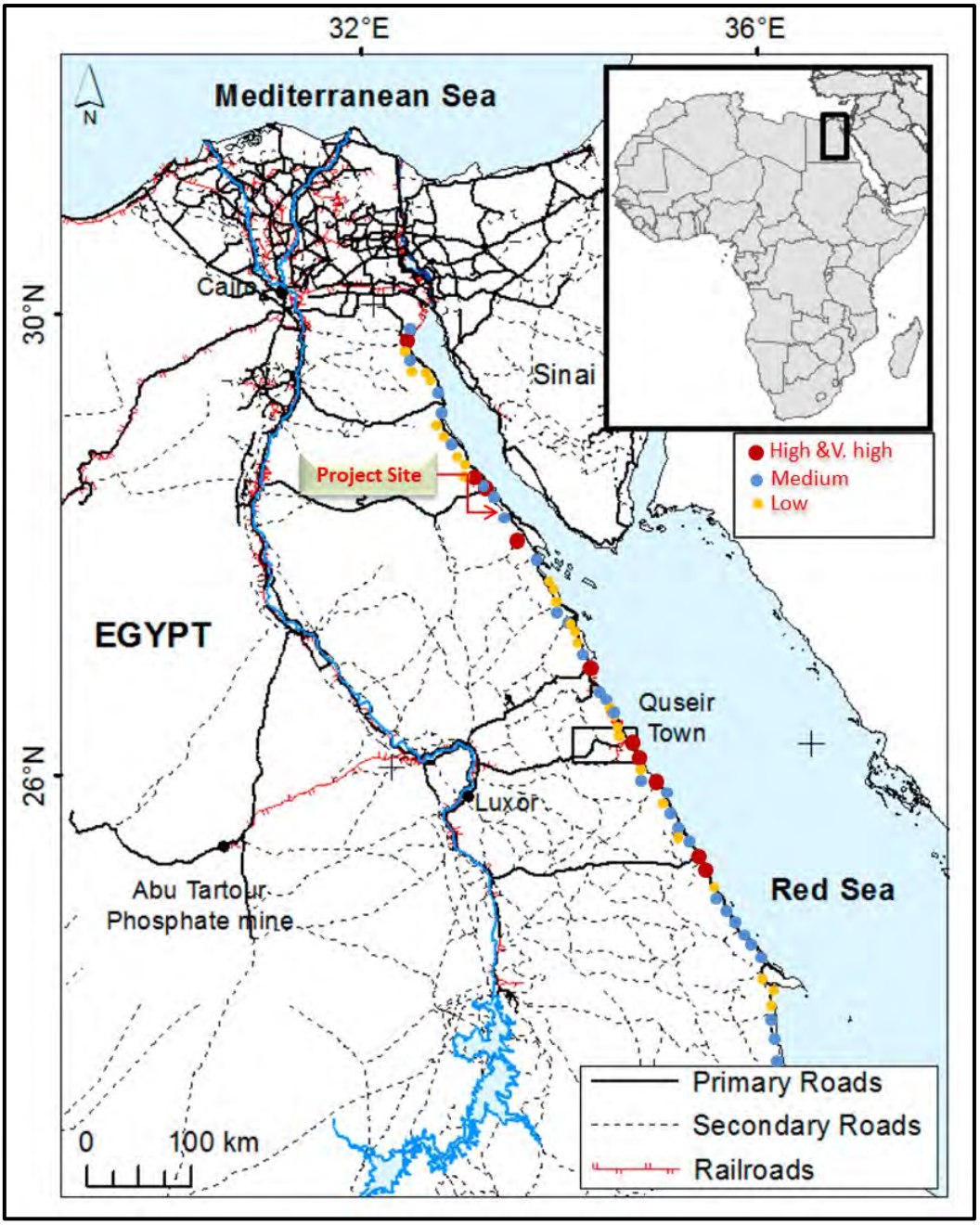

Figure 45: The likelihood flooding of the Red Sea area based on the historical record of the flash flooding.

Calculation Steps

The maximum (Max) and minimum (Min) values of the 23 Red Sea basin parameters were categorized into four levels: L1 to L4 (Table 20). For the five selected parameters, the difference between the higher and lower limits was divided by four to establish four category limits (C1 to C4) for each parameter (Table 19). The range of the four risk category levels — Low (1), Medium (2), High (3), and Very High (4) was calculated based on these category limits (Table 19).

Each of the selected five parameters contributes 20% to the overall severity of the expected flood. The values of the selected parameters for the two basins were compared against the four risk category limits (Table 20) to determine the risk category level for each parameter in each basin.

The severity percentages for the five parameters in the two basins were calculated based on the risk category level for each parameter (Table 21). The overall category level of severity for each basin was determined (Table 22).

The expected likelihood of flash floods with intensity levels — low, medium, high, and very high — was derived based on the historical flash flooding records for the Red Sea area, as shown in Figure 44. This figure indicates that the project site is in an area that has experienced medium to very high flooding at the outlets of some drainage basins.

The likelihood of flash floods was then categorized into four levels: (1) low, (2) medium, (3) high, and (4) very high. The flash flood risk matrix was calculated based on the severity and likelihood categories, as shown in Table 25.

Table 20: The morphometric parameters of the Red Sea basins categorized in four levels (L1 to L4)

	Parameters Range			Categories' Limits			
Parameters	Max	Min	(Max-Min)/4	L1	L2	L3	L4
Area (km2)	1796.5	2.8	448.4	451.2	899.7	1348.1	1796.5
Circularity Ratio (Rc)	0.52	0.13	0.1	0.2275	0.325	0.4225	0.52
Slope Index	13.4	0.9	3.1	4.0	7.2	10.3	13.4
Drainage Density (Km^{-1})	77.0	3.68	18.33	22.1	40.43	58.67	77.0
Net Flow	57.4	0.1	14.35	14.45	28.8	43.15	57.4

Table 21: The limits and risk levels of the selected 5 parameters according to the whole Red Sea basins

	Categories' Limits				**Risk Category Levels**			
Parameters	**C1**	**C2**	**C3**	**C4**	**Low (1)**	**Medium (2)**	**High (3)**	**V. High (4)**
Area (km2)	**451.2**	**899.7**	**1348.1**	**1796.5**	**2.8 - 451.2**	**451.2 - 899.7**	**899.7 - 1348.1**	**1348.1 - 1796.5**
Circularity	**0.2275**	**0.325**	**0.4225**	**0.52**	**0.13 - 0.2275**	**0.2275 - 0.325**	**0.325 - 0.4225**	**0.4225 - 0.52**
Slope index	**4.0**	**7.2**	**10.3**	**13.4**	**0.9 - 4**	**4 - 7.2**	**7.2 - 10.3**	**10.3 - 13.4**
Drainage density	**22.1**	**40.43**	**58.67**	**77.0**	**3.68 – 22.1**	**22.1 – 40.43**	**40.43 – 58.67**	**58.67 - 77**
Net flow	**14.45**	**28.8**	**43.15**	**57.4**	**0.1 – 14.45**	**14.45 – 28.8**	**28.8 – 43.15**	**43.15 – 57.4**

Table 22: The limits and risk levels of the studied two basins

	Basins		Risk Category levels (Likelihood)	
Parameters	W. N Dara	W. Dara	W. N Dara	W. Dara
Area (km2)	152.2	1170.9	1	3
Circularity	0.33	0.25	1	1
Slope index	0.92	1.15	1	1
Drainage density	3.95	3.68	1	1
Net flow $*10^6$ m^3	7.7	57.5	1	4

Table 23: The severity % of the selected 5 parameters on the two basins

Parameter	Category	Low (1)	Medium (2)	High (3)	Very high (4)
Area					
% limits		1 – 5%	6 – 10%	11 – 15%	16 – 20%
Red Sea Range		2.8 – 451.2	451.2 – 899.7	899.7 – 13481.1	1348.1 – 17.96.5
% of Severity	W. N. Dara	1.7			
	W. Dara			13.02	
Circularity					
% limits		1 – 5%	6 – 10%	11 – 15%	16 – 20%
Red Sea Range		0.3 - 0.4	0.4 - 0.6	0.6 - 0.7	0.7 - 0.8
% of Severity	W. N. Dara	4.1			
	W. Dara	3.1			
Slope index					
% limits		1 – 5%	6 – 10%	11 – 15%	16 – 20%
Red Sea Range		0.9 - 4	4 - 7.2	7.2 - 10.3	10.3 - 13.4
% of Severity	W. N. Dara	1.15			
	W. Dara	1.44			
Drainage Density					
% limits		1 – 5%	6 – 10%	11 – 15%	16 – 20%
Red Sea Range		5.4 - 23.3	23.3 - 41.2	41.2 - 59.1	59.1 - 77

% of Severity	W. N. Dara	0.89			
	W. Dara	0.83			
Net Flow					
% limits		1 – 5%	6 – 10%	11 – 15%	16 – 20%
Red Sea Range		0.1 – 8.15	1 - 1.9	1.9 - 2.8	2.8 - 3.7
% of Severity	W. N. Dara	2.7			
	W. Dara				5

Table 24: The category level of flood severity for the two studied basins

Basins	W1	w2
Area	1.69	13.03
Circularity	4.13	3.13
Slope gradient	1.15	1.44
Drainage Density	0.89	0.83
Net flow	2.66	5.01
Total %	10.52	23.43
Category level	1	1

Table 25: Matrix of the risk of the flash floods that could be expected in two studied basins

Severity ⇨ Likelihood ⇩	1	2	3	4
1	1	2	3	4
2	2	4	6	8
3	3	6	9	12
4	4	8	12	16

Low Medium High/Very High

Note:

- Both basins have a flood severity of 1
- The likelihood categories are 1 or 3 or 4
- The risk factor of the two basins is either 1, 3 or 4 (low risk)

In conclusion, based on the morphometrical analyses of about 38 parameters of the two studied basins in the framework of all basins in the Red Sea and Gulf of Suez taking into consideration the maximum rainfall received in the area in one day, the two basins have low flood risk severity.

7.6 Hydrogeologic Parameters

Bedair (2015) defined the extent, thickness, and geometry of the aquifer systems beneath the southern part of the site, specifically along the mainstream of Wadi Dara. By integrating previous studies, reviewing, and analyzing the detailed geological and hydrogeological settings of Wadi Dara, a survey of existing wells was conducted, and available data were collected. These data include water flow, groundwater levels, groundwater quality, and lithological descriptions of various units. Such information is crucial for supporting the groundwater model and addressing gaps in hydrogeological data. This study delineates the hydrogeological characteristics of the existing aquifer based on geophysical interpretations and well data, providing insights into deep-seated structures.

Calibration between the available drilled wells and the neighboring interpreted VES data provides a clear understanding of the subsurface geological and hydrogeological conditions. The geoelectrical sounding results were calibrated against borehole data in terms of layer thickness and resistivity values. Three VES points (6, 11, and 14) were aligned along cross-section GG and conducted near wells RIGW-2, Kanady-2, and Dara-5, respectively (Figure 46a).

The calibration process between VES-6 and the RIGW-2 well (Figure 46b) demonstrates a strong correlation between the interpreted geoelectric units and borehole data. However, the investigated sections have been classified into five distinct units with varying thicknesses and resistivity values, as detailed in the resistivity spectrum of the subsurface sequence (Table 26).

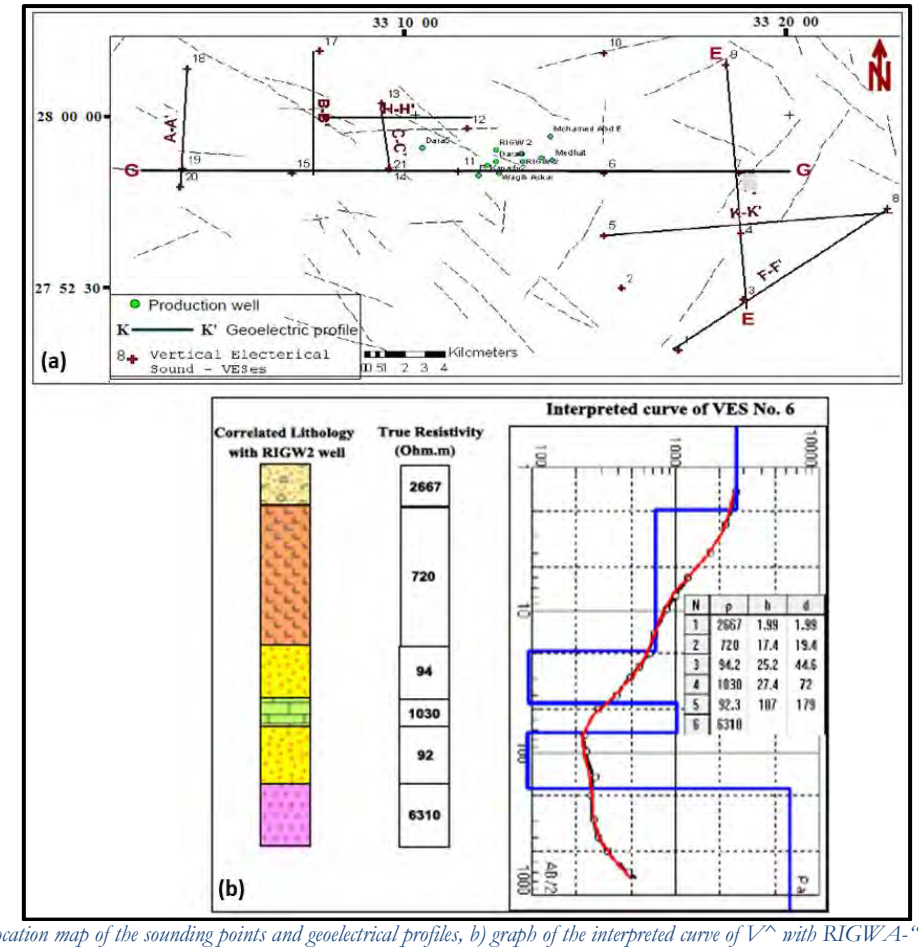

Figure 46: a) Location map of the sounding points and geoelectrical profiles, b) graph of the interpreted curve of V^ with RIGWA-" drilled well. (Bediar, 2015)

Table 26: Resistivity spectrum and its lithological units of geoelectrical sections. (Source, Bedair 2015)

Geoelectrical Unit	Resistivity (Ωm)	Description of the expected lithological Units	Common thickness (m)
First unite	240-3200	Surface deposits, pebbles, gravel, cobbles, sand, and hard cuttings (Gravelly sand)	8
Second unite	410-550	Fine to coarse grain of dry sand, shale intercalation.	15
Third unite	250-275	Green shale with dry sand, argillaceous in some parts.	22
Fourth unite	45-95	Water saturated zone, medium to coarse sandstone of different colors, argillaceous sandstone and clayey in some parts.	90
Fifth unite	6500-9800	/Basement rocks, blocky, v. hard, soft red color.	N - A
Sixth unite	1400-1600	Weathered evaporates and gypsum of pink color.	N - A

The constructed cross-sections E-E' and G-G (Figures 47 and 48) across the site area reveal that the topmost geoelectrical unit consists of a relatively thin layer with high resistivity values,

correlating with gravels, sands, and hard boulders. The second unit is thicker than the first due to the sculpturing effect of the underlying third layer. It exhibits lower resistivity values compared to the first unit and is interpreted as dry sand. Similarly, the third unit shows resistivity values indicative of predominantly dry conditions, like the two overlying geoelectrical units.

Notably, the top three geoelectrical units, with a combined thickness exceeding 45 meters, represent an unsaturated (dry) zone. This suggests that intensive infiltration of surface water significantly reduces surface flow volume and intensity. The upper 25 meters are primarily composed of highly porous and permeable gravel and sand, further facilitating infiltration.

The aquifer parameters of the Wadi Dara aquifer, as calculated by Sewidan and Himida (1991), indicate that the transmissivity (T) ranges from 198 to 3,580 m^2/day, while the storativity (S) ranges from 0.00164 to 0.00236, with both parameters increasing as the sand and gravel content increases.

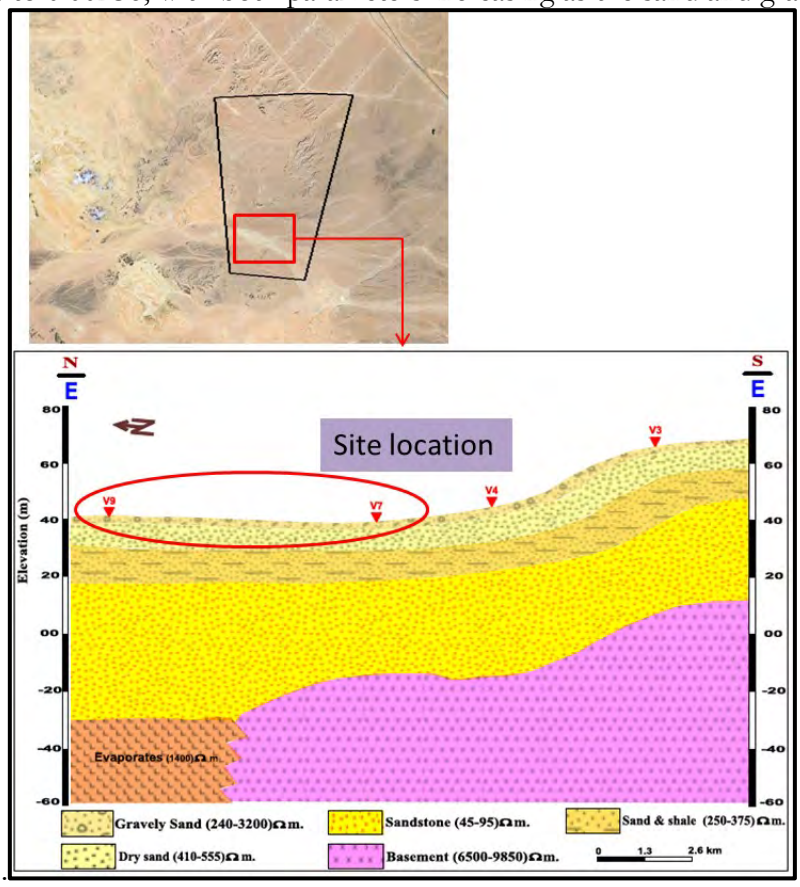

Figure 47: Geoelectrical cross section E – E and its lithologic unit at Wadi Dara. (Source, Bedair 2015)

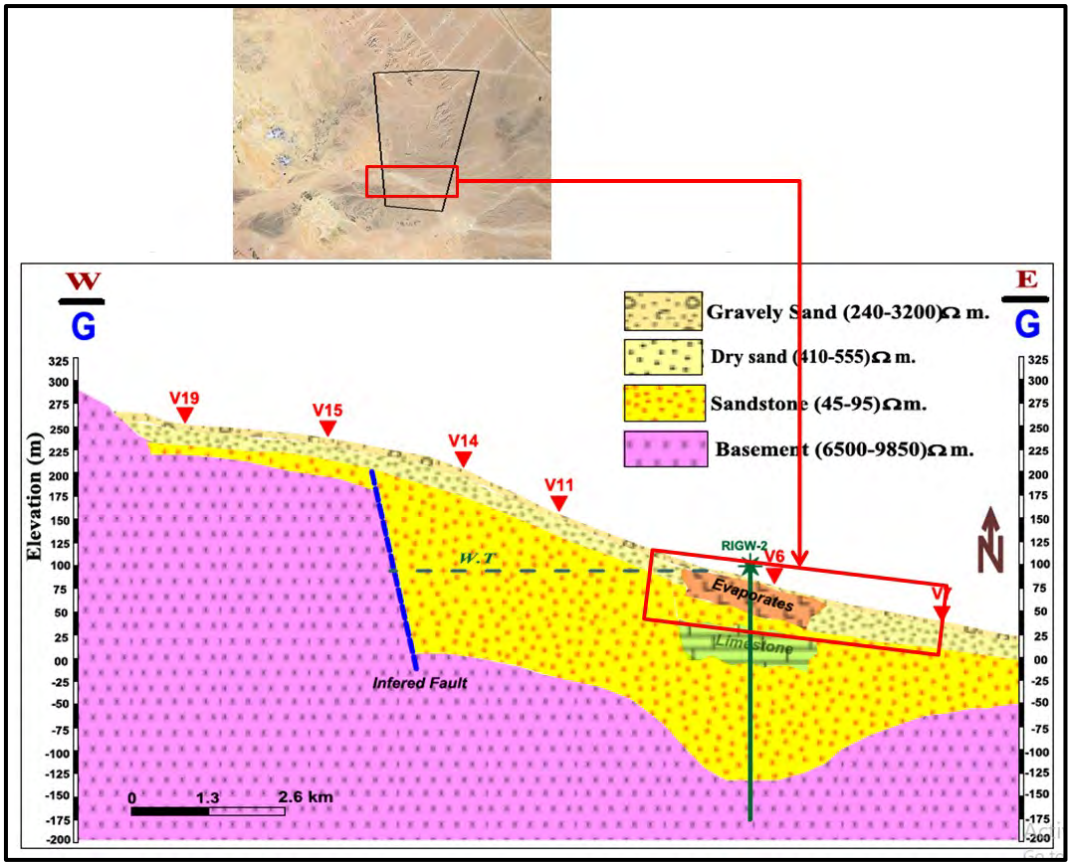

Figure 48: Geoelectrical cross section G – G and its lithologic unit at Wadi Dara. (Source, Bedair 2015)

The study concluded that the aquifer thickness ranges from 100 m to 300 m, with a general decrease westward, a finding that is also supported by data from drilled wells. The primary sources of aquifer recharge are direct infiltration from rainfall and leakage from the underlying water-bearing and fractured basement rocks along fault zones. The groundwater flow direction aligns with the regional topography and the slope of the underlying basement rocks, both of which trend eastward.

Based on the review of the hydrogeological parameters of the deposits covering the site and the depth to the groundwater level beneath the project site in relation to flood risk assessment, it can be stated that:

1) The upper unsaturated zone has a significant thickness and is primarily composed of coarse sand and gravel with high porosity and permeability. These characteristics enhance the infiltration capacity of surface water, reducing the intensity of surface flow during rainstorm events.
2) There are no water accumulation areas within the site or its immediate vicinity, indicating that the groundwater level is at a considerable depth.
3) Groundwater exploitation is not intensive in most parts of the project area, except along the mainstream of Wadi Dara. This suggests that surface flow and groundwater recharge are primarily influenced by the mainstream of large drainage basins, such as Wadi Dara.

4) Surface water infiltration occurs across the entire site due to the thick layer of highly porous and permeable deposits covering the area.

5) When considering the total project area in relation to the cumulative footprint of installations (e.g., turbine bases, paved roads), the project installations occupy a much smaller portion of the land. This implies that the overall natural infiltration rates remain largely unaffected by the installations. Additionally, since surface flow mainly occurs along mainstreams, these locations should be avoided when positioning turbines or should be considered for appropriate protective measures if necessary.

7.7 Site Visit

The field visit primarily focused on the project site to assess natural phenomena that indicate the intensity of rainfall, locations prone to flooding, the capacity of these floods, and their impact on the surrounding environment and nearby facilities.

At the project site, the visit inspected drainage lines that traverse the area to observe traces of severe surface runoff, particularly following the rainy season, and to evaluate the dimensions of these drainage lines.

The visit also dealt with places outside the boundaries of the site and identifying mitigation measures that were implemented to protect the facilities located in the main streams that are exposed to the impact of torrents.

7.6.1 Soil Cover and Sediment Transport

The entire site area is covered by Quaternary deposits of alluvial origin, forming successive terraces (Figure 49). These terraces are composed of sediments of varying sizes, primarily derived from exposed rocks in the upstream parts of the basins. The surface is covered with gravel and rock fragments embedded in a matrix of fine-grained sand and silt, exhibiting a gently undulating topography caused by gully erosion (NSSH, 2001). The soil texture ranges from sand to sandy

loam, with colors varying from very pale brown to yellow and light yellowish brown to brownish yellow.

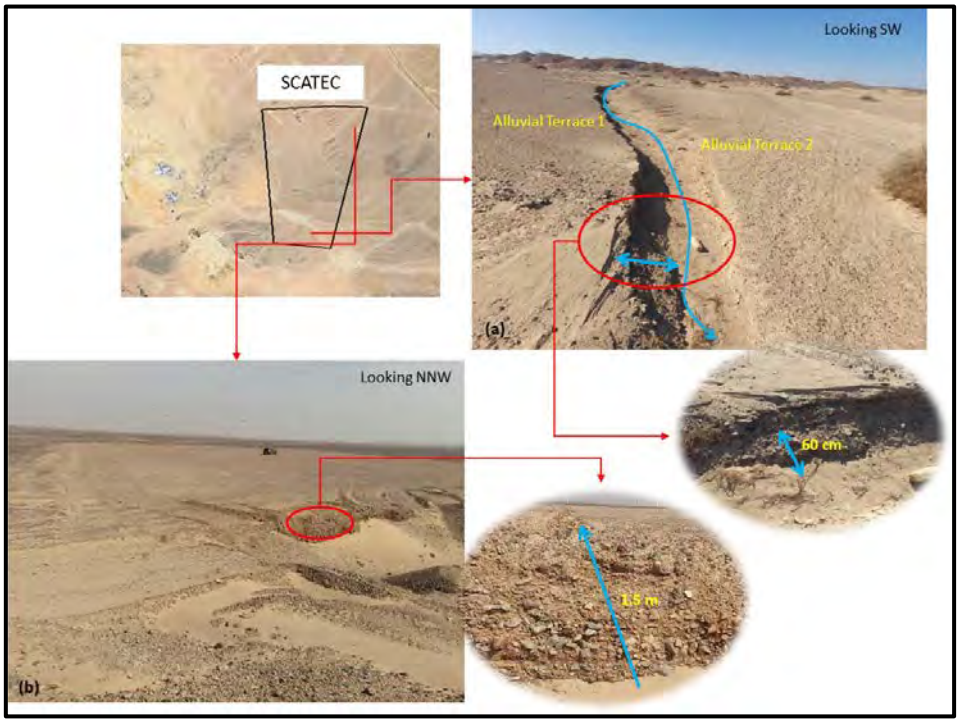

Figure 49: The grain size variation of the deposits covering the surface of the site.

The soil cover is characterized by high permeability and porosity, granting it a high infiltration capacity to absorb significant volumes of surface flow and recharge groundwater during rainfall events. The size of rock fragments decreases along the flow direction, particularly in the northwestern upstream part of Wadi N. Dara (Figure 50). The wadi fills sediments transition from boulder and gravel-sized fragments in the upstream areas (Figure 50a) to very coarse and coarse fragments embedded in fine-grained sand and clay in the elevated regions between drainage lines (Figure 50b). Further downstream to the east, the sediments consist of coarse fragments embedded in a matrix of fine to coarse sand and clay (Figure 50c).

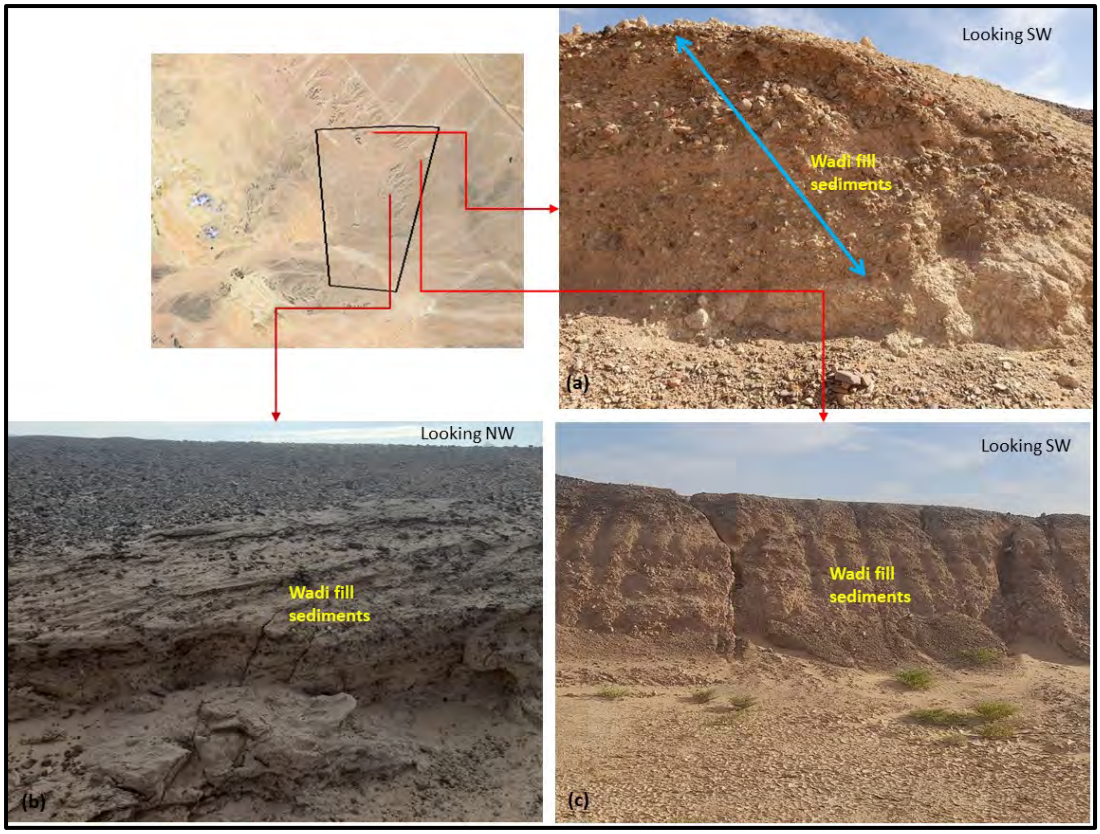

Figure 50: Filed photographs show the change in the grain size of the wadi fill sediments along the drainage lines.

The transport of sediments in dry wadis and their tributaries depends on the velocity of surface runoff during or immediately after rainfall. The size and distribution of sediments within the wadi channels provide evidence of the power of surface flow. In the drainage lines crossing the site, sediment size ranges from large to very large in the western part. Moving in the direction of water flow, sediment size decreases until being discharged into the Gulf waters.

In the northwest part of the site, the grain size of deposits does not vary significantly along the drainage lines, likely due to the relatively short distance between the upstream and downstream sections of the Wadi N. Dara drainage basin (Figure 50). However, along Wadi Dara, the upstream part of the drainage basin spans a much greater distance to the west. The middle and southern parts of the site feature gentle slopes toward the east, reducing surface flow velocity and its capacity to transport large sediment volumes.

Notably, clay and fine sand fractions dominate the drainage lines across the site, including the upstream portion of Wadi N. Dara. This indicates that the surface flow's volume and velocity are insufficient to transport all fine materials downstream along the drainage lines.

7.6.2 Ground Surface Relief and Topography

Close investigation of the topographic relief of the project site area as shown on the topographic profiles (Figure 51 the following points are observed:

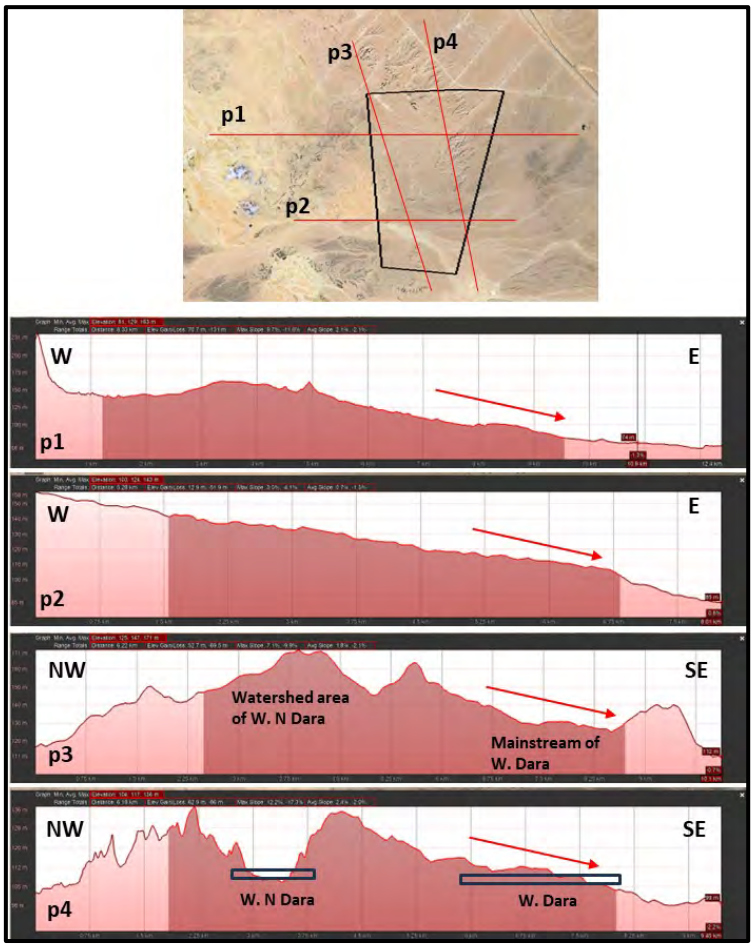

Figure 51: Topographic profiles developed from Google maps

- Two profiles (P1and P2) run in the direction of surface flow N-W, and two profiles (P3 and P4) are in NW-SE direction.
- The site is almost horizontal with a very gentle slope toward ESE with a slope degree ranging from 0.007 P1 to 0.008 P2, while the slope angle decreased in the SE direction to be of 0.002m P3 and 0.003 in P4.
- The northeast part of the site is characterized by elevated mountains reaching 165 m amsl. This area represents the watershed of Wadi N Dara drainage basin as it is dissected by slightly deep and narrow tributaries.
- The middle and southern part of the site, which is the outlet of Wadi Dara, is characterized by low relief and simple topography. The mainstream of W. Dara is very wide and shallow with small drainage lines passing along the mainstream.
- The site is highly accessible as there are no rough topographic elements like deep drainage basins or hills like features existed in the site area even in the NW part.
- The drainage lines crossing the site are very shallow and wide which reflects the weakness of surface flow. This is due to the small watershed area of Wadi N. Dara while W Dara

watershed is at a great distance to the West where the surface flow is obstructed by natural ridges of basement and sedimentary rocks along W. Dara before entering the project area.

- Field investigations reveal very weak surface flow action across the site, suggesting a low likelihood of flash flooding. However, strong surface flow could occur within the main streams of the drainage basins, particularly in Wadi N. Dara.
- The main courses of these tributaries are shallow, wide and their floor is covered by fine sediments, mainly clay which confirms the weakness in surface runoff even in high rainfall intensity events.

7.6.3 Possible Thickness of Surface Flow

The average thickness of surface water flow is indicated by the thickness of the recently developed terraces along the mainstream of the drainage lines. In the middle and southern parts, within the drainage lines of Wadi Dara, the thickness of these terraces does not exceed 60 cm (Figures 52 and 53). Additionally, the drainage lines in the elevated areas between the main streams are very shallow, further reflecting the weak surface flow during rainfall events (Figure 53b).

In the northern part, where the intensity of surface flow appears to be higher, the thickness of the recently developed terraces along the drainage lines is greater than in the southern part. This indicates that the surface water flow in the upstream section of Wadi N. Dara is faster compared to the flow in the middle and southern section's where Wadi Dara's drainage lines are located. Consequently, the likelihood of floods or severe surface runoff posing a threat to the site's infrastructure is minimal. However, in the event of high-intensity rainfall, the northeastern part of the site could be exposed to strong surface flow.

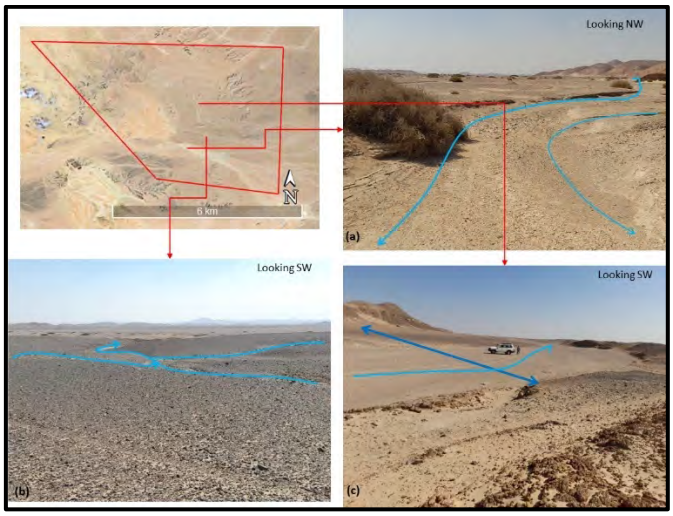

Figure 52: The shallow and wide drainage lines crossing the middle and southern parts of site

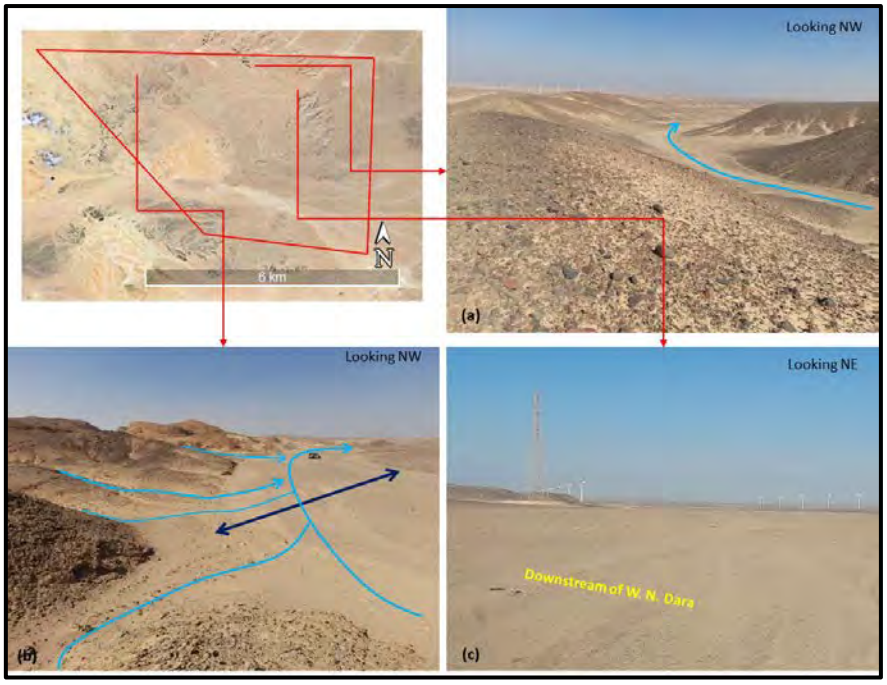

Figure 53: The main streams of the drainage lines crossing the northeastern part of the site.

7.6.4 Areas with Vegetation Cover

Vegetation density in the area is closely linked to the route of the drainage lines. The vegetation is sparse and sporadically distributed along the drainage line floors, suggesting either low rainfall intensity in the region or a high infiltration capacity of the soil, which limits water retention time. Observations during the site visit reveal an absence of vegetation along the mainstream of Wadi N. Dara (Figure 54a), while small, scattered vegetation can be found along the mainstream of Wadi Dara (Figure 54b).

Figure 54: Vegetations in the site area; (a) no vegetation at all in the mainstream of W. N Dara, (b) sporadic vegetation along the mainstream of Wadi Dara

7.6.5 Accumulation and Erosion Areas

Erosion primarily occurs along the sides of the drainage lines crossing the project site, with the floors of these lines serving as the main accumulation zones. Given that erosion factors in the area are currently considered very weak, the annual sediment deposit thickness does not exceed a few millimeters. This is evident from the thin layers of sediment observed on the floors of the channels traversing the site and along the mainstream of the drainage lines.

7.6.6 Water Accumulation Areas

There are no field indications suggesting the possibility of water accumulation, even temporarily. During or just after the rainy period, surface runoff carries clay, which accumulates in the downstream parts or small lowlands of the drainage lines, forming a thin water screen. However, the accumulated water evaporates quickly, leaving behind a thin layer of cracked mud (Figure 55).

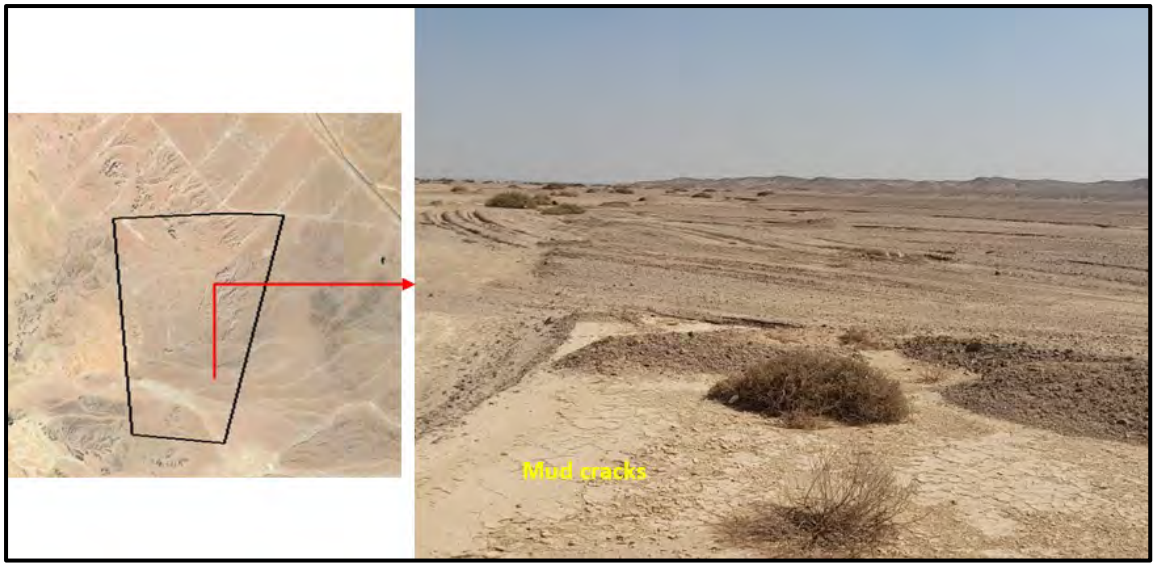

Figure 55: The area of surface flow accumulation at the eastern border of the site where a layer of mud cracks precipitated from the very recent rainfall event

7.6.7 Flood Mitigation Measures Applied

Upon inspecting the northern site location, it was observed that simple mitigation measures have been implemented for the facilities developed along the floor of the drainage lines (Figure 56). These measures include small culverts installed underneath the main road, located just to the north of the site. The culverts were specifically applied where the road crosses the trunk stream of Wadi N Dara (Figure 56). Additionally, on-site mitigations consist of simple concrete fences constructed around the bases of high-voltage towers positioned along the mainstream of the drainage lines (Figure 57).

These observations provide conclusive evidence that there is no expected danger to the site from flash floods originating from the Red Sea Mountain Ridges. The only potential concern is weak surface runoff in the drainage lines, which can be easily managed by implementing simple precautionary measures. These measures would protect any facility located in the paths of the tributaries from soil erosion and prevent exposure of the facility base to surface water flow.

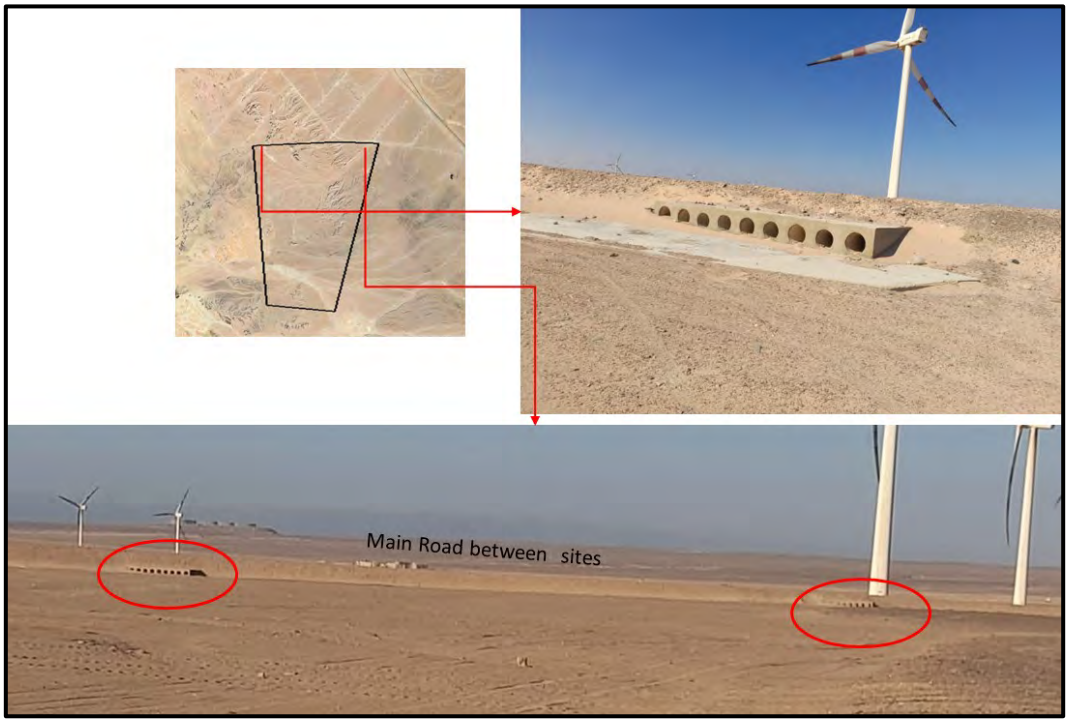

Figure 56: The flood mitigations applied off the project site. Culverts to protect the roads from the surface flow especially at the outlet of Wadi N Dara.

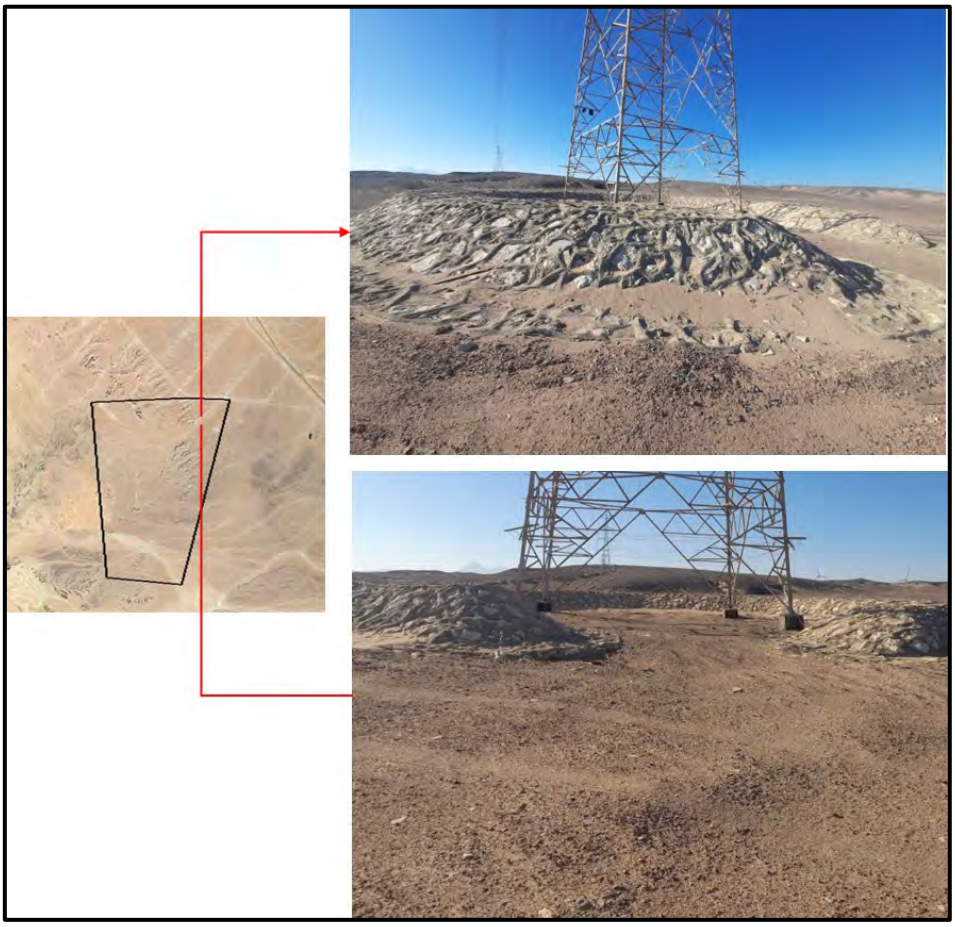

Figure 57: The concrete fences around the base of the high voltage towers

7.6.8 Flood Vulnerability Assessment

Floods are among the most destructive natural disasters, causing significant damage to human lives, property, and the environment. The severity of floods has been increasing and is expected to escalate further due to climate change-induced variations in monsoon precipitation. Given the country's exposure to flooding, assessing flood vulnerability is crucial for effective preparedness and mitigation strategies, particularly for the project site.

Based on the land use analysis within the project site and its vicinity, as outlined in the baseline assessment, the flash flood receptors in the area are limited. They primarily consist of engineering infrastructure, including main roads and associated services (such as checkpoints, ambulance stations, and fuel stations), power lines, communication and weather towers, and substations. Additionally, small population clusters and farming activities exist in Wadi Dara, alongside military units and crude oil and gas facilities. The only large, populated areas near the site are the cities of Ras Gharib and Ras Shukeir.

In Wadi Dara, the largest drainage basin crossing the southern part of the project site, no destructive floods have been recorded to date. Even during the severe flooding event of 2016 that submerged the city of Ras Gharib, Wadi Dara remained unaffected. Therefore, it can be confidently stated that the project site has a low flood vulnerability, with potential flood impacts only occurring in the event of exceptionally heavy rainfall.

Based on the comprehensive review of the flash flood potential for the project site, as outlined in previous studies and supported by field investigations into the site's geology, geomorphology, hydrogeology, hydrology and land use, the following map identifies areas that may be subject to strong runoff during heavy rainfall events. The area's most susceptible to strong surface runoff are primarily the floors of the mainstream drainage lines that cross the site (Figure 58).

If infrastructure is to be established in these areas, which are predominantly located in the courses of the mainstream drainage lines, it will be essential to provide adequate protection for these facilities against the risks posed by severe surface runoff during construction. To ensure the safety and durability of any infrastructure, a detailed site-specific study should be conducted, considering the nature of each site, the type of infrastructure, and its size. This study will allow for the development of targeted mitigation strategies to reduce the risks associated with runoff and flooding.

Figure 58: The proposed locations of strong surface runoff in the project sites which are mainly the floor of the mainstream of the drainage lines.

8. Summary and Conclusions

The flood risk assessment in the project area was conducted through several important stages.

Literature review of previous studies that addressed the prevailing climatic conditions, the historical record of flash flood events in the surrounding areas, and the flash flood vulnerability of the drainage basins crossing the project area. The literature review revealed that the project site is in a moderate flood hazard with a low flood vulnerability degree area. In the project area and its surroundings, about 40% of the annual precipitation contributes to surface runoff, while the remaining 60% is lost to infiltration and evaporation. Moreover, only about 11% of the total

surface runoff is generated by a single storm event. These results highlight the high absorption capacity of the soil layers in the project area, which effectively reduces the intensity of surface runoff.

Site visits were conducted to identify any actual evidence confirming the occurrence of flash floods specifically within the project area. Based on the literature review and site survey, the Wadi Dara basin, where the site is located, is considered a medium-hazard drainage basin in terms of flash flood events. Given the potential impacts of global warming and the anticipated changes in rainfall intensity over the area, it is recommended to develop flash flood models for the entire Dara basin. These models should incorporate various design storm intensities and return periods to assess the severity of flash flood risks in the event of significantly heavier rainfall than currently experienced.

The rainfall in the study area was analyzed based on the expected rainfall intensity extracted from the satellite images for weather and climate patterns and the actual recorded precipitation data collected from the nearest meteorological station. The data collected covers the period from 2015 to 2024, during which the digital files were analyzed and modeled to assess the spatial and temporal changes in rainfall patterns over the study period. Based on the rainfall data, either expected or recorded, it is obvious that no definite rainfall pattern has prevailed in the area. The expected rainfall is always much higher than the actual measured values. The rainfall depth for certain return periods (2, 5, 10, 25, 50, and 100 years) was calculated using the Log-normal statistical distribution (Maximum Likelihood Estimation). The predicted rainfall depth is approximately 3.31 mm for a 2-year return period, while it is expected to reach about 22.4 mm for a 100-year return period. The global warming phenomenon was taken into consideration when designing the rainstorms and their return periods through: 1) increasing the amount of recorded precipitation by about 25%, and 2) calculation based on the maximum rainfall depths recorded in one day at the station (October 2016). Rainstorms that recorded 51.3 mm at El Gouna station could correspond to a return period of about 26 years. The rainstorm depth recorded at El Gouna Station in one day during the occurrence of flooding in the Ras Gharib area (51.3 mm) could be expected in the study area in a period of more than 100 years.

Flood risk models were developed through morphometric analyses of the Earth's surface features from topographic maps, Landsat images and DEM that are supplemented by aerial, space and field measurements. Morphometric analyses of the studied basins (Wadi Dara and Wadi N. Dara), which mainly drain through the project site, were conducted. The morphometric parameters of the basin include basin dimensions (4 parameters), basin shape (4 parameters), topographic features (11 parameters), drainage network (9 parameters), and factors affecting the occurrence of flooding (11 parameters). From the statistical analyses of about 38 morphometric parameters of the two studied basins, in the framework of all basins in the Red Sea and Gulf of Suez, taking into consideration the maximum rainfall received in the area in one day, the two basins in the project site (Wadi Dara and Wadi N. Dara) have a low flood risk severity.

The entire site area is covered by Quaternary deposits of alluvial origin, forming successive terraces. These terraces are composed of sediments of varying sizes, primarily derived from exposed rocks in the upstream parts of the basins. The surface is covered with gravel and rock fragments embedded in a matrix of fine-grained sand and silt, exhibiting a gently undulating topography caused by gully erosion. The soil cover is characterized by high permeability and porosity, granting it a high infiltration capacity to absorb significant volumes of surface flow and recharge groundwater during rainfall events. Field investigations reveal very weak surface flow

action across the site, suggesting a low likelihood of flash flooding. However, strong surface flow could occur within the main streams of the drainage basins, particularly in Wadi N. Dara. The main courses of these tributaries are shallow, wide, and their floor is covered by fine sediments, mainly clay, which confirms the weakness in surface runoff even during high rainfall intensity events.

The following figure illustrated the processes conducted to finalize the flood risk assessment.

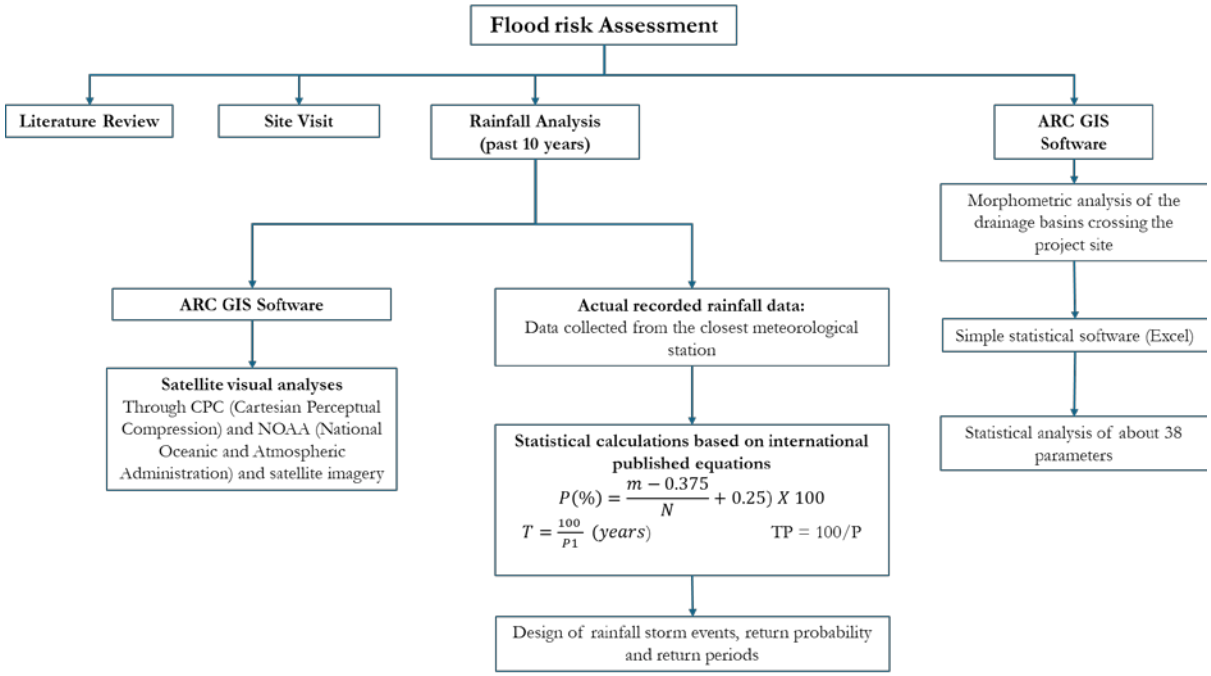

Figure 59: Illustrative Schematic of the Conducted Flood Risk Assessment

Based on the comprehensive review of previous studies on flash flood hazards in the area surrounding the project site, combined with a detailed field visit to investigate and document the actual signs of flash flooding indicators, the following conclusions can be summarized regarding the extent of dangerous floods that may occur on the site:

1) **Increased Flood Risks Due to Climate Change**: Over the past 15 years, Ras Gharib region has experienced an increase in the frequency and intensity of floods due to global warming and climate change, particularly during the rainy seasons. This shift has affected surrounding areas but has had a limited direct impact on the project site.
2) **Surrounding Wadi Flooding**: In 2016, rainwater collected in dry wadis to the north of the site, particularly in Wadi Abu Had and Wadi Al Darb, which affected the city of Ras Gharib. However, these flood events did not impact the Dara area or the project site directly.
3) **Downstream Characteristics of the Site**: The site lies at the downstream end of the Wadi Dara basin and the small Wadi N. Dara basin at the northeastern border. The rainwater collected through small tributaries creates weak surface flow that converges at the outlets of these wadis south of Ras Shukeir city. The flow remains relatively mild until reaching the site.

4) **Soil Permeability and Infiltration**: The site is characterized by soils with high porosity and permeability, which allows for substantial sub-surface infiltration of rainwater. This reduces surface runoff and minimizes the intensity of flow at the site, preventing significant flooding.
5) **Unsaturated Zone Thickness:** A thick unsaturated zone is present across the project site, consisting mainly of high-porosity and high-permeability sediments. This feature enhances the intensity of infiltration, effectively reducing the volume and velocity of surface water flow during heavy rainfall events. The substantial capacity of this zone to absorb water further lowers the likelihood of flood-related hazards.
6) **Gentle Relief and Shallow Drainage Lines**: The site has a simple, gently sloping relief towards the east and southeast. The drainage lines are wide and shallow, with no evidence of significant surface flow or vertical erosion of tributary paths. This further suggests a low risk of flooding from the surface runoff.
7) **Higher Elevations in the North**: The northwestern part of the site contains elevated hills, representing the watershed area for Wadi N. Dara. The drainage lines here are deeper than those in the southern and central parts of the site. However, these features do not significantly affect the risk of flooding within the project site.
8) **Surface Flow in Wadi N. Dara**: The surface flow along the mainstream of Wadi N. Dara appears to be faster compared to other areas, which is why simple flood mitigation measures, such as culverts, have been implemented near the site to protect infrastructure.
9) **Sediment Characteristics and Surface Flow**: The surface sediments on the site vary in size, from fine particles to large rocks. However, the surface runoff is weak and unable to transport larger sediments. As the runoff reaches the main wadi course, the flow intensity decreases significantly, leading to the deposition of fine sediments like clay and silt along the wadi course.
10) **Absence of Deep Wadis or Large Alluvial Fans**: There are no deep dry wadis or large alluvial fan deposits on the site that would indicate strong historical surface flow or significant erosion. This supports the conclusion that flood risk is low.
11) **Short, Shallow Drainage Lines**: The drainage lines that run through the site are short, wide, and shallow, further reinforcing the absence of significant flood risk. The only potential area for flooding could be at the outlet of Wadi N. Dara at the northeast of the site, but even this would be a low-impact event under typical conditions.
12) **Comparison of Expected vs. Recorded Rainfall Intensity:** A comparison between satellite-derived rainfall intensity estimates and actual recorded rainfall data from the nearest meteorological station reveals a significant discrepancy. On average, actual recorded rainfall intensity is no more than 10% of the expected values calculated from satellite images. This finding confirms that rainfall intensity at the site is generally lower than anticipated, further reducing the likelihood of severe flooding.
13) **Flash Floods Vulnerability Locations:** Although the entire site is classified as having medium flood vulnerability, severe surface flow has occasionally been observed at the outlets of the Wadi Dara and North Wadi Dara basins. These areas represent localized flood-prone zones within the broader project site and may require additional monitoring or mitigation strategies.
14) **Existing Flood Receptors on Site:** No significant flood receptors exist within the project site, except for established power line towers and the main road along the northern border. The lack of extensive infrastructure at risk further reinforces the low flood hazard level at the site.

15) **Existing Flood Mitigation Measures:** The most significant flood mitigation measures implemented at the site facilities include multi-slot culverts along the main road to facilitate controlled water flow and reinforced concrete fences around the base of the power line turbines. These fences, approximately 1.5 meters high, provide an added layer of protection against surface runoff. The turbines, primarily located within the mainstream drainage lines, are particularly susceptible to flash floods, making these protective structures essential in minimizing potential flood impacts and ensuring the stability and functionality of the infrastructure.
16) **Low Flash Flood Severity in the Project Area**: The entire site is expected to experience low flash flood severity. However, strong surface flow may occur at the outlets of Wadi Dara and Wadi N. Dara, particularly during heavy rainfall events. While these areas may experience localized flooding, the overall flood risk across the site remains low, making it a suitable location for project development with minimal flood-related concerns.

9. Recommendations

Based on the extensive studies conducted to assess the potential for dangerous flooding and surface runoff at the project site, as well as the simulation models developed from climate data, rainfall records, and digital elevation models, the following recommendations are made to mitigate potential risks:

1. Given the possibility of extreme rainstorms exceeding the maximum calculated estimates (i.e., events that might occur once every hundred years), it is recommended to construct a one-meter-high concrete fence around critical facilities, especially turbines or any infrastructure located within the mainstream of drainage lines. These areas are more susceptible to surface runoff, and this fence would provide an additional layer of protection against unexpected floods.
2. To mitigate flood risks, turbines should preferably be installed on **elevated terrain away from drainage mainstreams**, particularly at the outlets of **Wadi Dara and Wadi North Dara**. These locations are less susceptible to the accumulation of surface runoff, reducing the potential for flood-related damage. However, if avoidance is not possible, additional mitigation measures should be implemented to enhance resilience. These may include **reinforcing turbine foundations** to improve stability, **elevating turbine bases** above the projected flood level, or **constructing reinforced concrete fences** around turbine bases. The recommended **minimum height for these fences is 1.5 meters**, ensuring protection against potential surface runoff impacts. Proper site selection and structural reinforcement will significantly reduce the risk of turbine failure due to flooding.
3. The site's access roads, whether paved or asphalt, crossing the wide and shallow drainage lines. These areas exhibit weak to moderate surface runoff that does not concentrate on narrow, specific paths, meaning the impact on the roads is not significant. However, to minimize any potential disruptions, it is recommended to install simple cement culverts (with a maximum diameter of one meter) beneath roads that cross these drainage lines at identified points. This will allow surface water to flow through without blocking or damaging the road infrastructure.
4. As for the electricity cables, they must be buried under the ground at a depth of about a meter, while taking all measures for insulation and protection against subsurface infiltrated water.

5. While establishing an early warning system for floods is the responsibility of local authorities in the Gharb and Shukeir area, it is even more critical for the project team to develop an internal flood management plan. This plan should outline clear response protocols for handling flood emergencies, ensuring that all personnel are well-prepared to take appropriate actions. Key components of the plan should include monitoring rainfall data, identifying evacuation procedures, securing critical infrastructure, and implementing contingency measures in the event of severe flooding. By proactively preparing for flood events, the project can mitigate potential damages, reduce downtime, and ensure the safety of personnel and infrastructure.

References

Aggour TA, Sadek MA (2001) The recharge mechanism of some cases of the different groundwater aquifers, eastern Desert, Egypt. Bull Fac Sci Mansoura University 28(1):43–78

El Ghazawi A, Abdel Baki A (1991) Groundwater in Wadi Asel Basin, Eastern Desert, Egypt. Bull of Meneufia Uni V:25–44.

Elnazer AA., Salman S., Asmoay AS., 2017: Flash flood hazard affected Ras Gharib city, Red Sea, Egypt: a proposed flash flood channel. Nat Hazards (2017) 89:1389–1400

El Ramly IM (1972) Final report on geomorphology, hydrology planning for groundwater resources and reclamation in lake Nasser region and its environs. Cen And Des Inst, Cairo 603 pp

El Shamy IZ (1992) Recent recharge and flash flooding opportu- nities in the Eastern Desert, Egypt. Annals of Geological Sur- vey of Egypt. XVIII:323–334.

El- Shamy, I. Z., 1992b: New approach for hydrological assessment of hydrographic basins of recent recharge and flooding possibilities – 10th Symp. Quaternary and Development, Egypt, Mansoura Univ., 18 April, P. 15 (Abstract).

Ezz H., 2017: The Utilization of GIS in Revealing the Reasons behind Flooding Ras Gharib City, Egypt. International Journal of Engineering Research in Africa, 31, 135-142.

Ezz H., Gomaah M., Addelwars M., 2019: Watershed Delineation and Estimation of Groundwater Recharge for Ras Gharib Region, Egypt. Journal of Geoscience and Environment Protection, 2019, 7, 202-213.

Gregorgy , K. J. & Walling, D. E. (1973): Drainage Basins - Form and Process, Edward Arnold , London

Gomaa M A, Aggour TA (1999) Hydrogeological and hydrogeo- chemical conditions of carbonate aquifers in the Gulf of Suez region. Assiut Sci Bul Vol. 28., No. 2 pp 191–214

Gomaa, M.A. and Aggour, T.A.,(1999):"Hydrogrological and hydrogeochemical conditions of carbonate aquifers in the Gulf of Suez region,Egypt". Bull.Fac.Sci.Assiut Univ., pp. 191-214.

Horton,R., (1932): Drainage Basin Characteristics , Transactions of The American Geophysical Union, Vol.13

Khalil G, Hassan TM (1997) Hydrogeological aspcts of Karstified aquifer and its enviromntal impacts in Eastern Desert, Egypt. In: (ed. Gunay G. amd Johnson I.A) Proc.5th International symposium and field seminar on Karst waters and Enviomenatl Impacts. Antalya, Turkey, 10–20 Sep. :59–66.

Moustafa AR, Khalil MH (1995) Superposed deformation in the Northern Suez rift, Egypt: relevance to hydrocarbons explora-tion. J Pet Geol 18:245–266

RIGW (1988) Hydrogeological map of Egypt. scale 1, 2000,000. User guide, Ministry of Irrigation, Cairo, Egypt.

REGWA, 1991: Water resources for the area between Gharib and Quseir; Red Sea Development Organization. Submitted report to the Ministry of Housing, Development and New Communities. 271 p.

Sadek M., Li X., 2019: Low-Cost Solution for Assessment of Urban Flash Flood Impacts Using Sentinel-2 Satellite Images and Fuzzy Analytic Hierarchy Process: A Case Study of Ras Ghareb City, Egypt. Advances in Civil Engineering Volume 2019, Article ID 2561215, 15 pages

Said R (1990) The Geology of Egypt. A.A. Balkema /Rotterdam/ Brookfield, 734 pp.

Schumm, S. A.,.(1956): Evolution of Drainage System and Slopes in Badlands at Perth Amboy New Jersy, Bull. Geol. Soc. America, Vol, 67, pp. 597 – 646.

Strahler,A., (1985) : Dimensional Analysis Applied to Fluvial Eroded landforms, Bull. Geol. Soc. America, Vol. 63, pp. 279 – 300.

Strahler,A., (1964): Quantitative Geomorphology of Drainage Basin and Channel Net Work, in Chow, V. T (Editor), Handbook of Applied Hydrology, New York, pp. 39 – 76.

UNISDR 2017: Flood hazard and risk assessment.

Youssef AM., & Hegab MA., 2005: Using geographic information system and statistics for developing a database management system of the flood hazard of Ras Gharib area, Eastern Desart, Egypt. The 4th., international conference on the geology of Africa, Assuit, Egypy. 2, 1:15.